Biomechanical Multifunctionality of the Ghost Crab, *Ocypode quadrata*

by

Dwight Springthorpe, II

A dissertation submitted in partial satisfaction of the
requirements for the degree of
Doctor of Philosophy

in

Integrative Biology

in the

Graduate Division

of the

University of California, Berkeley

Committee in charge:

Professor Robert J. Full, Chair
Professor Robert Dudley
Professor Damian O. Elias

Fall, 2016

Biomechanical Multifunctionality of the Ghost Crab, *Ocypode quadrata*

Abstract

Biomechanical Multifunctionality in the Ghost Crab, *Ocypode quadrata*

By

Dwight Springthorpe, II

Doctor of Philosophy in Integrative Biology

University of California, Berkeley

Professor Robert J. Full, Chair

Bioinspired robotics has experienced unprecedented advancements. Robots can now run, swim and fly. Despite these advancements, the animals that inspired these robots remain substantially more versatile, using the same set of multifunctional appendages to perform many different tasks or behaviors. Understanding how biomechanics and behavior contribute to these capabilities will offer new insight into the science of animal movement and potentially inspire new multifunctional robotic technologies. Here, the ghost crab, *Ocypode quadrata*, was examined. These crabs, which are among the fastest land invertebrates, use relatively simple, unspecialized appendages to run, climb, burrow and dexterously capture prey. This dissertation focuses on ghost crabs' burrowing and climbing behaviors. Both of these involve complex behavioral suites that involve the walking legs, the chelae and the body. Crabs demonstrated specialized postures, locomotion in confined spaces and goal-directed manipulation of both the environment and themselves. Both burrowing and climbing strategies involved compensatory strategies that allowed the crabs to maintain performance across a wide range of environmental conditions. Crabs do not rely on specialized appendage features but rather on the ability to use all appendages together. The findings presented in this dissertation represent new insight into the biomechanics of multifunctionality and offer inspiration for new bio-inspired robots with multi-use parts that permit, not simply obstacle negotiation, but also modification of the environment.

For my mother

Contents

List of Figures

List of Tables

Acknowledgments

I give my heartfelt thanks to everyone that contributed to the long journey towards my doctorate degree. This dissertation would not have been possible without your innumerable contributions. To each of you, I offer my most sincere gratitude.

I am grateful for the support of my family. My mother, Suzanne Springthorpe, and father, Dwight Springthorpe, have been a constant source of inspiration. Without their inexhaustible reserves of understanding, optimism and encouragement, none of this would have been possible. To my siblings, Nicholas and Sarah Katherine Springthorpe, I offer my thanks for your help and support.

I also thank my adviser, Professor Robert Full, for providing the opportunity to pursue research at Berkeley and providing support and guidance whenever required. Professor Full is a truly exceptional scientist and a superb adviser who always puts his students' interests first. His dedication and support have defined and enabled both my career and the careers of many of my fellow students.

I have had the wonderful opportunity to collaborate with and learn from many excellent scientists. I would like to thank Professor Daniel Goldman for both his advice and generously allowing me to use his facilities for my research. I would also like to thank the current and former members of Professor Goldman's lab. In particular, Nick Gravish, Nicole Mazouchova, Daria Monaenkova and Sarah Sharpe all deserve special thanks for their advice and assistance. I also extend my thanks to the staff and faculty at the Duke Marine Lab and the Rachael Carson Marine Reserve in Beaufort, North Carolina. I thank Professor William Kirby-Smith for the use of his facilities and advice. I have also benefitted greatly from the Biomechanics community at U.C. Berkeley. This is a superb community of researchers and their constant support has enabled my work and helped me grow tremendously as a scientist. I offer special thanks to my qualifying exam committee members, Professors Mimi Koehl, Lucia Jacobs, Robert Dudley and Damian Elias, and to the members of my dissertation committee, Professors Robert Full, Robert Dudley and Damian Elias.

I thank the other current and former members of the Poly-PEDAL lab – Kaushik Jayaram, Nate Hunt, Thomas Libby, Chen Li, Ardian Jusufi, Jean-Michel Mongeau, Viktor Gudenus and Pauline Jennings. Their friendship, support and advice helped create a thriving and productive scientific community. It was an honor and privilege to work alongside them. I would also like to thank the undergraduate members of the Poly-PEDAL lab. Paulina Ng, Jayden Robert, Nicole Greene, Kimberly Penamora, Danield Corbett, James Saulsbury and Kiet Lam all deserve special recognition for their enthusiasm, efforts and creativity. It was a pleasure to mentor them and this dissertation could not have happened without them.

I also acknowledge those organizations that provided funding or other material support to my work. I thank the Army Research Lab, the National Science Foundation, the U.C. Berkeley Integrative Biology Department and the Center for Interdisciplinary Biological-inspiration and Education and Research (CiBER). In particular, the integrative graduate education and research traineeship (IGERT), provided by CiBER and the NSF provided me with critical training, funding and resources.

Finally, I offer my thanks to my wife, Leanne Springthorpe. Her love, encouragement and assistance made this dissertation possible in so many ways.

Chapter 1

Introduction and Summary

1.1 Introduction

The biology of multifunctionality, where an animal can accomplish multiple tasks with the same parts, such as appendages, is an exciting research frontier. Because a multifunctionality in animals represents a combination of biomechanical traits, neural programming and learned behavior, this field can identify principles of integration and complex optimization. Thus, findings have the potential to translate into new bio-inspired robots capable of transitioning smoothly between behaviors, moving rapidly through heterogeneous terrain and manipulating their environment to facilitate mission success. A comprehensive understanding of animal movement is also likely to translate into improved prosthetic devices and rehabilitative techniques.

Studying the ghost crab, *Ocypode quadrata*, is an excellent avenue for studying the general principles of multifunctionality (Figure 1). These crabs, which have a typical leg span between 5 cm and 15 cm and a body mass between 15 g and 70 g, maintain a semi-terrestrial existence on sandy beaches throughout the southeastern coast of North America as generalist predators and scavengers (Milne & Milne, 1946). Using the same set of relatively simple appendages, they can accomplish a wide range of behaviors including running, burrowing, climbing and dexterous manipulation. They are among the fastest land invertebrates, capable of running more than 2 m/s or 20 body lengths per second (Herreid & Full, 1988) in varied terrain that includes water, sand, stone and vegetation. Their chelae (i.e. claws) allow them to dexterously capture and manipulate a wide variety of prey. These crabs have been observed to capture, carry and consume live insects and small fish. Ghost crabs can also construct complex semi-permanent burrows up to 1 m long in varied substrates.

Understanding how ghost crabs are able to use their appendages together to enable so many different behaviors will offer new insight into the biomechanics of multifunctional appendage design. These biomechanical principles may inspire a new generation of robots with multi-use parts that permit, not simply obstacle negotiation, but modification of the environment, allowing them to move over and through highly diverse terrain.

Figure 1.1

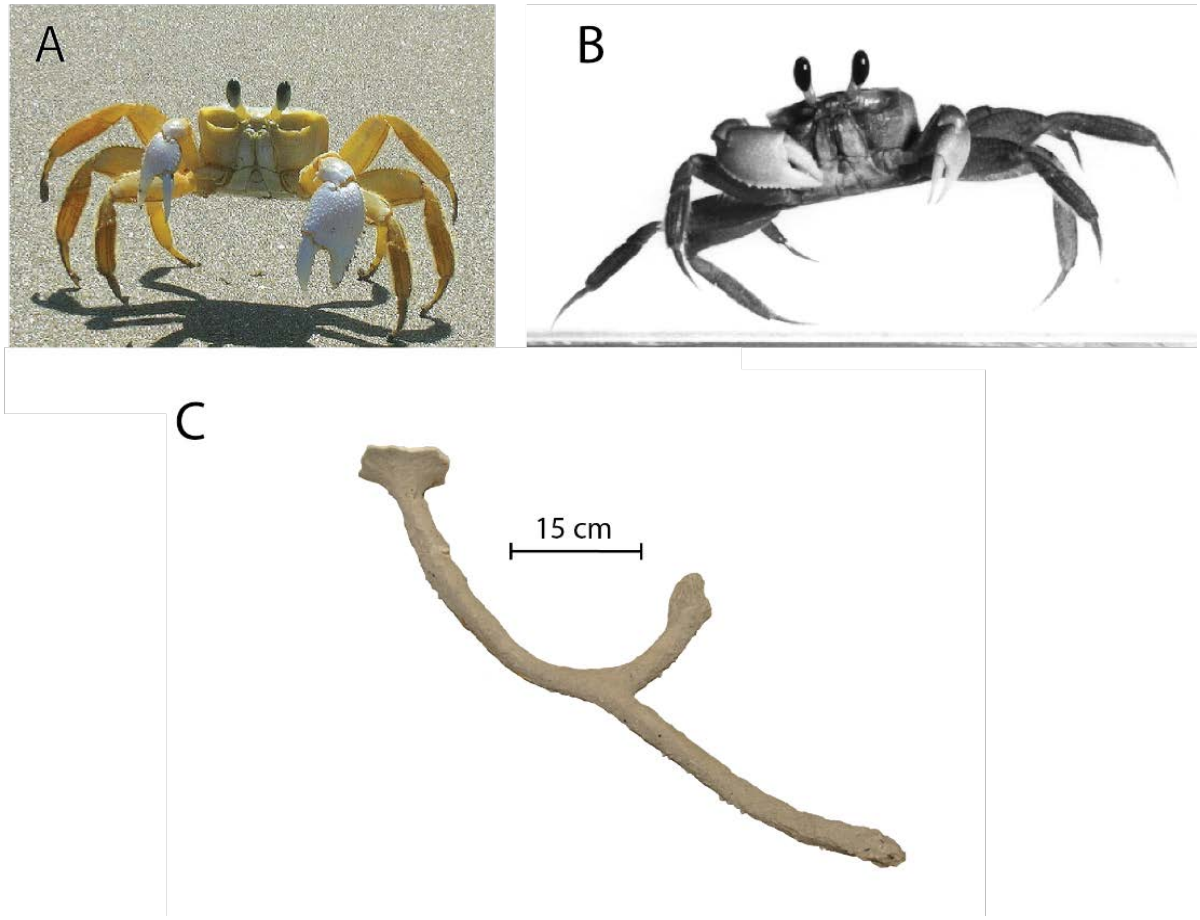

Figure 1.1: Introduction to the ghost crab (*Ocypode quadrata*). **A:** Photo of an adult ghost crab (CC BY 2.0; © Marina Campos Vinhal). Ghost crab leg span ranges from 5 – 15 cm and weigh from 15 – 70 g. Their habitat includes sandy beaches along the southeast coasts of North America. They are opportunistic scavengers, with a diet including carrion and small live animals, such as insects (Milne & Milne, 1946). **B:** Still from a high-speed video of ghost crab running. Ghost crabs are capable of running more than 2 m/s (Herreid & Full, 1988), making them one of the fastest land invertebrates. **C:** Cast of a typical ghost crab burrow. Burrows often have branching structures and may be more than 1 m long. These semi-permanent structures are constructed and maintained by a single ghost crab that uses the burrow for shelter from environmental stresses (Chan, et.al., 2006) and for protection from predators (Milne & Milne, 1946).

1.2 Summary

Chapter 2 describes novel x-ray imaging techniques used to identify the burrowing mechanisms of the ghost crab, *O. quadrata.* These studies revealed that ghost crab burrowing is a complex behavioral suite that involves the walking legs, the chelae and the body. The crabs demonstrated specialized postures, locomotion in confined spaces, and goal-directed manipulation of the substrate – all with the same appendages that allow them to run and manipulate prey.

Chapter 3 examines the mechanical energetics of ghost crab burrowing using a mathematical model based on current models of substrate mechanics and measured ghost crab morphometrics/kinematics. This model suggests that the instantaneous power requirements of excavation may be high but the overall power requirements of ghost crab burrowing are substantially lower due to prolonged periods of inactivity, allowing the crabs to recover from brief, high-intensity exertion. Burrow depth, substrate mechanics, burrowing kinematics and body size are predicted to substantially affect the energetics of burrowing.

Chapter 4 uses a combination of field and laboratory experiments to determine how ghost crab burrowing performance is related to the substrate's mechanical properties. Field studies revealed that the ghost crab habitat varies substantially with both location and with depth. Ghost crabs demonstrated the ability to construct comparable burrows in a wide range of conditions. The principal limiting condition on their ability to construct a burrow is moisture content. When the substrate's moisture content reaches saturation, it is no longer possible for the crabs to use the burrowing mechanisms discovered in Chapter 2. Laboratory studies revealed that the burrowing behaviors discovered in Chapter 2 are maintained in both vertical and horizontal burrowing and that ghost crabs can continue comparable burrowing performance across a wide range of substrate moisture contents. Together, these results suggest that ghost crab burrowing may be a robust behavior, allowing the crabs to burrow in a wide range of conditions using the same strategy.

Chapter 5 describes a novel climbing behavior in ghost crabs, termed hurdling, where the animals climbed over tall vertical walls up to 16 times their resting hip height. Three distinct hurdling strategies were observed, with each strategy being specific to a certain obstacle height range. The strategy used to climb the tallest obstacles is particularly interesting as it involves cooperative use of both the walking legs and the chelae. A follow-up study revealed that disabling the chelae removed the ability to climb tall obstacles. A quasi-static model of tall obstacle hurdling suggests that the chelae are required because they provide a mechanism for overcoming range-of-motion and torque limitations in the walking legs.

Chapter 2

Burrowing Behavior of the Ghost Crab

The general ability to burrow has been known in ghost crabs for some time (Milne & Milne, 1946). However, little is known about the specific mechanisms the crabs use to construct their burrows due to the inherent difficulty of observing behaviors in an opaque, subterranean environment. This chapter describes novel x-ray imaging techniques that enabled the first description of the entire suite of ghost crab burrowing behaviors. Overall, ghost crab burrowing represents a complex suite of goal-directed manipulation behaviors involving nearly all of a crab's appendages working together in a confined environment.

Summary

While ghost crabs appear specialized for rapid running, they can also construct semi-permanent burrows in sandy substrates. X-ray imaging combined with detailed body markers shows that ghost crabs employ their walking legs and chelae in a highly coordinated fashion to collect and transport material in the confined environment of their burrows. Specifically, the first three walking legs are used to remove material from the end of the burrow using a hook-and-pull motion that includes a combination of penetrating and shearing movements. The crabs supplement hook-and-pull burrowing with scratch digging, where the walking legs make repeated small-amplitude scratches that loosen material from the end of the burrow. Body rotations, where the crab spins about the principal axis of the burrow up to 270 degrees, occurred preparatory to or during other excavation behaviors. These rotations may stabilize the burrow walls through compaction and expand the crabs' workspace, permitting the crabs to change the direction of burrowing. Crabs transported the collected material using their walking legs and chelae. They demonstrated the ability to carry the collected material in a "basket", made from the first two walking legs and the chela on the down-burrow side. Additionally, the crabs were able to pass the collected material from one side of their body to the other inside the confines of the burrow. This is a highly coordinated movement that involves all walking legs, the chelae and the body. After passing the material across their bodies, crabs used their up-burrow walking legs to either push the material out of the burrow or compact the material, sealing the burrow. This is the first description of the complete burrowing cycle in ghost crabs and will likely inspire new designs for burrowing/running robots.

2.1 Introduction

Many animals across diverse taxa demonstrate the ability to burrow, either by moving within a substrate or by constructing a burrow (Dorgan, 2015). The mechanisms and strategies associated with burrowing vary enormously, depending on the animal's morphology and the material properties of the substrate (Ding et al., 2010; Dorgan et al., 2006). Some example strategies include localized rearrangement of the substrate, fluidization, mechanical boring (i.e. rasping) and excavation/transportation. The applicability and limitations of these general strategies are all different and are summarized in Table 2.1.

Localized rearrangement involves fracturing as observed in annelid worms (Dorgan et al., 2005) or compacting as observed in moles (Hildebrand, 1987) a small volume of the substrate, producing either temporary volume that the animal immediately moves into or a semi-permanent burrow. The annelid worm, *Nereis virens*, uses localized rearrangement (fracture) to move through marine muds (Dorgan et al., 2005). Similar mechanisms (using fracture and/or compaction) are widely used by many worms, bivalves and gastropods in muds and sands (Dorgan, 2015). Larger animals, such as the star-nose mole (*Condylura cristata*), also use compaction to produce larger burrows in loose soil (Hildebrand, 1987).

Fluidization relies on the non-Newtonian properties of granular substrates and allows the animal to move quickly within the material (Maladen, et al., 2009). The sandfish lizard, *Scincus scincus*, uses fluidization to move rapidly through dry sand (Maladen et al., 2009). Fluidization is also used in very wet sands by mole crabs (*Emerita;* Trueman, 1970).

Boring behaviors, where the animal produces a permanent cavity in a hard substrate, are common in invertebrates and may involve mechanical (Ansell & Nair, 1969) or chemical (Tresguerres, et al., 2013) means. The American piddock (*Petricolaria pholadiformis*), uses mechanical boring to produce permanent burrows in wood (Ansell & Nair, 1969). Other organisms, such as *Osedax* worms, may produce similar burrows using chemical, rather than mechanical, means (Tresguerres et al., 2013).

Excavation and transportation, which is employed by ghost crabs and many large vertebrates (Hildebrand, 1987) to produce relatively large semi-permanent structures, is particularly interesting since many of these burrowing animals must also perform other behaviors such as running and capturing prey. The ghost crab, *Ocypode quadrata*, produces semi-permanent burrows using excavation and substrate transportation. Excavation is also common among fossorial vertebrates such as rabbits, badgers, etc. (Hildebrand, 1987). Understanding what mechanisms enable an animal, such as the ghost crab, to run and burrow with the same set of appendages may offer new insight into the biomechanics of multifunctional appendage design.

Although burrowing behaviors are very common in crabs (Bellwood, 2002), little is known about the strategies ghost crabs use to produce their burrows. This is likely due to the inherent difficulty of visualizing the burrowing behaviors in the dense, opaque substrates in which the ghost crabs live. The burrowing mechanism of the mole crab (*Emerita*), a crustacean that inhabits the same sandy beaches as *O. quadrata*, has been examined in detail, finding that these animals use their thoracic legs (analogous to the ghost crab's walking legs) to rapidly burrow (Trueman, 1970). These strategies are unlikely to be employed by the ghost crabs, however, as mole crabs rely on specialized morphology and highly saturated substrates (Trueman, 1970). Burrowing behaviors have also been studied in other true crabs (e.g. Caine, 1974). Most of these crabs use their walking legs to burrow and a number of morphological adaptations to burrowing have been identified (Faulkes, 2012). The primary mechanical adaptations are short, broad burrowing appendages (Bellwood, 2002) similar to the adaptations generally observed in burrowing arthropods (Chapman, 1982) and vertebrates (Hildebrand, 1987). Ghost crabs, however, lack any obvious adaptations to a fossorial existence (Faulkes, 2012; Savazzi, 1985). Instead, ghost crabs have long, slender walking legs that are highly specialized for rapid running (Hafemann & Hubbard, 1969).

This chapter details behavioral experiments conducted to identify the principal mechanisms of ghost crab burrowing. The results of these studies offer insight into previously undescribed behaviors and provide necessary context for future work on ghost crab burrowing. Specifically, these experiments address the following questions:

1) What strategies do ghost crab use to remove material from the end of the burrow?
2) What strategies do ghost crabs use to transport collected material to the surface?
3) How much do burrow strategies vary between individuals?

Understanding how the ghost crabs can use their appendages, which are ostensibly unspecialized for burrowing, to manipulate and transport granular substrates may offer new insight into the biomechanics of excavation and animal multifunctionality.

Table 2.1

Mechanism of burrowing	Materials	Depth Limitation	Morphology and behavior
Localized fracture or rearrangement	Rearrangement: sand, mud Fracture: mud	Rearrangment: strong Fracture: weak	Wedge-shaped bodies Expansible elements
Fluidization	Sand, mud	Strong	Fast movement Fluid transport mechanisms
Chemical and mechanical boring	Rock, clay, wood, carbonate	Very weak	Hard ridges, scraping. Secretions (e.g. acid)
Excavation	Sand, mud	Weak	Appendages to collect and transport material

Table 2.1: Summary burrowing methods (derived from Dorgan, 2015). **Material** indicates the substrate in which this behavior is observed. Muds are elastic solids (Dorgan, 2015). Sands are granular materials, whose cohesion is related to moisture content (Mitari & Nori, 2006) and grain entanglement (Gravish, et al., 2012). Rock/clay/wood/carbonate are hard materials, which are non-cohesive once fractured. **Depth limitation** indicates how burrowing performance is related to burrow depth. Strong limitations indicate that performance declines sharply with depth, typically due to increased pressures. Strongly limited behaviors are typically confined to operation at or near the surface. The performance of weakly-limited may depend on depth (e.g. excavation costs increase with depth due to material transport costs), their operation is possible at a range of depths. **Morphology and behavior** briefly describes some of the common morphological and behavioral properties of the corresponding burrowing behavior.

2.2 Materials and Methods

Animals

Ghost crabs, *Ocypode quadrata*, were purchased from a commercial vendor (Gulf Specimen Marine Lab, Panacea, FL, USA), that captured wild ghost crabs from the Gulf Coast of Florida, USA. Crabs were stored individually in ventilated plastic containers, approximately 20 cm long, 15 cm wide and 15 cm tall. A small volume (approximately 25 ml) of fresh sea water substitute (Instant Ocean, Blacksburg, VA, USA) was placed into the container and changed every 1-2 days. The containers were stored at an approximately 10 degree incline, producing "wet" and "dry" sides, which the crabs were permitted to access freely. The crabs were provided with a diet of 1-3 live, medium-sized crickets (Petco, Atlanta, GA, USA) each day. Uneaten crickets were removed within 24 hours. The crabs were maintained at approximately 23 ^{o}C continuously. A window maintained a natural day:night cycle of approximately 13 hrs : 11 hrs. The behavioral data presented here came from 5 individuals (carapace width: 29 - 35 mm; mass: 21 - 25 g). Only complete, healthy crabs were used for behavioral trials. Any crab that was missing an appendage or that exhibited lethargic behavior was removed from the experimental cohort.

Artificial Beach Environment

An artificial beach environment was used for all behavioral experiments (Figure 2.1). This environment was constructed from 2.1 mm-thick optically-clear acrylic panels (McMaster-Carr, Elmhurst, IL, USA) and aluminum struts (MicroRAX, Auburn, WA, USA). The enclosure was 50 cm tall, 7.5 cm deep and 16 cm wide. The enclosure was filled to a depth of approximately 30 cm with clean damp sand (14% gravimetric moisture content). The sand was obtained from Jekyll Island, GA, USA, which is a known ghost crab habitat. To remove any voids and create a uniform burrowing substrate, the sand was tamped down by repeatedly tapping the enclosure on a table prior to inserting the crab. All ghost crabs used in these studies demonstrated the ability to move freely on top of the sand inside the artificial beach environment. In particular, crabs were able to move laterally and rotate, allowing them to initiate burrowing in any location on the top of the substrate.

X-ray Markers

Ghost crabs were found to be nearly transparent to x-rays. Thus, each crab studied here was equipped with a set of x-ray opaque markers, made from 1 mm-thick lead foil (McMaster-Carr, Elmhurst, IL, USA). Two types of markers were constructed: strips (1 mm-wide, cut to length) and dots (between 1 and 4 mm^2).

A candidate ghost crab was first placed into a cold chamber (approximately 5 ^{o}C) for a few minutes until quiescent. The crab was removed from the chamber and restrained with elastic

bands. Strips and dots were attached to the crab's body and appendages use cyanoacrylate adhesive (Loctite 1365882; Henkel Corp, Westlake, OH, USA). Strips were attached to each major segment of all walking legs (dactyls, propodus, carpus and merus) and to the dactyl and pollex of both cheale. Dots were attached to the carapace and to the merus of each walking leg. One dot was place on the dorsal surface of the carapace on the same side as the minor chela. Two dots were place on the dorsal surface of the carapace on the same side as the major chela. Each merus of each walking leg was equipped with a number of small dots equal to number of that walking leg (i.e. one dot for the first walking leg, two dots for the second walking leg and so on). This marking scheme is illustrated in Figure 2.2.

Ghost crabs were allowed at least six hours to recover from the marking procedure. Any crabs that exhibited lethargic behavior, appendage loss or damage were disqualified from behavioral experiments.

Figure 2.1

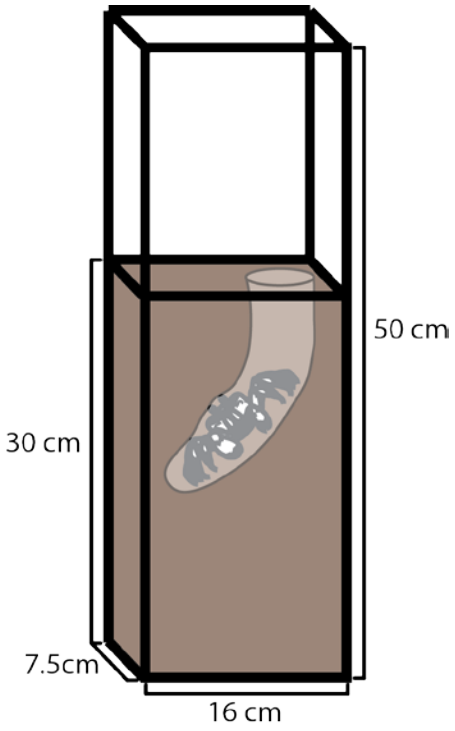

Figure 2.1: Figure illustrating the construction of the artificial beach environment. The crab was placed on top of a volume of damp sand (14% water by mass). The enclosure was constructed from aluminum framing, with clear acrylic panels.

X-ray Imaging

The artificial beach environment was placed into a customized fluoroscope (Complex Rheology and Biomechanics Lab; Georgia Technical University, Atlanta, GA, USA), as detailed in Figure 2.3. A ghost crab, equipped with x-ray markers, was placed inside the artificial beach environment and allowed to begin burrowing in a self-directed fashion. Due to imaging constraints, the room dedicated to x-ray imaging was kept completely dark while the crab was burrowing. The x-ray video was captured by a camera (Phantom v9.1, Vision Research, Wayne, NJ, USA). The ghost crab's behavior was continuously remotely monitored. If a crab did not begin burrowing within approximately 30 minutes, the trial was discontinued. Once a crab began burrowing, videos approximately four minutes in length were captured every eight minutes. The trial ceased once the crabs either burrowed below the visible region (approximately 20 cm depth) or when the crabs ceased burrowing for at least 30 minutes.

Figures 2.2 and 2.4 show part of a video still, detailing the recorded data. All markers, the undisturbed substrate and the crab's burrow were all clearly visible. Videos were analyzed with FIJI (http://fiji.sc) and Cine Viewer (Vision Research, Wayne, NJ, USA).

Figure 2.2

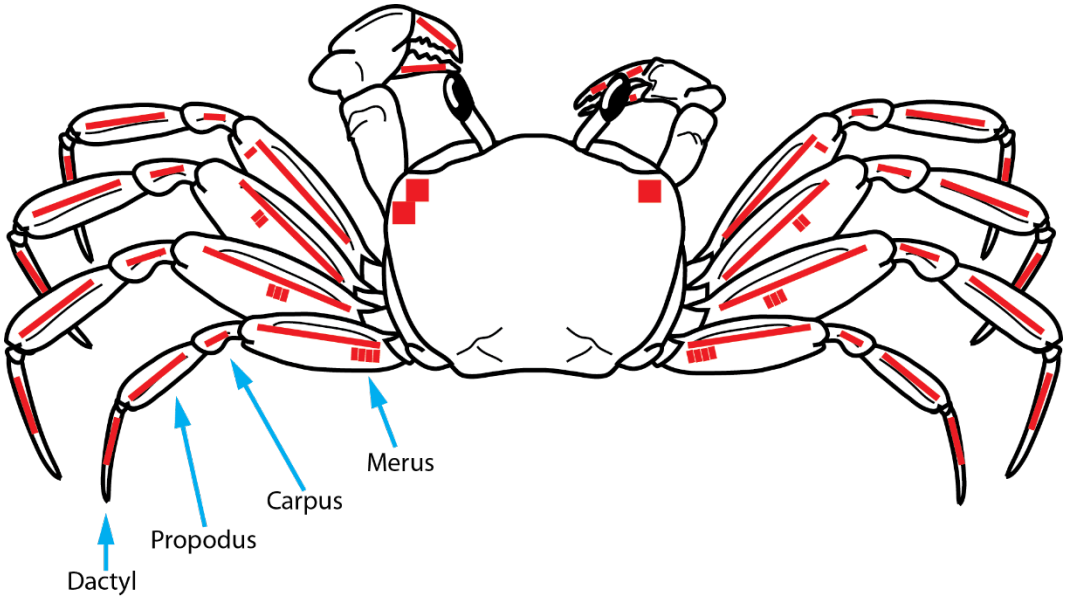

Figure 2.2: X-ray markers placed on subject crabs. To improve x-ray image contrast and assist with identifying appendage function, crabs were equipped with small lead markers, illustrated in red. Markers were attached with cyanoacrylate glue. Thin (1 mm width, 1 mm thick) strips of lead were attached to the dactyls, propodus, carpus and merus of all walking legs. These strips facilitate visualization of the function/motion of the walking legs' components during burrowing. Similar strips were also attached to the dactyl and pollex of both chelae. These markers permit identification of the position/motion of both chelae, as well as whether the crab opens/closes its pincers. Supplemental markers, made from the same 1 mm-thick lead sheet, were attached to each merus and to the left and right side of the crab's carapace. The merus markers identified the first, second, third and fourth walking legs using one, two, three and four tags respectively. These markers assisted with identifying the function/motion of the walking legs. The carapace markers distinguished the major and minor sides of the crab (two markers for the major side and one for the minor side), facilitating an understanding of the crab's body position.

Figure 2.3

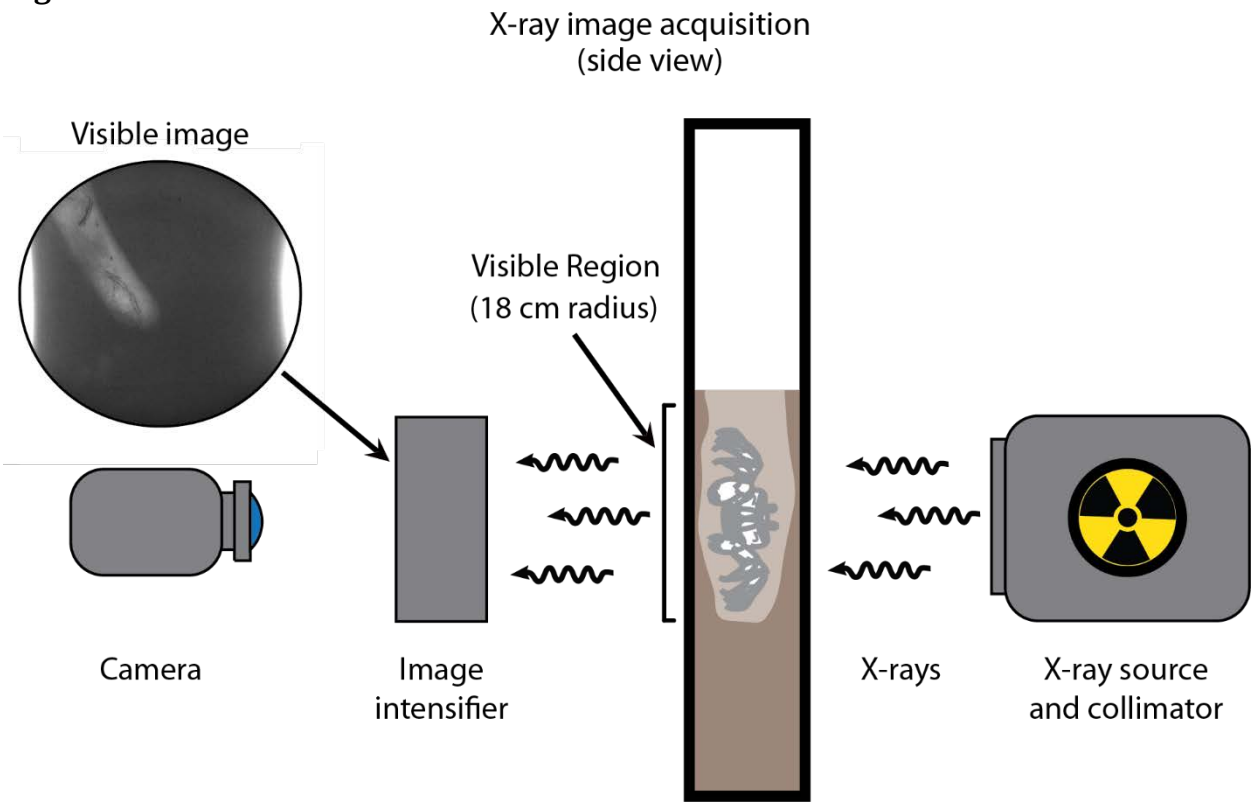

Figure 2.3: Diagram illustrating the function of the x-ray imaging system and the corresponding visible area. The x-ray source produced x-rays which pass though the enclosure. The Image intensifier converts the converted the x-rays into a visible image (video still shown), that was recorded by the camera. This configuration permitted a circular visible area, approximately 18 cm in diameter.

Figure 2.4

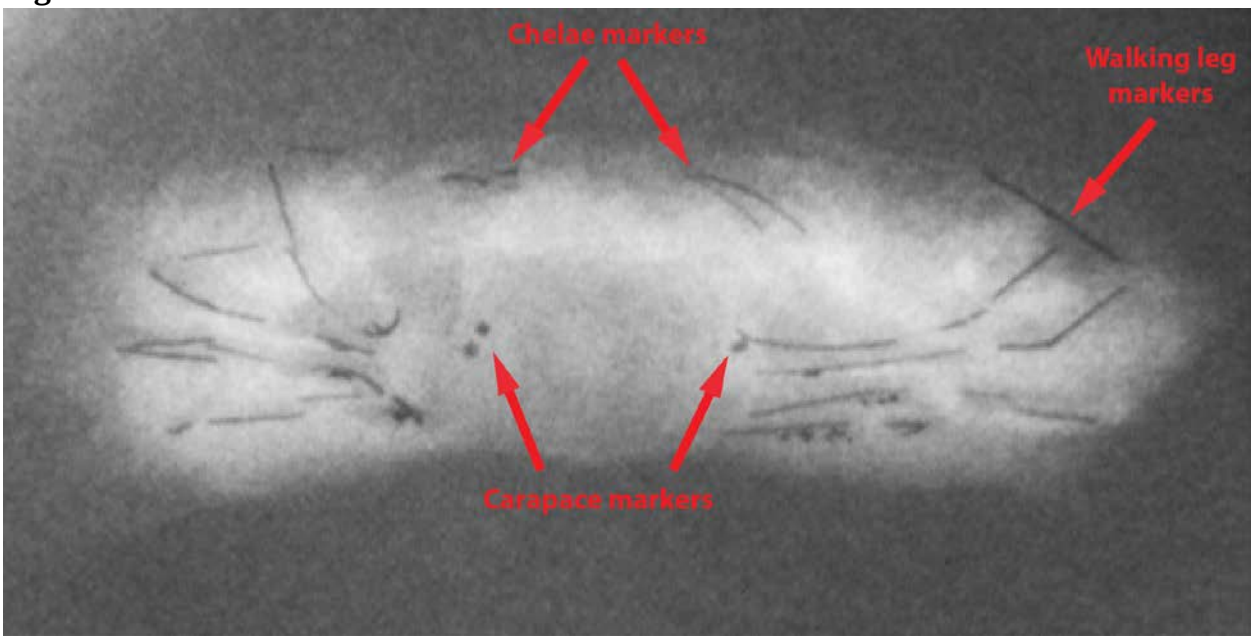

Figure 2.4: Still image from x-ray video showing a burrowing ghost crab. The carapace, chelae and walking leg markers are indicated (see Figure 2.2). The dark surrounding area was packed sand. The light-colored area surrounding the crab is the burrow.

2.3 Results and Discussion

A total of 3.5 hours of footage was recorded from 5 individuals. The subjects burrowed a total distance of 8 m, with each subject performing multiple trials (14 total trials, approximately 3 per individual). A total of 268 excavation cycles were observed and recorded.

An excavation cycle, diagramed in Figure 2.5, represents the basic high-level burrowing pattern observed in ghost crabs. Crabs move to the end of the burrow, collect material from the end of the burrow and then transport that material to the top of the burrow. For all results presented here, a cycle is defined as starting as soon as the crab begins collecting material from the end of the burrow. The excavation cycle ends when the crab begins collecting material again, after transporting the collected material and returning to the end of the burrow. Excavation cycle duration was approximately 1 minute. Each excavation cycle extended the burrow approximately 1 - 5 mm.

The excavation cycle can be subdivided into three broad categories: inactivity, excavation mechanisms and manipulation. These behaviors and their occurrence within the excavation cycle are illustrated in Figure 2.6.

Inactivity is any period of time in which the crab remained stationary. These durations may last anywhere from seconds to minutes and occurred at any time in the excavation cycle. These periods of inactivity may have substantial effects on the energetics of burrowing as discussed in Chapter 3.

Excavation mechanisms are any behaviors occurring while the crab removes material from the end of the burrow. Three major behaviors were observed: hook-and-pull, scratch digging and body rotation. The crabs were observed to alternate between these or employ them in parallel. For example, a crab may alternate between hook-and-pull and scratch digging or execute a hook-and-pull while simultaneously performing a body rotation.

Manipulation includes those behaviors crabs use to transport and manipulate collected material. These behaviors were always observed following excavation mechanisms. That is, crabs were not observed to resume excavating until after they finished transporting the collected material. Manipulation can be broken down into three principal behaviors that occur in series: carrying, cross-body transfer and pushing/packing.

Although the crabs used their chelae in various ways during different parts of the excavation cycle, crabs were never observed pinching the material or collecting material with their chelae.

Figure 2.5

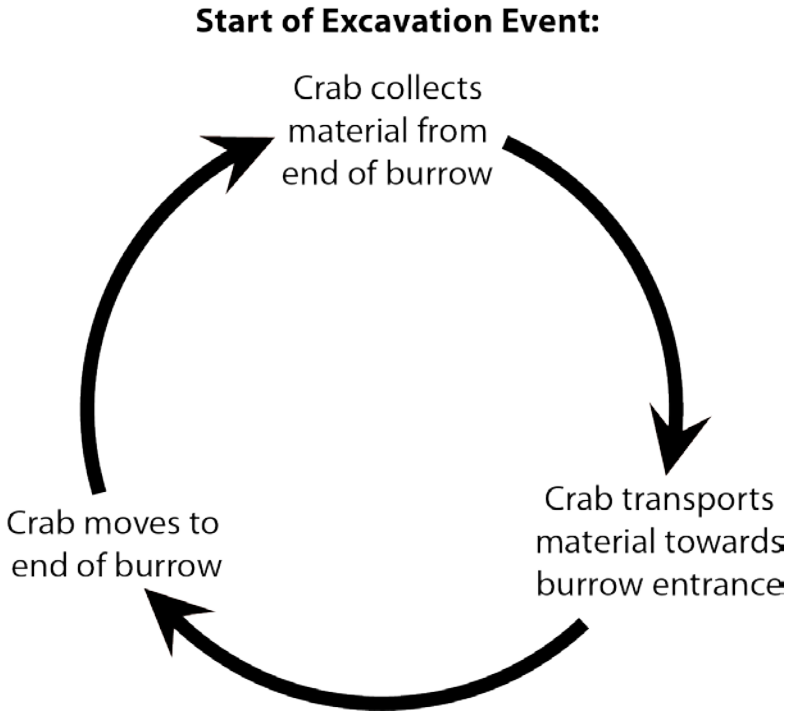

Figure 2.5 Diagram illustrating the definition of an excavation event. An excavation event began when the crab started collecting material from the end of the burrow. When the crab collected sufficient material, the crab transported that material and then returned to the end of the burrow. The excavation cycle ended (and a new one began) when the crab started to collect material again.

Figure 2.6

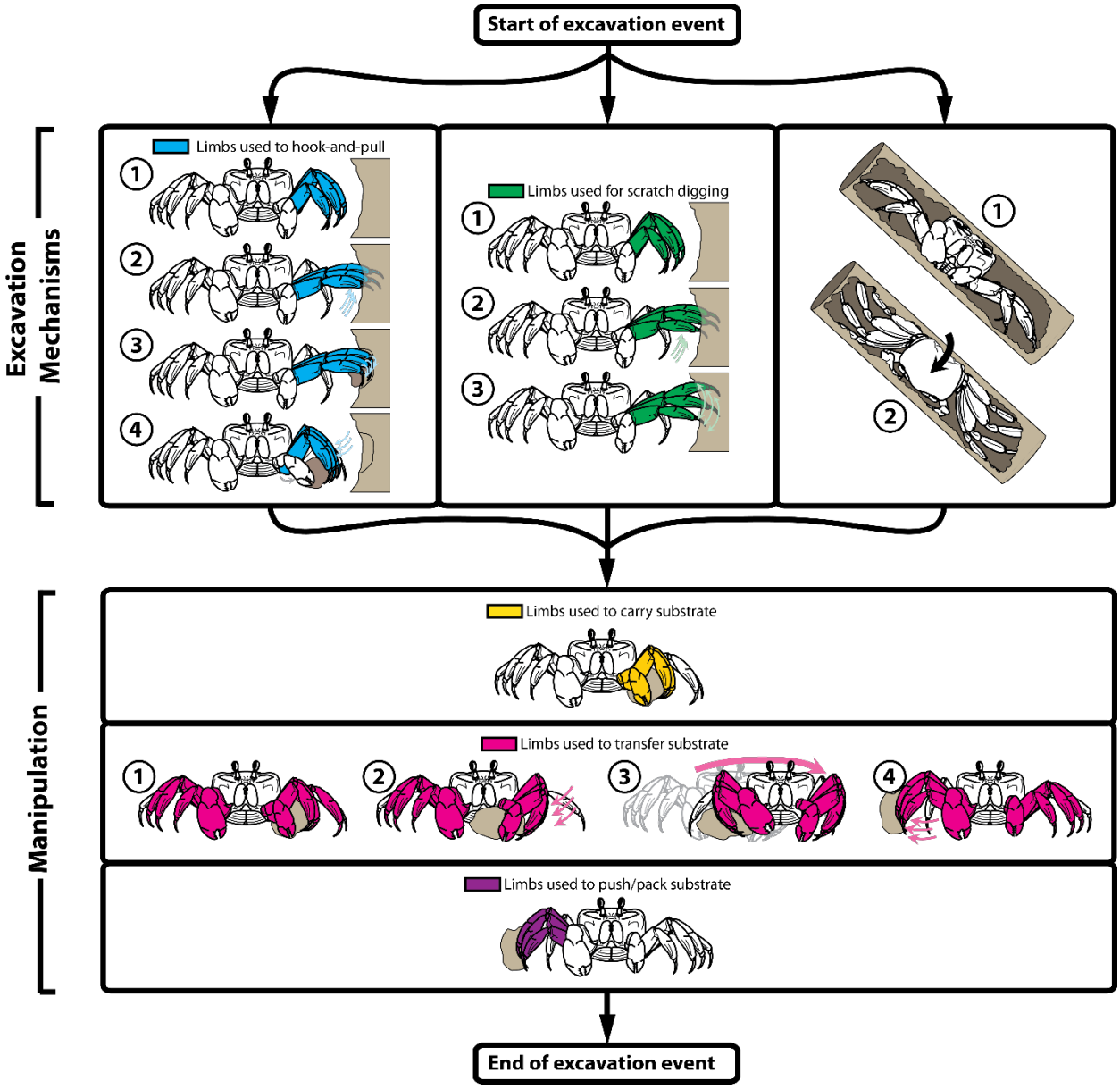
Start of excavation event
Excavation Mechanisms
Limbs used to hook-and-pull
Limbs used for scratch digging
Manipulation
Limbs used to carry substrate
Limbs used to transfer substrate
Limbs used to push/pack substrate
End of excavation event

Figure 2.6: Figure summarizing the behaviors used in ghost crab burrowing and their occurrence during an excavation cycle. Periods of inactivity, where the crab remained completely stationary, were not illustrated as they may occur at any point during the excavation cycle. After approaching the end of the burrow, crabs performed hook-and-pulls, scratch digging and body rotations. The crab may alternate or combine these behaviors (e.g. performing a hook and pull while also performing a body rotation). Every observed excavation cycle included at least 3 hook and pulls. Typically, the crab will also perform scratch digging and/or body rotations to varying degrees. However, some observed excavation cycles included neither of these behaviors. After the crab has collected a volume of material, the crab transitioned to manipulation behaviors. The crab began by carrying the material and may perform only this manipulation behavior for the remainder of the excavation cycle. Crabs carrying sand may instead perform a cross-body transfer and then push or pack sand. If the crab chooses to seal the burrow, then transfers and pushing/packing was required.

Hook-and-Pull

Hook-and-pull excavation was the principal mechanism used by the ghost crabs to remove material from the end of the burrow. This behavior is diagramed in Figure 2.7.

Generally, a crab began by inserting the dactyls of the first three down-burrow walking legs into the substrate up to the dactyl/propodus joint. The crab then contracted the walking legs, starting with the dactyls. This sheared material away from the end of the burrow and drew the loosened material towards the crab's body. This behavior generally resembles the hook-and-pull behavior observed in some mammals (e.g. Anteater; Hildebrand, 1987). The crab repeated this behavior approximately 3 to 7 times in a single excavation cycle, amassing a larger volume of collected material with each hook-and-pull. The duration of a single hook-and-pull was approximately 1 to 2 s.

Figure 2.7

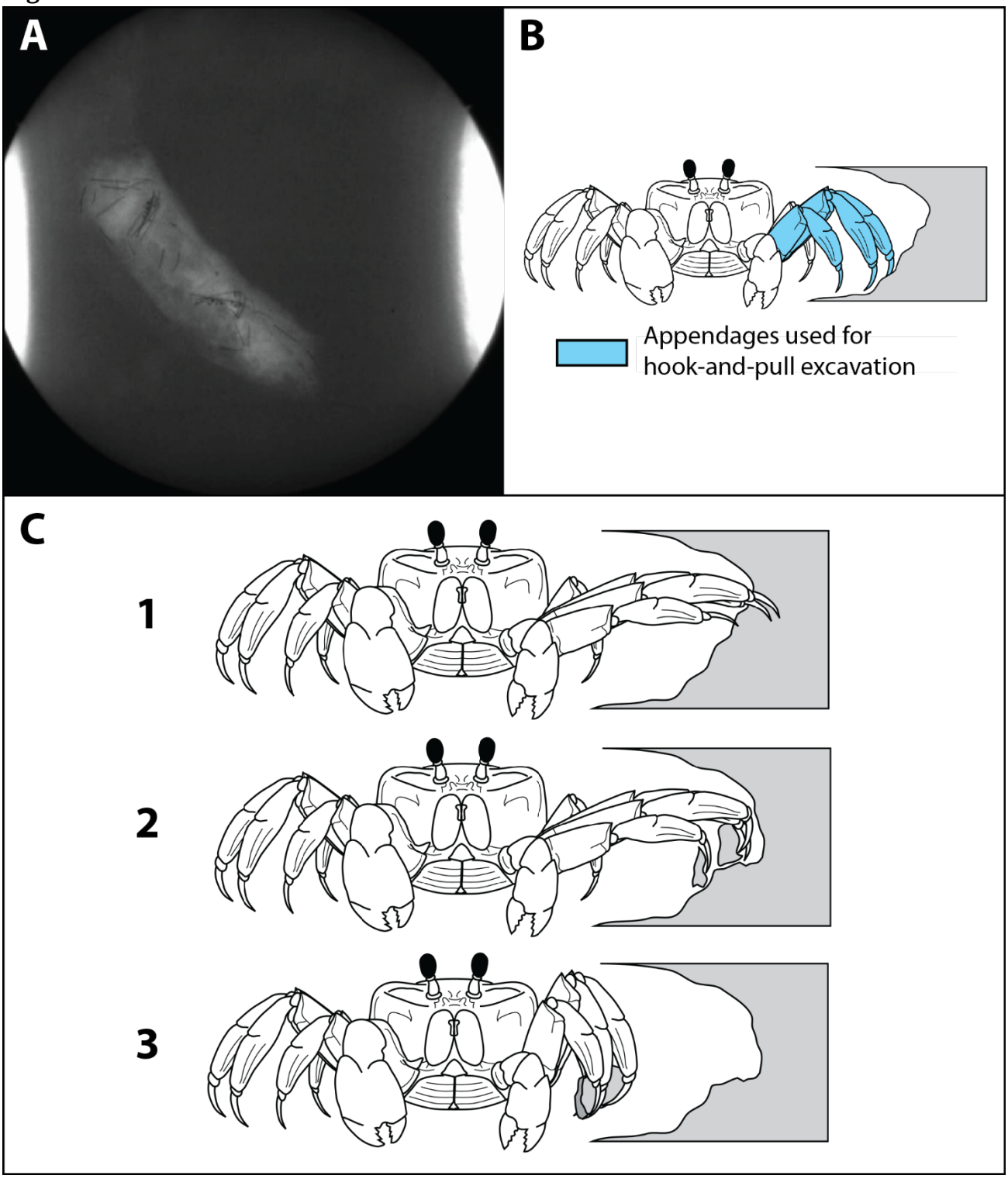

Figure 2.7: Description of the "hook-and-pull" excavation behavior. **A**: A still image from and x-ray video, showing the crab performing hook-and-pull. The crab's down-burrow walking legs are extended into the material at the end of the burrow. **B:** Illustration showing which appendages are used to hook-and-pull. Only the first three walking legs on the down-burrow side (highlighted in blue) are used for this behavior. **C:** The sequence in which the crab moves its legs during a hook and pull. First (1), the crab extends the dactyls of the walking legs into the end of the burrow. Second (2), the crab sharply contracts the dactyls, loosening material from the end of the burrow. Third (3), the crab contracts its legs, drawing loosened material from the end of the burrow towards its body.

Scratch Digging

Scratch digging was a secondary excavation behavior that generally occurred preparatory to a hook-and-pull. This behavior is diagramed in Figure 2.8.

During scratch digging, a crab repeatedly applied small-amplitude scratches to the end of the burrow with the dactyls of the first three down-burrow walking legs for a duration of 1 to 3 s. Superficially, this behavior resembled the scratch digging behaviors observed in many small mammals, where repeated shallow scratching loosens material (Hildebrand, 1987). In ghost crabs, however, this behavior does not appear to remove material from the end of the burrow. Instead, scratch digging loosened the substrate at the end of burrow. Since packing density has been correlated with drag forces in granular materials (Gravish, et al., 2010), scratch digging may be a mechanism for reducing the forces required for hook-and-pull excavation.

Figure 2.8

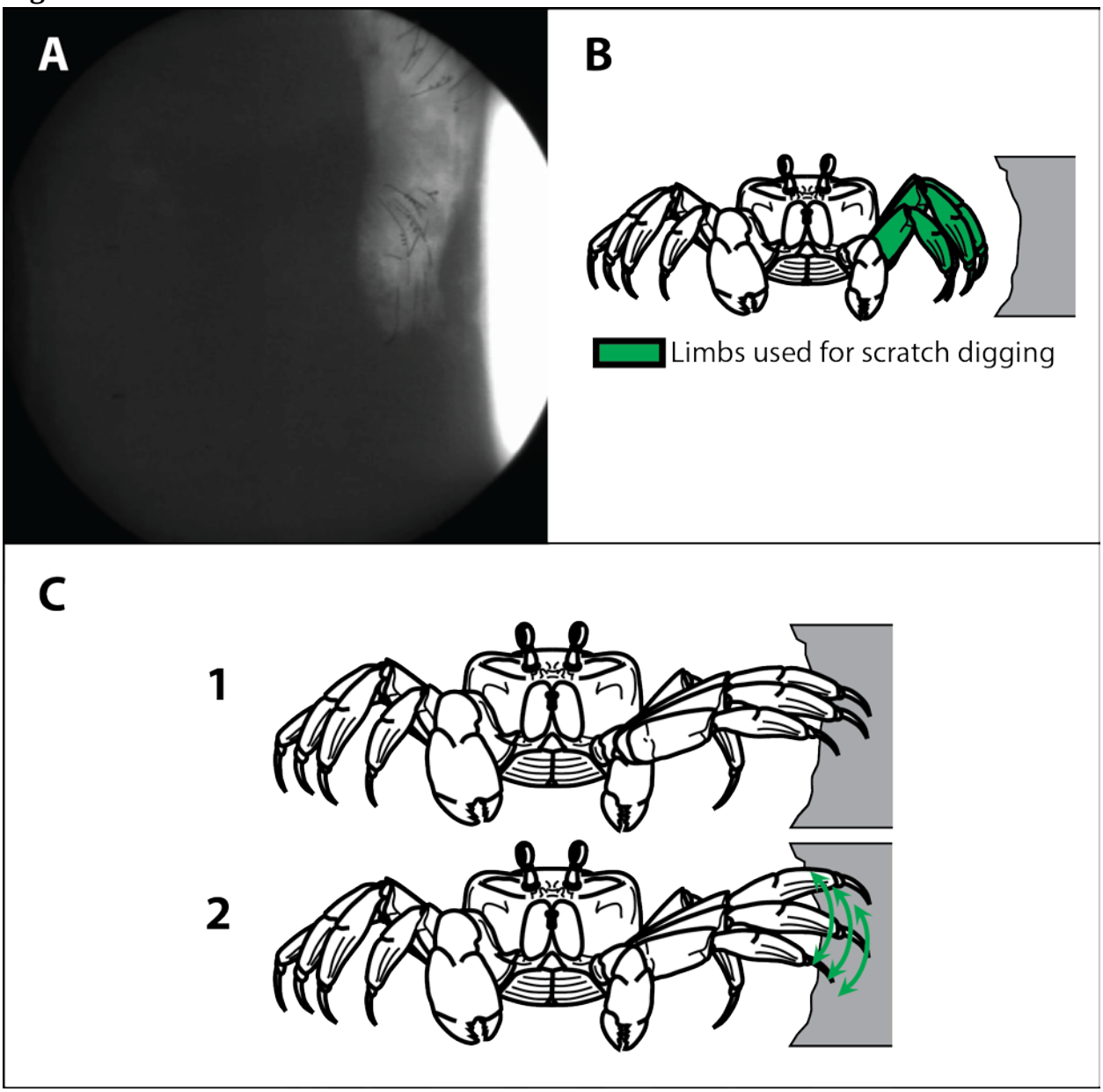

Figure 2.8: Description of the "scratch digging" burrowing behavior. **A:** A still image from an x-ray video, showing the crab performing scratch digging. The crab's down-burrow legs are currently extended into the material at the end of the burrow. **B:** Illustration showing which appendages are used to scratch dig. Only the first three walking legs on the down-burrow side (highlighted in green) are used for this behavior. **C:** The sequence in which the crab moves its legs during scratch digging. First (1), the crab inserts the dactyls of the first three down-burrow walking legs into the end of the burrow. Second (2), the crab loosens material using repeated small amplitude scratches.

Body Rotation

Body rotation was a secondary excavation behavior. Body rotations may be performed preparatory to or simultaneously with other excavation behaviors. This behavior is diagramed in Figure 2.9.

A crab engaged in body rotation spins about the principal axis of the burrow. The crab began by planting the rear of the carapace and the chelae into the walls of the burrow. Then, the crab rotated within the burrow, using the chelae and all walking legs to “walk” along the walls of the burrow. Body rotations were observed in all crabs and burrowing trials, regardless of the crabs’ angle with respect to gravity. The total angular displacement of a body rotation varied, but rotations of 180 to 270 were commonly observed. This behavior may serve two purposes in ghost crab burrowing: expanding the workspace and stabilizing the burrow.

Due to the crabs’ morphology and range of motion, they are unable to perform hook-and-pull behaviors above the transverse plane of the carapace. If the crabs maintained a single orientation within the burrow, they would be unable to remove material above their bodies, potentially limiting their ability to control the direction of burrowing, their ability to burrow around obstacles, and their ability to produce the branching structures frequently observed in the natural burrows. By rotating their bodies within the burrow, the crabs avoided these limitations by expanding their workspace, permitting access to the entire surface of the burrow.

Body rotations may also stabilize the burrow structure through localized compaction of the burrow walls. Pressing the relatively large, smooth surfaces of the carapace and dorsal faces of the chelae may re-compact material loosened by excavation behaviors and increase the stability of the burrow walls (Jaeger & Nagel, 1992). While the crabs were not observed to use localized compaction to actually extend their burrows, the mechanics and utility of this behavior may be similar to the burrowing strategies observed in moles, which use their large forelimbs to compact their burrowing substrates, producing semi-permanent burrows (Hildebrand, 1987).

Figure 2.9

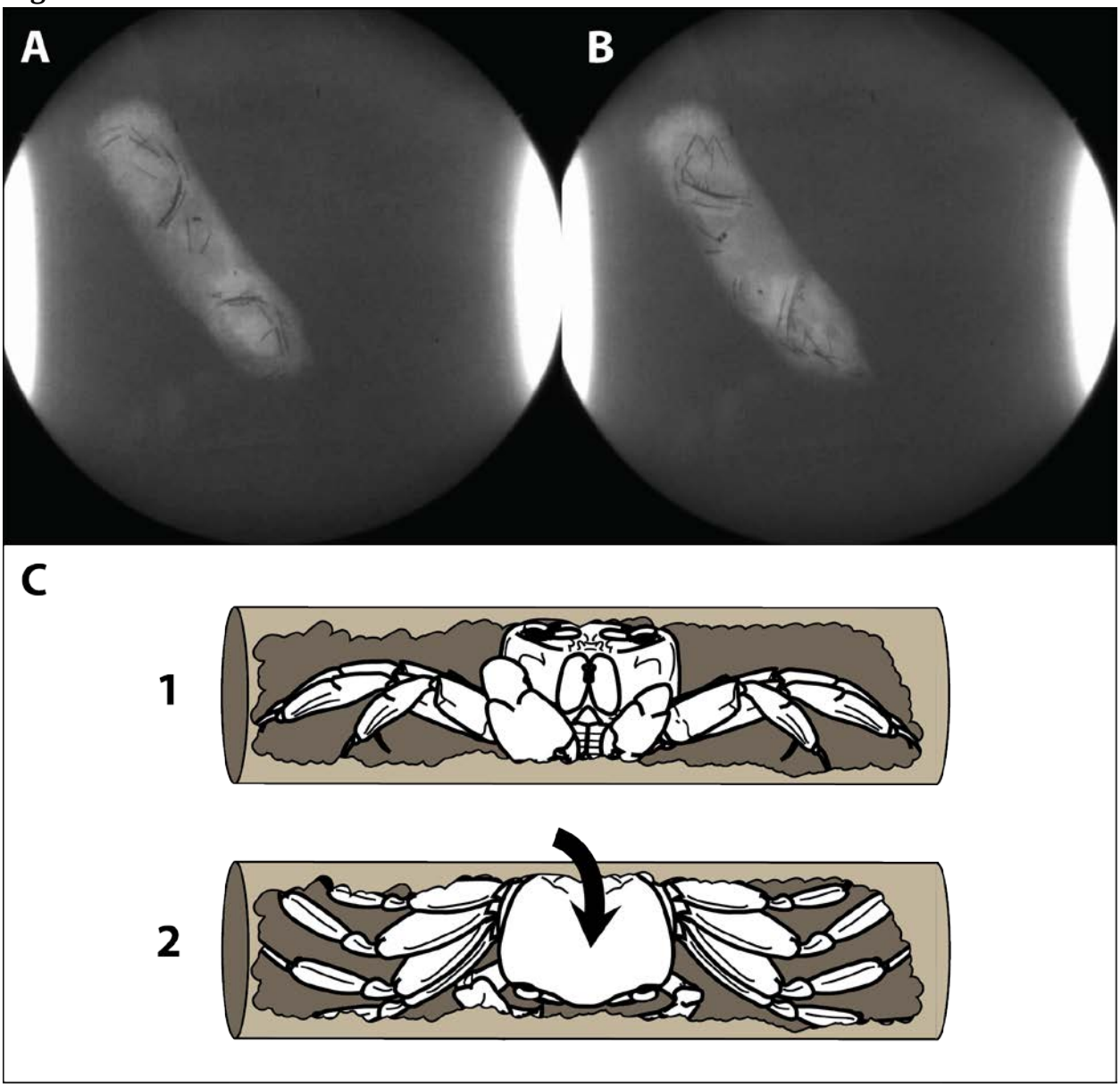

Figure 2.9: Description of the "body rotation" behavior. **A:** A still image from an x-ray video, showing the crab prior to performing a body rotation. **B:** A still image from an x-ray video, show the crab after performing a body rotation. The crab has performed an approximately 180-degree rotation. **C:** The crab begins a body rotation by pressing its chelae and the rear of its carapace into opposite sides of the burrow (1). Then, the crab uses its chelae, carapace and walking legs together to rotate inside the burrow. Rotations up to 270 degrees were observed.

Carrying

Carrying was the first manipulation/transportation behavior. Although this behavior frequently preceded passing and pushing behaviors, crabs demonstrated the ability to remove a volume of collected material exclusively with the carrying behavior. The carrying behavior is summarized in Figure 2.10.

Carrying was performed with the first two walking legs and the chela on a crab's down-burrow side. These appendages formed a "basket" that retained the collected material while the crab used its other appendages to walk or climb inside the burrow. While every excavation cycle included the carrying behavior to some degree, it can be the sole means of material transport when the burrow is open. If the crab has sealed the burrow, then carrying must be supplemented with a cross-body transfer and pushing behaviors.

Cross-Body Transfer

The cross-body transfer was a highly coordinated behavior where a crab moved a volume of collected material from the down-burrow side to the up-burrow side. This behavior, which occurred entirely within the confines of the burrow, is summarized in Figure 2.11.

Cross-body transfers began from the posture described in the carrying behavior, where the crab has gathered a volume of collected material into a space created by the first two walking legs and the chela on the down-burrow side. The crab then used its down-burrow walking legs and chela to push the collected material so it was directly underneath the crab's carapace. Then, the crab shifted its carapace towards the down-burrow side while simultaneously drawing the up-burrow walking legs and chela to the down-burrow side of the collected material. Finally, the crab used the up-burrow walking legs and chela to push the material up the burrow into the pushing behavioral posture. Thus, this behavior represents a bridge from the carrying to pushing behavioral modes. The total duration of a cross-body transfer is typically 2 to 4 seconds.

Figure 2.10

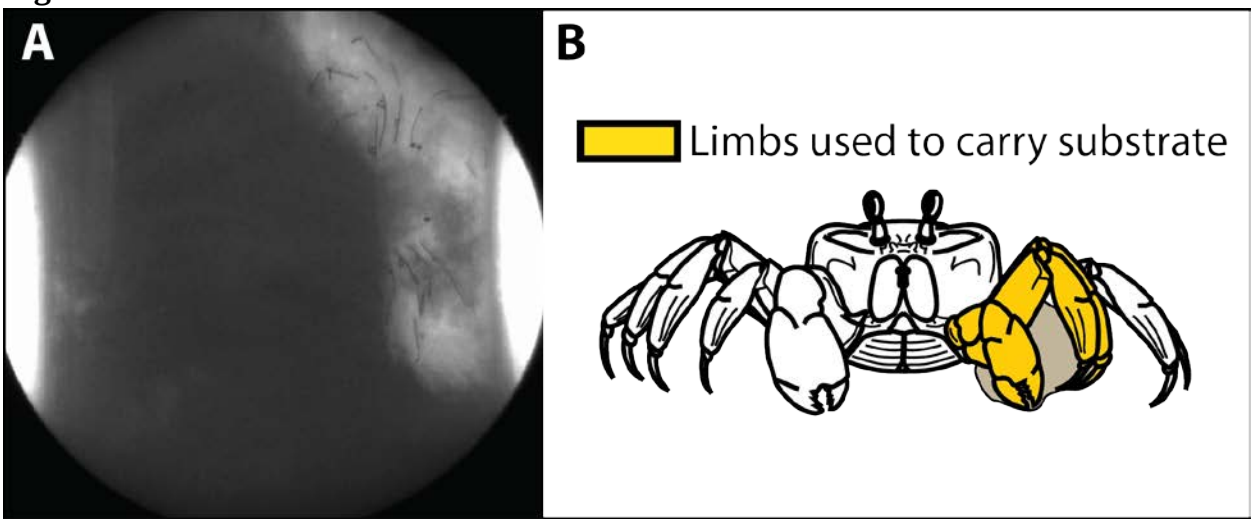

Figure 2.10: Description of the "carrying" behavior. **A:** A still image from an x-ray video, showing the crab carrying sand. A volume of sand is being carried up a vertical section of burrow. **B:** The appendages used to carry sand (highlighted in yellow). Crabs used the first two walking legs and the chela on the down-burrow side to transport volumes of collected material (highlighted in brown). The remaining appendages are used for locomotion.

Figure 2.11

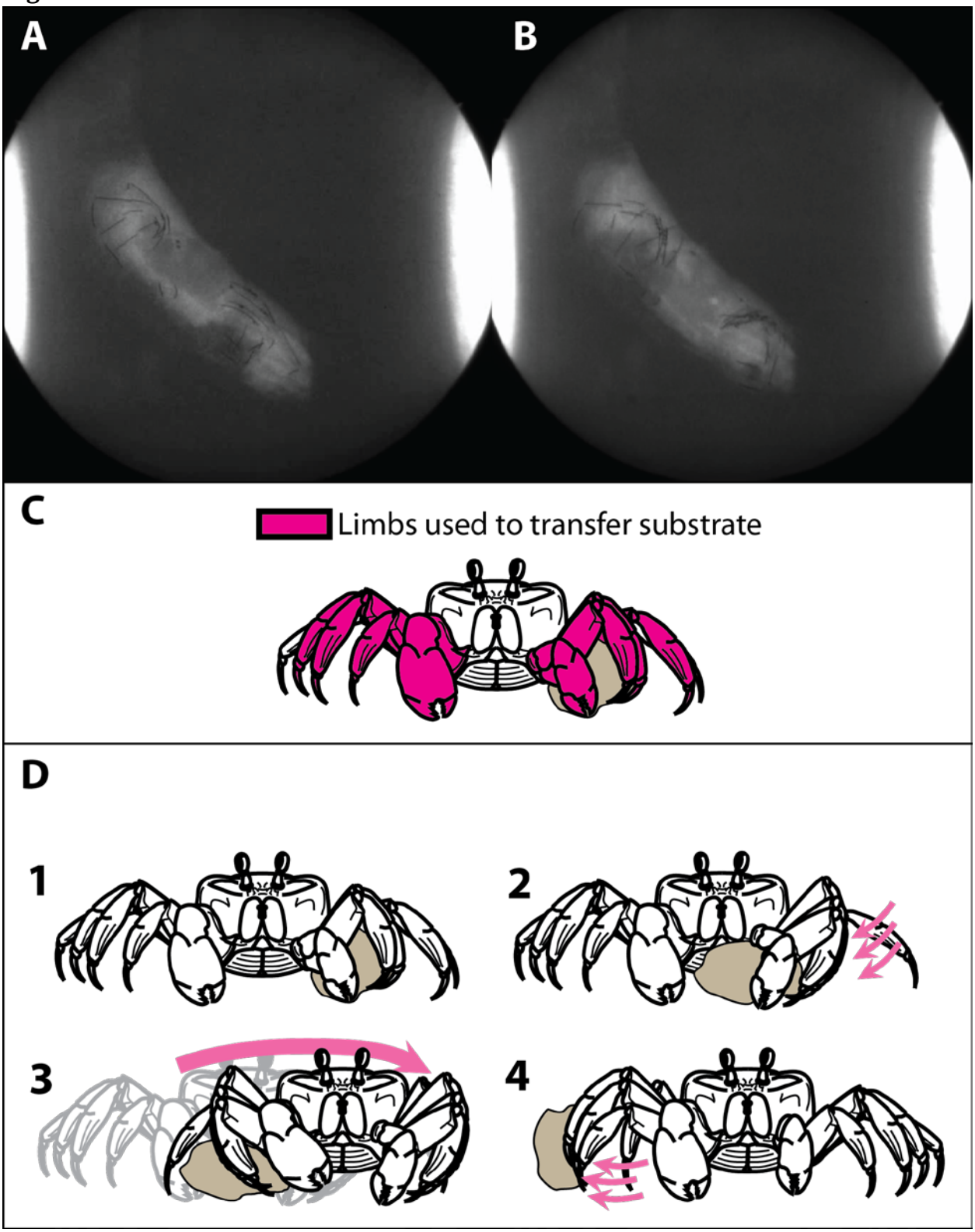

Figure 2.11: Description of the "cross-body transfer" behavior. **A:** A still image from an x-ray video, showing the crab prior to transferring sand from one side to the other. The crab collected a volume of sand approximately equal to the volume of its carapace. This volume is being retained by the crab's first two walking legs and the chela on the down-burrow side. **B:** A still image from an x-ray video, showing the crab after transferring the sand. Note that the volume is now on the crab's up-burrow side. **C:** Illustration showing which appendages (highlighted in magenta) are used to transfer material. Crabs use all of their appendages except for the fourth walking legs. **D:** The sequence in which a crab moves to transfer material across its body. The crab begins (1) with a volume of sand, held in the first two walking legs and chela on the down-burrow side. Then (2), the crab uses the down-burrow walking legs and chela to draw the material towards it body. Third (3), the crab shifts its body down-burrow and positions its up-burrow walking legs and chela behind the material. Finally (4), the crab pushes the material towards the burrow entrance using its up-burrow chela and walking legs.

Pushing and Packing

Pushing and packing represent a second mechanism for removing material from the burrow as well as a means of sealing the burrow. This behavior is summarized in Figure 2.12.

Once a crab has achieved the pushing behavioral posture, where the first three up-burrow walking legs were entirely behind the collected material, the crab can push the volume of material inside the burrow. The crab used its other appendages to walk or climb inside the burrow. If the burrow was open, then the crab pushed the material all the way to the burrow entrance, removing the material from the burrow entirely. However, if the burrow was sealed, then the crab compacted the collected material into the upper end of the burrow using the dorsal surfaces of the first three up-burrow walking legs.

Figure 2.12

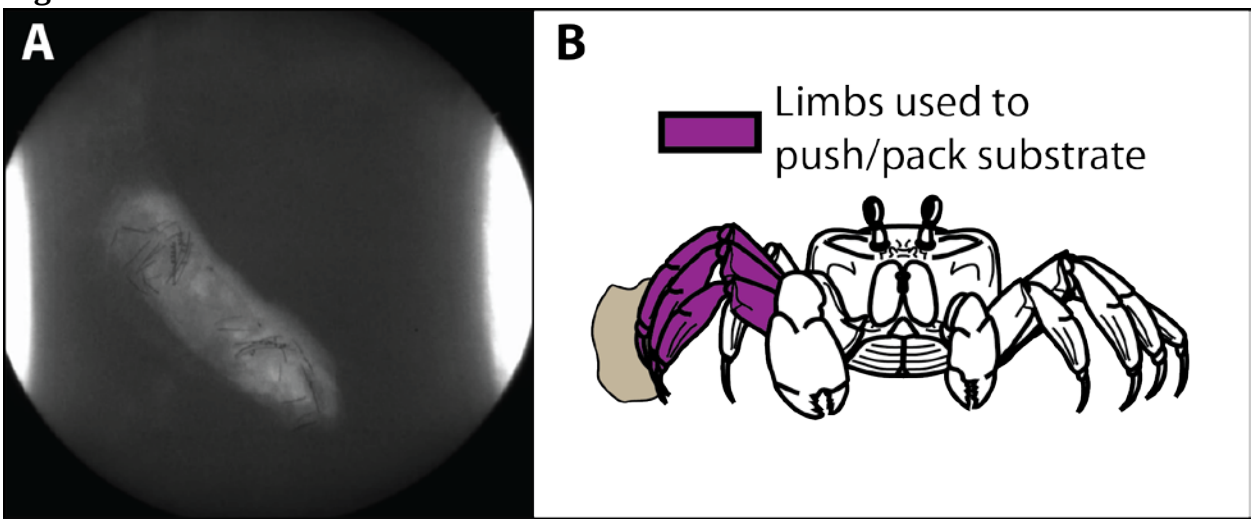

Figure 2.12: Description of the "pushing/packing" behavior. **A:** A still image from an x-ray video, showing the crab pushing sand. A volume of sand, approximately equal to the volume of the crab's carapace, is being pushed towards the upper end of the sealed burrow (the crab is extending the burrow rightwards). The crab has already sealed the burrow by packing material during previous excavation cycles. **B:** The appendages used to push and pack sand (highlighted in purple). Crabs use the first three walking legs on the up-burrow side to push and pack material.

Behavioral Variation

Overall, little variation between or within individuals was observed in the behaviors documented here. All subjects demonstrated all of the behaviors in the same overall pattern described in Figure 2.6. In 12 of 14 trials, ghost crabs chose to burrow with the minor chela facing down-burrow. However, no substantial behavioral differences were observed in the two trials where the crabs chose to burrow with their major chela facing down-burrow. To further quantify variation in burrowing performance, the following metrics were compared:

1) Excavation event duration, the total time from the start to the end of one excavation cycle (Figure 2.13).
2) Hook-and-pull duration, the duration of a single hook-and-pull event (Figure 2.14)
3) The number of hook-and-pull events occurring in a single excavation cycle (Figure 2.15).

Analysis was focused on the hook-and-pull behavior because it is the primary mechanism used to extend the burrow.

No statistically significant differences were observed between individuals in excavation event duration (ANOVA: $F(4,15) = 1.91$, $p = 0.16$), hook-and-pull duration (ANOVA: $F(4, 116) = 2.11$, $p = 0.8$) or the number of hook-and-pulls in a single excavation cycle (ANOVA: $F(4,74) = 1.58$, $p = 0.19$). This suggests that ghost crab burrowing may be somewhat stereotyped. However, the studies here represent only a single combination of substrate conditions and body size. It is entirely possible that body size and substrate properties will significantly alter ghost crab burrowing behavior (Che & Dorgan, 2010; Dorgan et al., 2006).

Figure 2.13

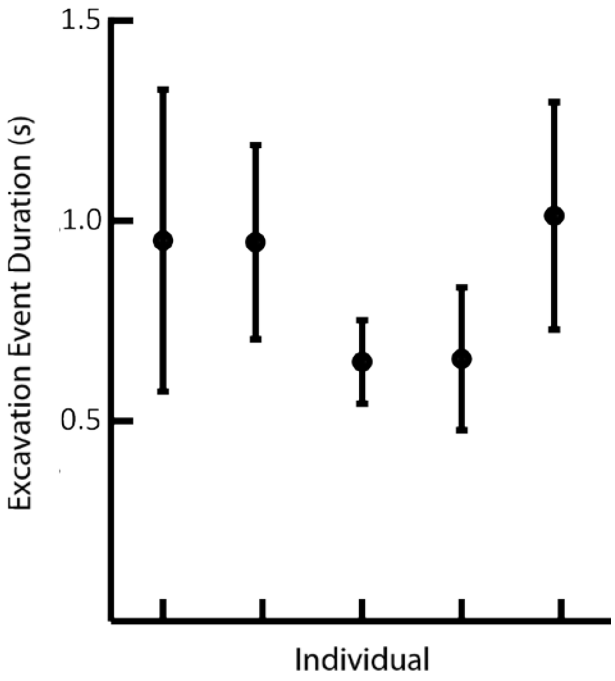

Figure 2.13: Graph showing the number of complete excavation events per minute, grouped by individual. Each data point combines all available data for that individual. Points indicate that individual's average. Error bars indicate +/- 1 s.d.. No significant difference was observed.

Figure 2.14

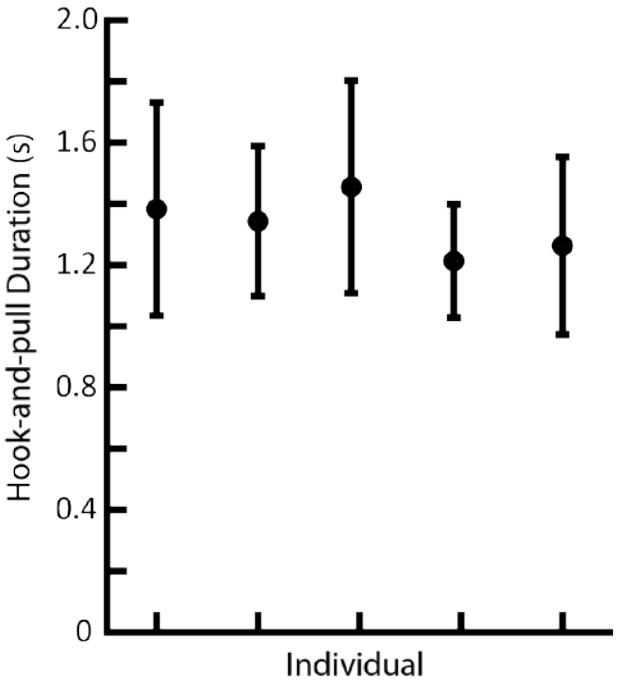

Figure 2.14: The duration of a single hook-and-pull event, grouped by individual. Each data point represents all available data for that individual. Points indicate that individual's average. Error bars indicate +/- 1 s.d. No significant difference was observed.

Figure 2.15

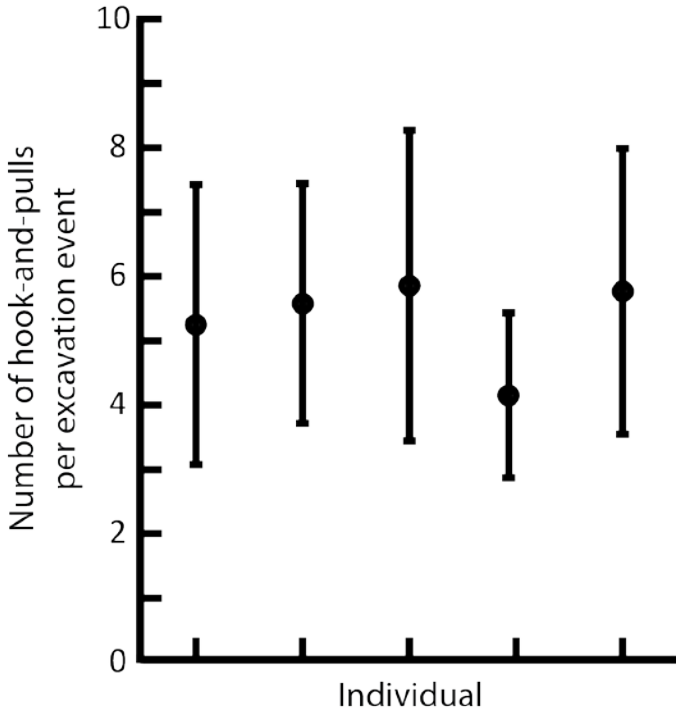

Figure 2.15: The number of hook and pull events performed during a single excavation event, grouped by individual. Each data point represents all available data for that individual. Points indicate that individual's average. Error bars indicate +/- 1 s.d. No significant difference was observed.

2.4 Conclusions

Ghost crab burrowing represents a complex, multifunctional behavioral suite that involves locomotion in confined environments and goal-directed manipulation of a granular substrate. Nearly all of the crabs' appendages are used in at least one part of the excavation cycle.

Ghost crabs use three different strategies in parallel to remove material from the end of the burrow: hook-and-pull, scratch digging and body rotation. While hook-and-pull (Figure 2.7) and scratch digging (Figure 2.8) are analogous to excavation behaviors observed in mammals (Hildebrand, 1987), they do not resemble burrowing strategies commonly associated with crustaceans (Bellwood, 2002; Faulkes, 2012). The body rotation behavior (Figure 2.9) that appears to expand the workspace of the other excavation behaviors is particularly interesting as it may also stabilize or expand the burrow though localized compression of the substrate.

Ghost crabs demonstrated three distinct strategies for transporting and manipulating collected material. These strategies included carrying (Figure 2.10), cross-body transfer (Figure 2.11) and pushing/packing (Figure 2.11). Unlike excavation behaviors, the transportation/manipulation behaviors were executed in serial, rather than parallel. Overall, substrate transportation involved highly coordinated manipulation inside of a confined environment. The observed manipulation behaviors were substantially more complex than the relatively simple grasping/capture behaviors typically associated with arthropod manipulation (Dollar, 2001).

The strategies observed appear to be consistent across individuals. All the individuals examined employed the same strategies in the same overall pattern (Figure 2.6). Nor were any significant differences in burrowing kinematics observed (Figures 2.13, 2.14, 2.15). However, these results are only for ghost crabs of consistent size burrowing in a single uniform substrate. Burrowing strategies have been shown to change significantly with body size in other animals (Che & Dorgan, 2010). Granular materials are also quite complex (Jaeger & Nagel, 1992). It is possible that ghost crab burrowing strategies change with both body size and substrate properties.

Unlike many burrowing animals, ghost crabs are specialized for running (Hafemann & Hubbard, 1969) and do not possess any of the most common morphological adaptations associated with burrowing behaviors (Faulkes, 2012). While burrowing specialists, such as the mole crab, are able to move through sandy substrates much faster than the ghost crabs, these burrowing specialists often have limited running capabilities (Trueman, 1970). Thus, the mechanisms used by the ghost crab for burrowing represent one potential way that legged robots could re-purpose their appendages for manipulating the substrate and enhancing their locomotive capabilities. These capabilities and a better understanding of how robots interact with the substrates on which they operate will be critical to next-generation mobile robots, such as those used in extra-planetary exploration (Iagnemma & Dubowsky, 2010).

Chapter 3

Mechanical Energy of Burrowing in Ghost Crabs

Understanding the energetic costs of ghost crab burrowing is critical to understanding the effectiveness of the behavior and its role in the crabs' energy landscape (Shepard et al., 2013). This chapter describes a mathematical model that uses empirical models of the substrate's mechanics and measured ghost crab morphometrics and kinematics to estimate the mechanical energy required during the principal burrowing behaviors observed in Chapter 2.

Summary

The energetic model, including both collection and transportation behaviors, suggests that the average mechanical power requirements of burrowing are approximately 12 mW for a typical burrowing ghost crab. However, some components of the excavation cycle, such as penetrating the substrate with the walking legs, have substantially higher estimated instantaneous power requirements. These high-intensity behaviors are generally brief, however. The lower average mechanical cost of burrowing is primarily due to long periods of inactivity. In addition to allowing a crab to recover from periods of anaerobic activity, these resting periods may enhance a crab's burrowing endurance (Weinstein & Full, 1992). The total mechanical energy costs of an excavation cycle are estimated to increase linearly with depth. Body size also affects the energetic costs of an excavation cycle, with the total cost being proportional to the third and fourth powers of the crab's carapace width.

3.1 Introduction

Burrowing is generally considered an energetically expensive behavior. The energetic costs of burrowing have been found to be much higher than the costs of other locomotion modes, including swimming, running and flying (Hunter & Elder, 1989). Despite these costs, burrowing behaviors are common throughout the animal kingdom (Dorgan, 2015). Animals may be willing to pay the relatively high energetic costs of burrowing because it provides protection from predators (Hunter & Elder, 1989).

The metabolic costs of burrowing have been widely examined, particularly in small burrowing mammals. For example, respirometry has been used to quantify burrowing energetics in gophers (Vleck, 1979), mole rats (DuToit, et al., 1985) and moles (Seymour, et al., 1998). The costs of burrowing in many soft-bodied invertebrates have also been examined by estimating the external mechanical power output (Hunter & Elder, 1989; Trevor, 1978). In almost every case, the cost of transport by burrowing (the energy required to move a given distance) was orders of magnitude greater than the costs of transport by walking/running (White, 2001). While the energetic costs of burrowing per unit distance are high, burrowing animals tend to move slowly, resulting in low overall energetic costs (Dorgan, et al., 2011).

While very little is known about the energetics of burrowing in the ghost crab, *O. quadrata*, the mechanics and energetics of ghost crab running have been well studied (Blickhan & Full, 1987; Full, 1987). By supplementing the existing data on running energetics with an estimate of the energetic costs of the ghost crabs' burrowing behavior, a more complete energy landscape (Shepard et al., 2013) can be constructed, placing all of the ghost crabs' behaviors into a broader ecological context. This chapter provides an initial estimate of the mechanical energy of burrowing in ghost crabs by addressing the following specific questions:

1) What are the mechanical energy requirements of the penetration and shearing actions observed in the hook-and-pull behavior described in Chapter 2?
2) What is the mechanical energy cost of substrate transportation?
3) How do these costs depend on the substrate's physical properties?
4) How do the mechanical energy requirements compare to the known mechanical costs of level-ground locomotion in ghost crabs?
5) How are these costs expected to change with burrow depth and body size?

These estimates will also suggest the relative difficulty of different components of the excavation cycle, potentially indicating conditions where the effectiveness of the ghost crabs' burrowing strategies will be limited.

3.2 Model of Mechanical Energy Costs

The model attempts to estimate the energetic costs of ghost crab burrowing based on measured substrate properties, ghost crab morphology and kinematics. While this model only represents a first-order approximation of burrowing energetics, it will estimate the overall mechanical costs of excavating/transporting the substrate and how these costs would be expected to change according to substrate properties and body size.

Model Derivation

This model of ghost crab burrowing energetics has three principal components: penetration, sheer and transport. Penetration represents the initial phase of a hook and pull action, where the crab inserts its dactyls into the substrate. Sheer follows penetration and represents how the crab contracts its dactyls within the substrate, loosening and collecting material. Transport is the final phase, where the crab transports itself and the collected material to the surface.

The total energy (E_{Total}) of an excavation cycle is defined as follows:

$$E_{Total} = E_{Penetration} + E_{Shear} + E_{Transport}$$

$E_{Penetration}$ is the energy expended to insert dactyls into the substrate. E_{Shear} is the energy expended while shearing material away from the end of the burrow. $E_{Transport}$ is the energy required to transport both the crab and the collected material to the top of the burrow.

Although there are other behaviors involved in ghost crab burrowing that may have substantial energetic costs (e.g. locomotion within the burrow, scratch digging and body rotation), these are not represented in this model because it is impossible to reasonably estimate their costs from the data available. Instead, the goal of this model is to estimate the costs of collecting and transporting material in the context of ghost crab burrowing. This model also estimates how these costs may be related to environmental conditions, burrow depth and ghost crab size.

Penetration Energy

In the context of an excavation cycle, $E_{Penetration}$ can be expressed in terms of both the number of hook-and-pull cycles (n_{HP}) and the number of legs used (n_L):

$$E_{Penetration} = \sum_{1}^{n_L} \sum_{1}^{n_{HP}} E_{P,L}$$

The total energy expended during penetration is the energy required to insert a single dactyl on a single given leg ($E_{P,L}$), summed over the number of times that leg was used and summed over the total number of legs used.

This model assumes that all of the dactyls are identical in form, structure and the mode of employment. This simplifies the total penetration energy and allows $E_{Penetration}$ to be represented in terms of E_P, the energy required to insert one generalized dactyl into the substrate a single time:

$$E_{Penetration} = n_L n_{HP} E_P$$

E_P can be determined by integrating the frictional forces, F_P, from insertion (l = 0) to the maximum depth (l = L):

$$E_P = \int_{l=0}^{l=L} F_P dl$$

Several assumptions are needed to translate the frictional forces, F_P, into a function, expressed in terms of the crab's physical dimensions and the substrate's material properties:

1) The frictional forces on the dactyl are independent of speed, as per current empirical models (Seguin, et al., 2011).
2) Any transient or unsteady forces are ignored.
3) Frictional forces are linearly related to cross-sectional area and depth. For a given depth, d, the pressure, P, is determined by $P = c_p d$, where c_P resistance to penetration per unit depth (N/m^3).

These assumptions permit E_P to be expressed as follows:

$$E_p = \int_{l=0}^{l=L} A(l)P(l)dl$$

A(l) is the cross-sectional area of the dactyl as it is inserted. P(l) is the force per unit area as a function of insertion depth.

If the dactyl is approximated as an elliptical cone (length: L, width: W, height: H) that is inserted into the substrate perpendicularly, A(l) can be expressed thusly:

$$A(l) = \frac{\pi H W l^2}{L^2}$$

As assumed, P(l) can be expressed in terms of depth, l, and the substrate's resistance to penetration, c_P:

$$P(l) = c_P l$$

This allows the following expression of E_P:

$$E_p = \int_{l=0}^{l=L} \frac{c_P \pi H W l^3}{L^2} dl$$

Which reduces to:

$$E_p = \frac{1}{4} c_P \pi H W L^2$$

Shear Energy

After the crab has inserted its dactyls into the substrate, it sheers the material away from the end of the burrow by rotating the dactyls about the dactyl/propodus joint. The total energy required for this operation, E_{shear}, can expressed in terms of the number of hook-and-pull cycles, n_{HP}, the number of legs employed, n_L, and $E_{S,L}$ the energy required for an individual dactyl to complete a single given shear:

$$E_{Shear} = \sum_{1}^{n_L} \sum_{1}^{n_{HP}} E_{S,L}$$

This model assumes that all of the dactyls are identical in form, structure and the mode of employment, simplifying the expression and representing it in terms of the E_S, the energy required to perform a single shearing action with one dactyl:

$$E_{Shear} = n_L n_{HP} E_S$$

E_S can be determined by integrating the total drag force, F_S, along the dactyl's arc from θ_{start} to θ_{end}:

$$E_S = \int_{\theta_{start}}^{\theta_{end}} F_S d\theta$$

By making the following assumptions, F_S can be estimated from the crab's known dimensions and the properties of the substrate:

1) The frictional forces are independent of the dactyl's velocity, as per current empirical models (Gravish et al., 2010).
2) Frictional forces are constant along the entire path.
3) Frictional forces are proportional to the cross-sectional area of the dactyl. For a given total cross-sectional area, A, the frictional force, F_S, will be equal to $F_s = c_s A$, where c_S is the shear strength of the substrate (N/m^2).

These assumptions permit E_S to be calculated by integrating the cross sectional width, W(l), and the total distance travelled, D(l), for each element of the dactyl from l = 0 (proximal end) to l = L (distal end):

$$E_S = \int_{l=0}^{l=L} c_s W(l) D(l) dl$$

Assuming that the dactyl has a triangular cross section of width, W, and length, L, W(l) can be expressed as follows:

$$W(l) = -l\frac{W}{L} + W$$

If the dactyl moves in a circular arc about the proximal end, the total distance traveled by a point along the dactyl can be easily expressed in terms of the total angular displacement of the dactyl, θ:

$$D(l) = \theta l$$

Thus, E_S becomes:

$$E_S = \int_{l=0}^{l=L} c_s(-l\frac{W}{L} + W)\theta l dl$$

This reduces to:

$$E_S = \frac{1}{6} c_S \theta W L^2$$

Transportation

To extend the burrow, the crab must transport both the collected material and itself to the top of the burrow. The cost of this behavior can be easily estimated by finding the change in gravitational potential energy of both the collected material and the crab. Unlike penetrating and shearing behaviors, transportation occurs only a single time during an excavation cycle.

The total energy required for transportation, $E_{Transport}$, is composed of two main parts: E_M, the collected material's increase in gravitational potential energy, and E_B, the increase in the crab's gravitational potential energy:

$$E_{Transport} = E_M + E_B$$

This model makes the following assumptions:

1) The density of the substrate, ρ, is uniform and does not change.

2) The mechanical energy costs of locomotion are dominated by the required increase in gravitational potential energy.
3) The burrow is entirely vertical.
4) The mechanical costs of descending locomotion within the burrow are disregarded and crabs do not recover energy while descending.

E_M is related to the substrate density, ρ, the volume of collected material, V, and the burrow's vertical depth, h, by the following:

$$E_M = \rho V g h$$

If the collected material forms a sphere of diameter, d, then this becomes:

$$E_M = \frac{4}{3}\pi\,(d/2)^3 \rho g h$$

E_B is simply related to the crab's mass, m:

$$E_B = mgh$$

Total Energy

The initial expression of an excavation cycle's total energy requirements is:

$$E_{Total} = E_{Penetration} + E_{Shear} + E_{Transport}$$

Using the expressions derived in the preceding sections, this can be expressed in a more detailed form that includes the number of legs used (n_L), the number of hook-and-pulls (n_{HP}), the physical dimensions of the ghost crab's dactyls (H, height; W, width; L, length), the angular displacement of the dactyls (θ), the material properties of the substrate (density, ρ; shear strength, c_S; and penetration resistance, c_P), the volume of collected material (sphere of diameter, d) and the crab's mass (m):

$$E_{Total} = n_L n_{HP}\left(\frac{1}{4}c_P \pi H W L^2 + \frac{1}{6}c_S \theta W L^2\right) + \frac{4}{3}\pi\,(d/2)^3 \rho g h + mgh$$

Power

Using the energetic estimates, the power output of the crab can be estimated for both individual activities and for an entire excavation cycle.

The average power required during an excavation cycle, P_{Total}, is related to the total power, E_{Total}, and the duration of that excavation cycle, T_{Total}:

$$P_{Total} = \frac{E_{Total}}{T_{Total}}$$

Note that T_{Total} includes both the time spent actively performing burrowing behaviors and periods of inactivity between behaviors.

The power required for penetration, $P_{Penetration}$, is related to the energy required for a single dactyl to penetrate the substrate, E_P, the number of dactyls employed, n_L, and the duration of a single penetration event, T_P:

$$P_{Penetration} = n_L \frac{E_P}{T_P}$$

Unlike T_{Total}, T_P does not include periods of inactivity since crabs have not been observed to pause while inserting their dactyls into the substrate.

The power required for shearing the substrate can be calculated using the same relationship as used for $P_{Penetration}$. E_S is the shearing energy required for a single dactyl and T_S is the duration of the shear.

$$P_{Shear} = n_L \frac{E_S}{T_S}$$

Transportation power requirements (material, P_M, and body, P_B) are related to the crab's mass and vertical velocity of the crab's ascent, v:

$$P_M = \frac{4}{3}\pi\,(d/2)^3 \rho g v$$

$$P_B = mgv$$

Energy Requirements and Body Size

The energy requirements of ghost crab burrowing depend on the physical dimensions of the crab, meaning the energy requirements will change as the characteristic size of a crab increases.

Assuming geometric scaling, the following dimensions can be related to the crab's carapace width, w_c, and fixed scaling values, s:

$$H = s_H w_c$$

$$W = s_W w_c$$

$$L = s_L w_c$$

$$d = s_d w_c$$

$$m = s_m (w_c)^3$$

All scaling values are unitless, except for s_m which has units of kg/m^3.

If these scaling relationships are substituted into the total energy relationship and the ascent velocity is assumed to be constant, then total energy, E_{Total}, can be expressed as a function of carapace width, w_c, burrow depth, d, and material properties (density, ρ; shear strength, c_S; and penetration resistance, c_P):

$$E_{Total} = n_L n_{HP}\left[\frac{1}{4}c_P \pi s_H s_W (s_L)^2 (w_c)^4 + \frac{1}{6}c_S \theta s_W (s_L)^2 (w_c)^3\right] + \frac{4}{3}\pi\left(\frac{s_d w_c}{2}\right)^3 + s_m (w_c)^3 gh$$

Specifically, the following relationships between individual energy requirements become clear, assuming that the mechanics of the excavation cycle remain constant as body size changes:

$$E_{Penetration} \propto c_P w_c^4$$

$$E_{Shear} \propto c_S w_c^3$$

$$E_{Transport} \propto \rho d w_c^3$$

3.3 Materials and Methods

Estimation of Model Parameters

The model was supplied with morphometric, kinematic and material property values typical for the crabs and substrates involved in the experiments described in Chapter 2, Section 2. These values are listed in Table 3.1.

Substrate properties were estimated by directly measuring experimental substrates described in Chapter 2. Resistance to penetration was measured using a penetrometer (No. 77114; Forestry Suppliers, Jackson, MS). The penetrometer measures the pressure (in kgf/cm^2) required to insert a circular foot (2.54 mm diameter) to a depth of 6.35 mm into the substrate. Shear strength was measured using a torsional vane shear tester (No. 77299; Forestry Suppliers, Jackson, MS). This instrument measured the shear pressure (in kgf/cm^2) required to break a 40-mm diameter disc free of the substrate. Substrate density was measured by collecting known volumes of substrate and weighing them on a scale.

Ghost crab morphometrics were estimated by measuring the experimental subjects described in Chapter 1. Carapace width and appendage dimensions were directly measured using calipers. Body mass was measured using a scale. Values for all individuals (n = 5) were averaged to produce the typical values presented in Table 3.1. Ghost crabs have been shown to scale geometrically in previous studies (Burrows & Hoyle, 1973). This fact was used to predict how mass and appendage dimensions will change with body size, allowing the model to predict how burrowing energetics will change with increasing body size. The volume of collected material is also assumed to scale geometrically with ghost crab body size.

Ghost crab kinematics, including n_L n_{HP}, T_P, T_S, v and d, were estimated by digitizing behavioral videos described in Chapter 2. Values for each individual (n = 5) were obtained by counting or measuring using ImageJ (https://fiji.sc/). These individual values were averaged to arrive at the typical parameter values presented in Table 2.1. Kinematic values were assumed to be constant for all ghost crabs, regardless of body size.

Table 3.1

Symbol	Description	Value	Units
c_S	Shear strength	5.9×10^4	N/m^2
c_P	Penetration resistance	1.9×10^7	N/m^3
ρ	Substrate density	1.6	g/cm^3
g	Gravity	9.8	m/s^2
n_L	Number of legs used	3	--
n_{HP}	Number of hook-and-pulls	5	--
θ	Angular displacement	90	degrees
h	Burrow depth	20/100	cm
v	Ascent velocity	2.5	cm/s
T_P	Duration of penetration	0.29	s
T_S	Duration of shear	0.29	s
w_C	Carapace width	33	mm
H	Dactyl height	2.5	mm
W	Dactyl width	5	mm
L	Dactyl length	12	mm
d	Diameter of collected material	17	mm
m	Crab mass	27	g
s_M	Body mass scaling coefficient	740	kg/m^3
s_H	Dactyl height scaling coefficient	0.16	--
s_W	Dactyl width scaling coefficient	0.08	--
s_L	Dactyl length scaling coefficient	0.4	--
s_d	Collected material scaling coefficient	0.6	--

Table 3.1: The values supplied to the model to estimate energetic costs.

3.4 Model Results and Discussion

Total Energetic Requirements

Mechanical energy requirements were calculated for excavation at 20 cm depth (Table 3.2) and 100 cm depth (Table 3.3). The mechanical energy requirements are predicted to increase linearly with burrow depth, due primarily to the increased change in gravitational potential energy of the crab and its payload. Overall, excavation is a relatively costly activity. Based on Blickhan & Full (1987), burrowing to 20 cm depth requires the crab to output mechanical energy equivalent to walking approximately 2.1 km. Burrowing to 100 cm depth requires the mechanical energy equivalent of walking 12 km.

This model also assumes that the material properties of the substrate do not change with depth. Since this model predicts that the total energy required during an excavation cycle is proportional to both the penetration resistance and shear strength, any changes in these properties as depth increases will change the costs accordingly. While it is known that ghost crabs burrow in a very heterogeneous environment and that substrate properties vary with depth (Jaeger & Nagel, 1992; Seguin et al., 2011), it is difficult to estimate how the specific values of c_P and c_S a crab encounters will change with depth.

Power Output

The instantaneous power requirements for the component behaviors, along with the average power requirements for an excavation event at 20 cm depth are estimated in Table 3.4. The average instantaneous mechanical power generated during one excavation event lasting one minute (0.012 W) is twice the mechanical power at the maximum aerobic speed (Blickhan & Full, 1987; Full, 1987). The maximum aerobic speed represents the speed at which maximal oxygen consumption is attained and endurance decreases rapidly with a further increase in speed. Direct measurements of endurance show that the ghost crabs can sustain locomotion for approximately 10 minutes at this rate of mechanical power. At the average instantaneous mechanical power rate of excavation, endurance data are consistent with crabs sustaining repeated excavation events without the likelihood of fatigue. Moreover, given the intermittent nature of the burrowing, it is likely that the benefit of exercise and rest cycles further extend endurance as has been shown during ghost crab intermittent terrestrial locomotion (Weinstein & Full, 1992).

Table 3.2

Behavior	Mechanical energy required for one excavation event at 20 cm (J)	Total mechanical energy required to reach 20 cm (J)
Penetration	0.55	44
Shear	0.11	8.8
Material Transport	0.01	0.41
Body Transport	0.06	56
Total	**0.73**	**56**

Mechanical energy per distance traveled during excavation event:	**280 J/m**
Distance walked to generate equivalent mechanical energy to burrowing 20 cm:	**2.1 km**

Table 3.2: Estimated mechanical energy requirements for excavation at 20 cm depth. The mechanical energy required for one excavation event is indicated in the center column, calculated using the energetic model presented here and the values shown in Table 3.1. The total mechanical energy to reach 20 cm is indicated in the right column. This value was determined by adding mechanical energy for all depths from 0 cm to 20 cm, assuming that the crab increases the depth by 0.25 cm per excavation event (80 total events to reach 20 cm depth).

Table 3.3

Behavior	Mechanical energy required for one excavation event at 100 cm (J)	Total mechanical energy required to reach 100 cm (J)
Penetration	0.55	220
Shear	0.11	44
Material Transport	0.05	10
Body Transport	0.30	60
Total	**1.0**	**330**

Mechanical energy per distance traveled during excavation event:	**330 J/m**
Distance walked to generate equivalent mechanical energy to burrowing 100 cm:	**12 km**

Table 3.3: Estimated mechanical energy requirements for excavation at 100 cm depth. The mechanical energy required for one excavation event is indicated in the center column, calculated using the energetic model presented here and the values shown in Table 3.1. The total mechanical energy to reach 100 cm is indicated in the right column. This value was determined by adding mechanical energy for all depths from 0 cm to 100 cm, assuming that the crab increases the depth by 0.25 cm per excavation event (400 total events to reach 100 cm depth). The energy per distance traveled is higher at 100 cm depth than 20 cm depth because transportation costs (both body and material) increase with depth.

Table 3.4

Behavior	Energy required for one excavation event at 20 cm (J)	Duration of behavior within one excavation event (s)	Instantaneous power used within one exaction event (W)
Penetration	0.55	1.45	0.379
Shear	0.11	1.45	0.076
Material Transport	0.01	8.00	0.001
Body Transport	0.06	8.00	0.008
Inactivity	0	41.1	0
Total	**0.73**	**60**	**0.012**

Table 3.4: Estimated mechanical power output within one excavation event at 20 cm depth, as determined by the model and values listed in Table 3.1. The duration of penetration and shear was estimated by assuming five of each event with each event lasting 0.29 s. The duration of transport behaviors was determined by dividing the depth of the burrow (20 cm) by the typical ascent speed (2.5 cm/s).

Effect of Body Size

The total energy required for an excavation event is predicted for a range of crab body sizes in Figure 3.1. These estimates assume that the crabs scale geometrically and the burrowing strategies (e.g. n_{HP} and n_L) and locomotion speed remain constant as body size changes.

The model predicts that overall energetic costs increase with ghost crab size. The majority of terms that compose the total required energy are proportional to w_c^3. However, the energy required to penetrate the substrate is proportional to w_c^4. Thus, larger crabs must supply disproportionally more energy to burrow to the same depth as a smaller crab, an effect that magnifies with depth.

The estimates depend on geometric scaling in ghost crabs, which is well-documented for ghost crabs (Burrows & Hoyle, 1973). However, smaller crabs (e.g. other species or juvenile ghost crabs) may exhibit different scaling relationships, due to the mechanical requirements of burrowing. For example, studies on burrowing worms found that smaller worms required blunter, thicker bodies to compensate for their reduced force production (Che & Dorgan, 2010).

It is also possible that burrowing strategies or locomotion speeds change with body size. Larger crabs have the ability to exert greater forces and also lower costs of locomotion (Full, 1987), potentially changing the patterns observed within an excavation cycle.

Figure 3.1

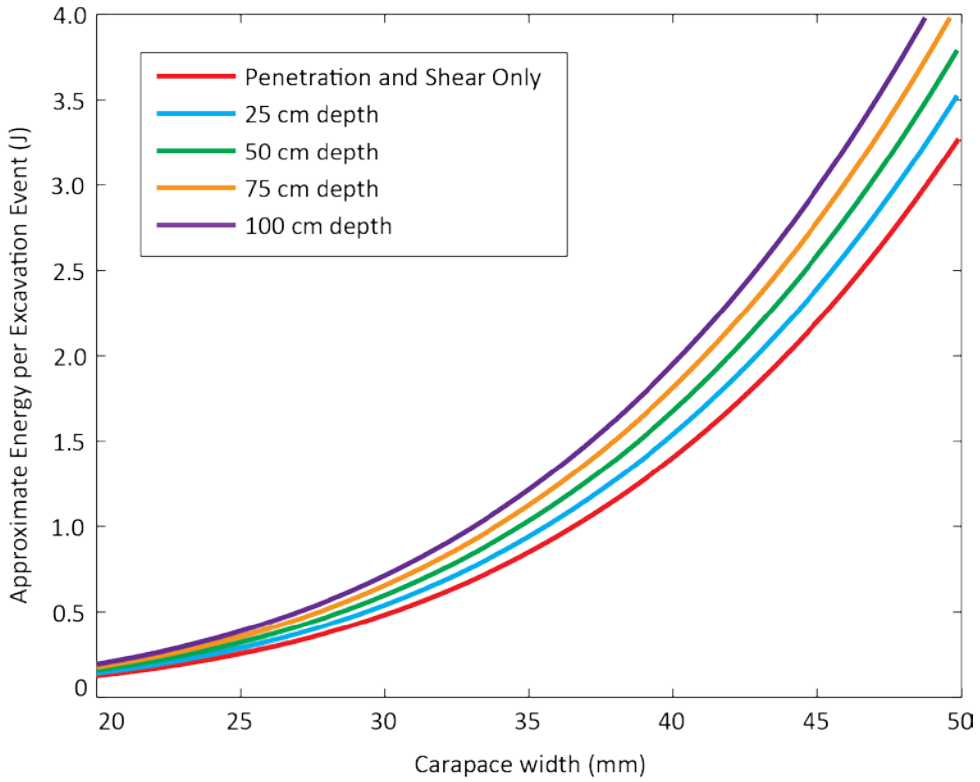

Figure 3.1: The estimated mechanical energy cost of an excavation event as a function of body size. Line color indicates how this relationship changes with burrow depth. **Penetration and Shear Only** (red) is the base cost of removing material from the end of the burrow, assuming that material properties are constant. Lines for **25 cm** (cyan), **50 cm** (green), **75 cm** (orange) and **100 cm** (purple) include the costs of material and body transport for a purely vertical burrow of the indicated depth. Generally, the energy cost is dominated by the material properties of the substrate.

Assumptions and Limitations

The model presented here represents a useful approximation of the energetic requirements of ghost crab burrowing. However, this model has several significant limitations.

This model's first limitation is related to the estimation of locomotion costs within the burrow. First, the model disregards the costs of descent inside the burrow. While descending nominally returns gravitational potential energy to the crab, it is unlikely that crabs can recover much of the energy expended during the ascent because descent requires continual damping and probably does not support energy conserving mechanisms observed in level locomotion (Blickhan & Full, 1987). Second, transporting a payload, regardless of appendage use, has been shown to significantly increase the costs of locomotion (Herreid & Full, 1986). Third, the burrow and all locomotion within it is assumed to be purely vertical. Natural ghost crab burrows, however, generally exhibit a range of inclines (see Chapter 4). Since the increase in locomotion costs relative to level locomotion is proportional to the incline (Full & Tullis, 1990), burrowing at a non-vertical angle may reduce the instantaneous power requirements while increasing the total energetic requirements by increasing the distance the crab must travel. Finally, all of the observed burrowing behaviors likely involve substantial production of isometric muscle forces. Since the appendage displacement of an isometric behavior is zero, it makes no contribution to the mechanical power output. However, producing an isometric force can have has a substantial metabolic cost, affecting the overall metabolic costs of locomotion (Kram, 2000).

This model also makes several assumptions about the kinematics and material properties of ghost crab burrowing, which may contribute to the high estimated mechanical energy and power output of excavation behaviors (particularly penetration). For example, the dactyls are assumed to penetrate the substrate at a right angle. If crabs instead insert the dactyls at an angle, they may be able to reduce the penetration forces, which are proportional to depth (Seguin et al., 2011). Likewise, shear forces are related to packing density (Gravish et al., 2010), which is assumed to be constant in this model. If the crab can reduce the packing density through alternate means, such as scratch digging, then shear forces could be substantially lessened. Due to the short duration of penetration and shearing behaviors, unsteady effects (e.g. Gravish et al., 2010) may also play a substantial role in the energetic costs of burrowing. The kinematics of burrowing were also assumed to be constant, regardless of ghost crab size. It is possible that larger (or smaller) ghost crabs adopt different burrowing strategies. For example: penetration forces are proportional to the square of penetration depth. Large ghost crabs may reduce burrowing forces by inserting their dactyls a shorter distance into the substrate.

There are also other environmental effects which will require consideration. For example, ambient temperature, which generally decreases with burrow depth (Chan et al., 2006), has been shown to change ghost crab performance (Weinstein & Full, 1994) and endurance (Weinstein & Full, 1998).

Resolving these limitations will require a two-pronged approach that includes an empirical model of the forces involved in excavation and metabolic measurements of burrowing ghost

crabs. The empirical model could be developed using similar methods to those employed by Gravish et al., (2010), incorporating substrate properties, effector morphology and kinematics. This model will provide a more accurate estimate of burrowing forces and energetic requirements. Combining the metabolic measurement techniques described in Full (1987) and Vleck (1979) could enable direct measurements of the metabolic energetic costs of behavioral components that are difficult to model or estimate. Although this would be a technically demanding experiment, it would provide valuable metabolic information and a deeper understanding of the crabs' energy landscape (Shepard, et al., 2013).

3.5 Conclusions

The mechanical energy required to perform a series of hook-and-pull behaviors can be broken down into two distinct components: penetration and shear. The cost of penetration is related to the length and cross-sectional area of the dactyls and the penetration resistance of the substrate. The cost of shearing is related to the length and cross-sectional area of the dactyls, the shear strength of the substrate and the angular displacement of the dactyl. Penetration represents the majority of the mechanical energy costs of burrowing (Tables 3.2 and 3.3). Shearing also represents a major component of the cost of burrowing (Tables 3.2 and 3.3). These costs, however, are very sensitive to the substrate's material properties and the kinematics of excavation. A number of factors, including substrate packing density, dactyl insertion angle and dactyl insertion depth could reduce the mechanical power output of excavation by more than a factor of ten.

The mechanical energy costs of substrate and body transportation are generally a small component of the overall costs of burrowing (Tables 3.2 and 3.3), though they increase with depth. As the overall mass of the collected material is generally small, the cost of substrate transportation is the smallest component of the total costs, even at depths of 100 cm. The mechanical energy costs of vertical locomotion also increase with depth, with a total cost of approximately twice the cost of substrate transportation. The mechanical costs of transporting a crab's body to the surface is substantially higher (Tables 3.2 and 3.3). While the cost is low at 20 cm depth, the body transport costs begin to exceed the shear costs at approximately 50 cm depth.

The mechanical costs of burrowing are linearly related to the burrow depth, penetration resistance, shear strength and density of the substrate. Costs are also proportional to the third and fourth power of body size (Figure 3.1).

While this model predicts that burrowing requires high instantaneous power output, the average mechanical power output is much lower (Table 3.4). This is due to short periods of high-intensity activity followed by relatively long periods of inactivity. The periods of inactivity within the excavation cycle may serve an important purpose; intermittent activity can substantially increase the crabs' endurance (Weinstein & Full, 1992). This may also represent larger trend in animal

burrowing. For example burrowing gophers also demonstrate short bursts of activity followed by relatively long resting periods (Vleck, 1979).

This model suggests several additional research questions, which could be addressed with direct measurements of a crab's metabolic expenditure. First, what are the metabolic costs of locomotion within a burrow, particularly while carrying a payload? Payloads have been shown to substantially increase locomotion costs (Weinstein & Full, 1994) but what is the magnitude of these costs relative to the mechanical costs of burrowing? Second, do larger crabs adopt different burrowing strategies to minimize the forces required for burrowing? Assuming that small and large crabs scale geometrically (well supported by Burrows & Hoyle (1973)) and that muscle physiology is constant, the maximum force produced by a crab should be proportional to the square of carapace width (Alexander, 2006). Since this model predicts that the force required to penetrate the substrate with the dactyls increases with the fourth power of carapace width, it seems likely that larger crabs may modify the kinematics of burrowing to compensate. Finally, this model predicts that ghost crabs could maintain the same power output while increasing the burrow extension rate if the strength (compressive or shear) of the substrate is reduced. Testing ghost crab burrowing performance in a variety of substrates may offer some insight into the overall metabolic costs of burrowing.

These questions will be best addressed with a substantially more comprehensive experimental apparatus that combines x-ray imaging with simultaneous oxygen consumption analysis (similar to that employed by Vleck (1979)), providing direct energy metabolic energy measurements. Experimentally testing this model's predictions will provide new insight into the ghost crab's energy landscape and potentially indicate the applicability and limitations of crab-inspired burrowing robots.

Chapter 4

The Effect of Substrate Properties on Ghost Crab Burrowing

Ghost crab burrowing is a complex, multifunctional behavior that involves highly coordinated appendage use in a confined environment, as demonstrated in Chapter 2. Burrowing behaviors are, however, intrinsically related to the material properties of the substrate (Dorgan, 2015). This chapter assesses how ghost crab burrowing performance correlates with substrate properties and environmental conditions, using both field and laboratory studies.

Summary

Field studies, conducted on a barrier island in North Carolina, USA, found that ghost crabs construct burrows in a highly variable environment that includes substantial changes in moisture content, sheer strength and compressive strength. Despite this, the density and size of ghost crab burrows was not correlated with environment type. Plaster casts of ghost crab burrows found a significant linear correlation between ghost crab size and burrow diameter. No correlation was found between ghost crab size and burrow depth, burrow length or burrow structure. The primary limitation on ghost crab burrowing appears to be moisture content. Laboratory studies examined the performance of ghost crabs engaged in horizontal and vertical burrowing. Ghost crabs are able to burrow significantly faster in horizontal conditions, mainly due to reduced periods of inactivity. A second laboratory study tested the hypothesis that ghost crab burrowing performance is correlated with substrate moisture content. However, ghost crabs maintained consistent performance across the entire range of tested moisture contents.

4.1 Introduction

Many animals demonstrate the ability to burrow in a variety of substrates (Dorgan, 2015). These animals and their strategies exhibit varying degrees of substrate specialization. Some strategies are limited to a very specific material (e.g. *Osedax* worms burrow only in bone; Tresguerres et al. (2013) while other animals are able to produce burrows in a range of substrate properties (e.g. ants can produce burrows in clay, silt, sand and gravel; Espinoza & Santamarina, (2010)).

The applicability and effectiveness of a burrowing strategy is closely related to the substrate properties (Ding et al., 2010; Dorgan et al., 2006). These properties (Figure 4.1) have an experimentally demonstrated capacity to change how animals interact with the substrate. For example, mysid shrimp are completely unable to burrow if the substrate grain size is too large (Nel, et al., 1999). Substrate compaction significantly changes the frictional properties of a granular material (Gravish et al., 2010), which alters locomotion strategies in animals (Mazouchova, et al., 2010) and locomotor effectiveness in robots (Li, et al., 2009). Even if material properties remain constant, an animal's body size and shape can significantly affect the effectiveness of burrowing. Larger worms are able to exert higher forces whereas smaller worms have shorter, blunter bodies to increase the effectiveness of their lower force output (Che & Dorgan, 2010). Likewise, aspect ratio has a strong effect on razor clam burrowing efficiency and velocity (Jung, et al., 2011).

Burrowing in crustaceans is very common (Bellwood, 2002), with different degrees of specialization and adaptability (Faulkes, 2012). Specifically, ghost crabs produce long, semi-permanent burrows in sandy beaches. These burrows are used for protection from predators and environmental stresses (Milne & Milne, 1946). Even short burrows of 25 cm depth can reduce the ambient temperature by up to 16 ^{o}C, substantially reducing a ghost crab's risk of overheating and desiccation (Chan et al., 2006). Some studies have found correlations between burrow structure and location relative to the tide line (Hill & Hunter, 1973), though other results dispute this (Duncan, 1986). Notably, ghost crabs are not apparently specialized for burrowing (Savazzi, 1985), lacking the short broad burrowing appendages that are typically associated with fossorial crustaceans (Faulkes, 2012). Instead, ghost crabs are rapid running specialists (Hafemann & Hubbard, 1969), capable of running more than 2 m/s or 20 body lengths per second (Herreid & Full, 1986). Despite this, the results of Chapter 2 conclusively demonstrate that ghost crabs are competent burrowers that use highly coordinated, goal-directed manipulation strategies to produce semi-permanent structures.

The overall objective of this chapter is to determine whether and how ghost crab burrowing performance is related to the substrate's mechanical properties. Specifically, is ghost crab burrowing a general-purpose behavior that can accommodate a variety of substrate properties or are the crabs limited to a specific range of conditions? This chapter describes a two-pronged approach to answering this question. Field studies were used to assess the natural variation in the ghost crabs' habitat and to correlate these environmental conditions with burrowing preferences and burrow structure. Laboratory studies examined how performance and burrowing strategies were related to specific environmental variables.

Figure 4.1

Property	Schematic Diagram	Effect of variation
Moisture content	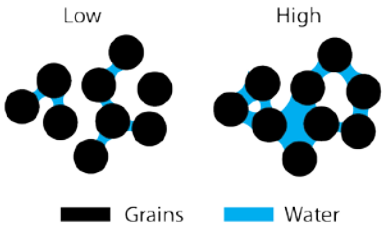	Increasing moisture non-monotonically changes cohesive forces. For low moisture contents, increasing moisture content will increase cohesive forces. At high moisture contents, cohesive forces collapse.
Entanglement	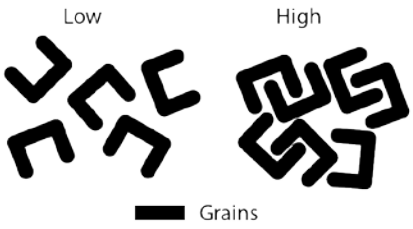	Increasing entanglement increases the grain-to-grain friction through particle interpenetration. In bulk, this translates to increased material strength (e.g. sheer and tension).
Bulk density	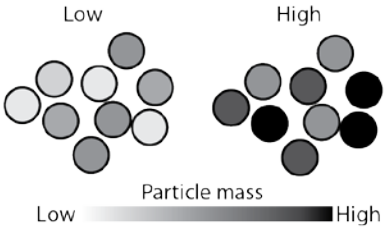	Increasing the bulk density of the material increases the ratio of gravitational forces to cohesive forces (e.g. moisture content). Bulk density also increases transportation costs.
Packing density	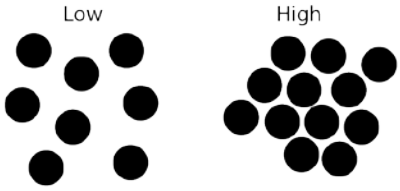	Increasing packing density increases the bulk density. Increased packing density also increases resistance to penetration. If the material contains water, increased packing density increases the density of capillary bridges, altering cohesive forces.
Grain size	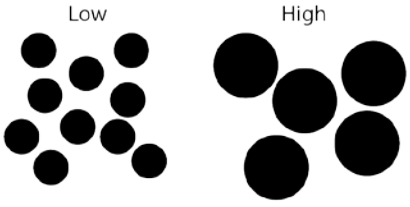	Increasing grain size increases the ratio of gravitational forces to cohesion forces. Depending on particle shape and packing density, increasing grain size may also change bulk density.

Figure 4.1: Substrate properties and the effects of their variation. **Moisture content** produces non-monotonic changes in cohesive forces. Completely dry sand is non-cohesive (absent other effects, such as entanglement). As the moisture content increases, capillary bridges form between grains creating inter-grain cohesion. Further increasing moisture content increased the density of capillary bridges, increasing cohesive forces. However, if moisture content is sufficiently increases, the granular material will become a slurry and cohesive forces will collapse. (Mitari & Nori, 2006). **Entanglement** refers to mechanical interpenetration of grains. The potential for grain entanglement depends on the grain shape and material. Increased entanglement increases local friction forces. On a bulk material level, this results in increased material strength (e.g. sheer, tension). Unlike the cohesive forces from moisture content, the inter-grain bonds will not spontaneously form; some kind of mechanical agitation (e.g. compression, vibration) is required to produce entanglement (Gravish et al., 2012). **Bulk density** refers to the overall mass per unit volume of the material. Increased bulk density will result in higher metabolic costs of material transportation (Bernal & Mason, 1960). Increased bulk density will also increase the ratio of gravitational forces to cohesive forces (Mitari & Nori, 2006). This may affect burrowing strategies (i.e. by reducing burrow stability). **Packing density** is the volume ratio of empty space to material. Increased packing density may change bulk density, depending on grain size and shape (Bernal & Mason, 1960). Increased packing density also increases the resistance to penetration by a foreign object (Umbanhower & Goldman, 2010). Increase packing density may also increase the density of capillary bridges, leading to altered material cohesion due to moisture content (Mitari & Nori, 2006). **Grain size** refers to the average size of a grain within the material. If the ratio of grain size to animal size is sufficiently large, altered burrowing strategies may be required (Dorgan, 2015). Depending on grain packing density and shape, changing grain size may also change the bulk density (Bernal & Mason, 1960). Increasing grain size may also change the density of capillary bridges, leading to altered material cohesion due to moisture content (Mitari & Nori, 2006).

Burrowing Preferences and Environmental Conditions

Initial field work examined how material properties change throughout one beach inhabited by ghost crabs and how burrow size and density correlate with these properties. Although prior studies (Duncan, 1986; Hill & Hunter, 1973) have attempted to correlate burrowing preference in ghost crabs with body size and location relative to the shore, the results are conflicting and did not attempt to relate burrowing with the mechanical properties of the substrates. This chapter offers more data on ghost crab burrowing to address the following questions:

1) Do the substrate properties in the ghost crabs' natural habitat vary substantially with location and/or depth?
2) If the substrate properties do vary substantially, do ghost crabs burrow more frequently in some substrates versus others?
3) Does substrate preference change with ghost crab size?

Answering these questions will provide necessary background for future studies on ghost crab burrowing by quantifying the natural variation ghost crabs can expect to encounter. If ghost crabs demonstrate a preference for certain substrates over others, then this study may also suggest what conditions are optimal or limiting for ghost crab burrowing.

Burrow Casting

The mechanical properties of a substrate may vary substantially as depth increases (Jaeger & Nagel, 1992). Since ghost crabs are known to produce complex burrows that extend up to a meter below the surface (Duncan, 1986; Hill & Hunter, 1973), a second series of field studies used burrow casting to examine burrow structure and how it was related to substrate properties and ghost crab size. Specifically, these studies examined the following questions and hypotheses:

1) Is burrow structure (i.e. depth, length, diameter, or branching structure) predicted by ghost crab size?
2) Are there any substrate properties (i.e. compressive strength, shear strength, moisture content) that are correlated with the burrow's maximum depth?
3) What is the typical performance envelope of ghost crab burrowing

Resolving these questions may reveal which substrate conditions limit ghost crab burrowing and how these limits are related to body size. Many previous studies have found that burrowing strategies and performance change significantly with body size (Che & Dorgan, 2010), so this studies' results would be expected to show that smaller crabs produce significantly different structures from larger crabs.

Figure 4.2

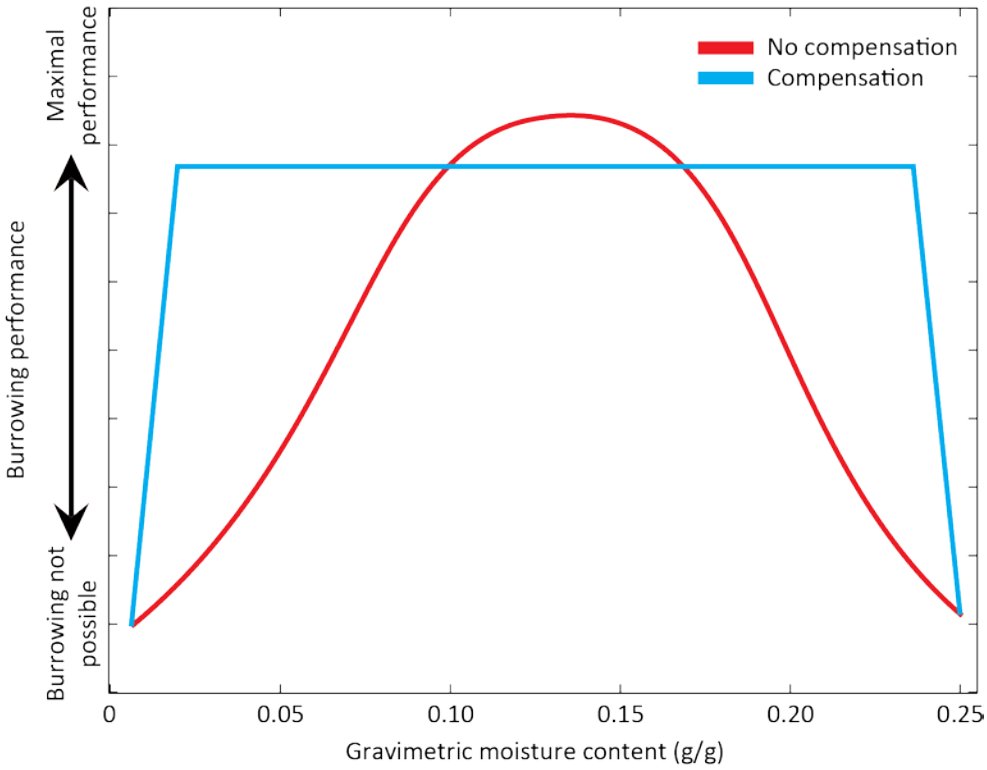

Figure 4.2: Hypothesis showing how burrowing performance may be related to substrate moisture content. Burrowing performance is expressed in a generalized form. Examples of specific burrowing performance metrics include (but are not limited to) maximum burrow depth and burrow extension rate. Two hypotheses are represented here: no compensation (red) and compensation (blue). If cohesive forces due to substrate moisture content are the primary limiting factor in ghost crab burrowing and crabs do not employ compensatory mechanisms, then burrowing performance would be expected to correlate with moisture content.

Horizontal vs. Vertical Burrowing

Ghost crabs may be able to burrow in a wide variety of conditions. However, the previous two field studies are unable to address whether the ghost crabs adopt alternate behaviors to compensate for changing substrate properties. A follow-up experiment to the results presented in Chapter 1 addresses this by presenting ghost crabs with horizontal and vertical burrowing challenges. As per the energetic model presented in Chapter 3, the costs of substrate transportation contribute substantially to the overall costs of burrowing. When the crabs burrow horizontally, these costs can be reduced while the substrate's other properties remain constant. This study addresses the following specific questions and hypotheses:

1) Does ghost crab burrowing performance differ between horizontal and vertical conditions?
2) Do the burrowing strategies used by ghost crabs change between horizontal and vertical conditions?

Answering these questions will demonstrate how responsive ghost crabs are to their burrowing environment and may offer some insight into the performance targets burrowing crabs appear to attain. For example, it is possible that crabs attempt to maintain a constant rate of burrow extension. If this is true, then performance and strategies would not be expected to differ between horizontal and vertical conditions. However, Chapter 3 suggests that crabs could extend their burrows faster while maintaining a constant metabolic expenditure if the energetic costs of burrowing are reduced. In this case, horizontal burrow extension rates would be expected to be significantly higher than vertical extension rates.

Effect of Moisture Content on Burrowing Performance

Substrate moisture content substantially alters the material properties of a granular substrate (Mitari & Nori, 2006) and has been shown to affect burrowing performance in ants (Espinoza & Santamarina, 2010; Monaenkova, et al., 2013). While ghost crabs may burrow in substrates with a range of moisture contents, it is unclear if their burrowing performance remains consistent throughout the range of conditions they encounter. To address this, a laboratory study quantifying ghost crab burrowing performance in substrates of varying moisture contents was performed.

The central hypothesis of this section is that ghost crab burrowing performance is correlated with substrate moisture content. If the ghost crabs' burrowing behavior is tuned for a narrow range of moisture contents, then this hypothesis predicts that performance will peak at some intermediate value, similar to the substrate specialization observed in other beach-dwelling burrowers (Nel et al., 1999). However, it is also possible that ghost crabs can employ compensatory mechanisms that permit them to burrow in a range of moisture contents. If this is the case, then burrowing performance is expected to be consistent across a broad range, similar to the burrowing

performance observed in some burrowing generalists (Alexander, et al., 1993). These two competing hypotheses are illustrated in Figure 4.2. Specifically, this study addresses the following questions:

1) Does burrow depth depend on moisture content?
2) Is the burrow's total length dependent on moisture content?
3) Does the average or maximum burrow extension rate depend on moisture content?
4) Do crabs spend more time actively extending their burrows in some substrate moisture contents than others?

While casual observation shows that ghost crabs cannot burrow in either completely dry or completely saturated substrates, their performance at intermediate conditions is currently unknown. Based on results from other burrowing animals (Espinoza & Santamarina, 2010; Monaenkova et al., 2013), it is reasonable to expect the metrics of ghost crab performance studied here to peak at an intermediate moisture content.

Broader Implications

Understanding how burrowing performance in ghost crabs is related to the substrate properties may also offer insight into beach ecology, by both clarifying the ghost crabs' energy landscape (Shepard et al., 2013) and exposing the limits of crab-induced bioturbation (Jones, et al., 1997). Prior studies have found that a substrate's compressive strength have significant effects on locomotor performance. Appendage designs that reduce foot pressure were found to improve running performance by passively decreasing the foot's penetration into the substrate (Qian et al., 2015). Quantifying ghost crab burrowing performance and its relation to substrate properties lead to similar models of how the physical properties of the substrate affect burrowing performance in general. These findings may translate into new legged robots, capable of both running and burrowing in heterogeneous terrain.

4.2 Materials and Methods

Field Studies

Field Site

All field studies were conducted at the Rachael Carson Reserve (Beaufort, NC, USA; Figure 4.3) in July/August, 2014. The reserve is an undeveloped barrier island with a large native population of ghost crabs, *Ocypode quadrata*. The island includes sandy high-energy beaches, sand dunes and tidally-dominated marshy inlet.

The environment was divided into four sub-environments: high-tide, inter-dune, marsh-like and dune. These environments and their locations within the reserve are shown in Figure 4.4. While these environments have several features in common, including general composition (fine grained sand moistened by sea water), they differ substantially. The high-tide environment is the typical high energy beach, which is often associated with the ghost crab habitat (Milne & Milne, 1946). The inter-dune environment is similar to the high-tide line except that it is not regularly exposed to wave action. The marsh-like sub-environment occurs on the island's inner shore. This environment is characterized by low-amplitude wave action and generally high moisture content. The dune environment, also commonly associated with ghost crab inhabitation (Duncan, 1986; Hill & Hunter, 1973), are relatively high above the high-tide line. Dune surfaces are generally dry and covered with small grasses and shrubs.

Vertical Transects

Vertical transects were used to characterize how the substrate properties in each sub-environment varied with depth. Transects began at the surface by sampling the compressive strength, shear strength and gravimetric moisture content (GMC). Then, a thin trench was produced with a sharp spade, minimizing the disturbance to the substrate. As the trench was excavated, the compressive strength, shear strength and GMC were measured every 10 cm of depth down to 50 cm. The trench was extended vertically to the saturation depth, where the substrate's moisture content increases sufficiently to prevent further excavation. The saturation depth was measured with a tape measure.

Figure 4.3

Figure 4.3: The Rachel Carson Reserve, in Beaufort, North Carolina, USA (Map data ©2016 Google). The reserve is an undeveloped island that is part of the North Carolina Outer Banks (see inset). Ghost crabs inhabit most of the island, particularly the sandy beaches on the south-facing shore of the island. The field studies detailed here were conducted in the northwest corner of the island, highlighted in orange.

Figure 4.4

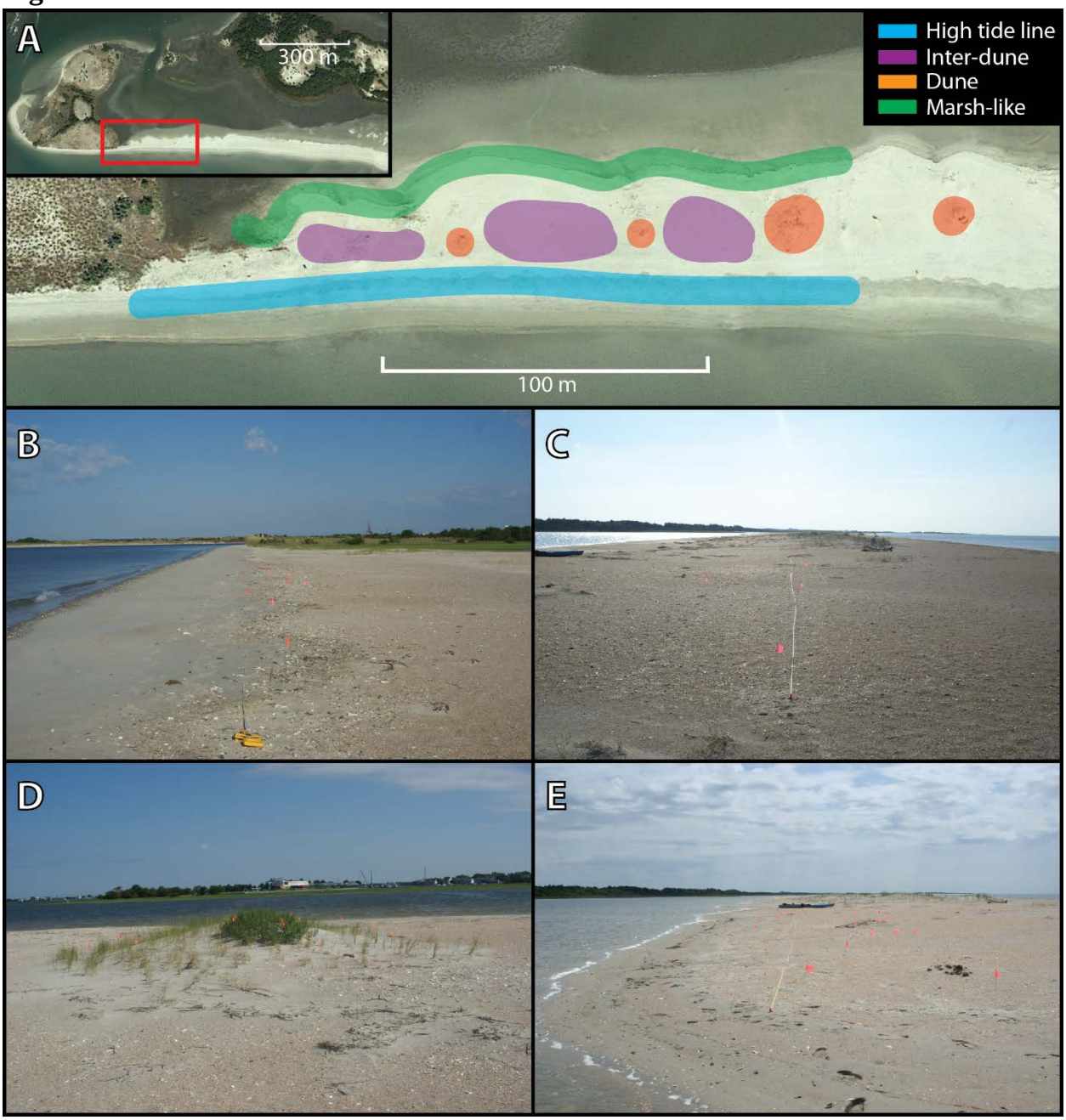

Figure 4.4: Habitat types observed and sampled. **A:** The area of the Rachael Carson Reserve that was surveyed. Inset shows high-level view of the Reserve, showing the survey area in red. The survey area was subdivided into four different habitat types. Blue indicates the high tide line. Purple indicates the inter-dune region. Orange indicates dunes. Green indicates marsh-like areas. (Map data ©2016 Google) **B:** The high tide line habitat. This habitat is characterized by high-amplitude wave action and limited vegetation. Large debris (washed up plant matter, shells) is common at the surface and below. Constant exposure to wave action maintains a moderate substrate moisture content, defined as the fraction of water mass to overall substrate mass. The region in which ghost crab burrows is approximately 50 cm above the saturation depth. **C:** The inter-dune region is a largely flat, open area distinguished by little vegetation and no exposure to waves. Moisture content is maintained by seepage from the ocean and rain. The area in which ghost crabs burrow is typically 60 cm above the saturation depth. **D:** A sand dune. Dunes are distinguished relatively dense vegetation (grasses and small shrubs). The surface is dry and loose but the substrate is moist below. The entrances to ghost crab burrows are typically found 80 cm above the saturation depth. **E:** The marsh-like area, which occurs on the island's central lagoon. This area is characterized by low-amplitude wave action and occasional vegetation (e.g. marsh grasses). The substrate moisture content in this area is generally high. The area in which ghost crabs burrow is typically 20 cm above the saturation depth.

Surface Transects

Surface transects in each sub-environment were used to assess the number and size of ghost crab burrows. Where possible, transects were rectangles 30 m long by 4 m wide. When the dimensions of a sub-environment did not permit the rectangular transect to be placed entirely within the boundaries of that sub-environment, ellipsoidal transects were used instead. The area of the ellipsoidal transects were determined by measuring the major and minor axes.

Burrow density was determined by counting the total number of open burrows one cm in diameter or larger inside the transect boundary. It is unlikely that the counted burrows were constructed by animals other than *O. quadrata* because no other burrowing animals of equivalent size were observed in this environment. This conclusion is reinforced by the frequent observation of distinctive ghost crab tracks (four parallel lines in the sand) surrounding the burrows.

The diameter of each burrow inside a transect was measured with a ruler. Burrow diameter has been correlated with body size in related ghost crabs (Chan et al., 2006).

Substrate Properties Measurement

The substrate properties measured here included gravimetric moisture content (GMC), compressive strength and shear strength. All three of these properties have been correlated with burrowing performance in other animals (Brown & Trueman, 1991; Monaenkova et al., 2013).

Gravimetric moisture content, the water mass to total sample mass, was measured by collecting approximately 5-10 ml of soil using a tubular soil sampler (No. 76971; Forestry Suppliers, Jackson, MS, USA). This sample was stored in a sealed plastic sample container and transported back to a nearby laboratory. The wet granular material was weighed, dried in an oven and re-weighed. The gravimetric moisture content is defined as follows:

$$GMC = \frac{Wet\ Mass - Dry\ Mass}{Wet\ Mass}$$

Resistance to penetration was measured using a penetrometer (No. 77114; Forestry Suppliers, Jackson, MS). The penetrometer measures the pressure (in kgf/cm^2) required to insert a circular foot (2.54 mm diameter) to a depth of 6.35 mm into the substrate.

Shear strength was measured using a torsional vane shear tester (No. 77299; Forestry Suppliers, Jackson, MS). This instrument measured the shear pressure (in kgf/cm^2) required to break a 40-mm diameter disc free of the substrate.

Burrow Casting

To understand what substrate properties may limit burrowing and to correlate burrow structure with ghost crab morphology, burrow casts and the resident crabs were collected from the field site.

Active burrows were first identified by looking for signs of recent ghost crab inhabitation. These included fresh tracks around the burrow entrance, recently excavated material or actual sightings of the resident crab. Candidate burrows were slowly filled with plaster of Paris (DAP Products, Inc, Baltimore, MD, USA). The porosity of the substrate and slow filling speed ensured that any branches were completely filled. Burrow casts were allowed to cure for at least two hours and then excavated carefully with a spade. Each burrow's length, depth and structure were recorded.

Shear strength, compressive strength and GMC were measured from the substrate immediately surrounding the burrow as the burrow was excavated. Measurements were taken at 10 cm depth and the burrow's maximum depth. A third measurement was taken at one-half of the burrow's maximum depth if the total depth exceeded 30 cm.

Ghost crab capture and measurement

In most cases, the resident crab would evacuate the burrow as the burrow was filled with plaster. This permitted the crab's capture and measurement. If a crab was not captured during casting, then the burrow was carefully broken apart and a crab, if found, was carefully removed and measured.

Laboratory Studies

Animals

Ghost crabs, *Ocypode quadrata*, were purchased from a commercial vendor (Gulf Specimen Marine Lab, Panacea, FL, USA), that captured wild ghost crabs from the Gulf Coast of Florida, USA. Crabs were housed individually in ventilated plastic containers, approximately 20 cm long, 15 cm wide and 15 cm tall. A small volume (approximately 25 ml) of fresh sea water substitute (Instant Ocean, Blacksburg, VA, USA) was placed into the container and changed every 1-2 days. The containers were stored at an approximately 10 degree incline, producing "wet" and "dry" sides, which the crabs were permitted to access freely. The crabs were provided with a diet of 1-3 live, medium-sized crickets (Petco, Atlanta, GA, USA) each day. Uneaten crickets were removed within 24 hours. The crabs were maintained at approximately 23 ^{o}C continuously. A window maintained a natural day:night cycle of approximately 13 hrs : 11 hrs. Only complete, healthy crabs were used for behavioral trials. Any crab that was missing an appendage or that exhibited lethargic behavior was removed from the experimental cohort.

Data for the horizontal and vertical burrowing trials came from 5 individuals (carapace width: 29 - 35 mm; mass: 21 - 25 g).

Data for the trials examining the effects of moisture content on burrowing performance came from 4 individuals (carapace width: 30 ± 2 mm; mass: 18 ± 3 g). Only complete, healthy crabs were used for behavioral trials.

Horizontal and Vertical Burrowing Environments

An artificial beach environment was used for all behavioral experiments. This environment, derived from the artificial beach environment described in Chapter 2, could be configured in either a vertical (Figure 4.5A) or horizontal (Figure 4.5B) configuration. This environment was constructed from 2.1 mm-thick optically-clear acrylic panels (McMaster-Carr, Elmhurst, IL, USA) and aluminum struts (MicroRAX, Auburn, WA, USA). The enclosure was 50 cm tall, 7.5

cm deep and 16 cm wide. The enclosure was filled to a depth of approximately 30 cm with clean damp sand (14% gravimetric moisture content). The sand was obtained Jekyll Island, GA, USA, which is a known ghost crab habitat. To remove any voids and create a uniform burrowing substrate, the sand was tamped down by repeatedly tapping the enclosure on a table prior to inserting the crab. In the vertical condition, crabs were inserted on top of the packed substrate. In the horizontal condition, the crabs were inserted adjacent to the packed substrate.

X-ray Markers

The same marking scheme detailed in Chapter 2, Section 2 & Fig. 2.2 was used for this experiment. Each crab was equipped with a set of x-ray opaque markers, made from 1 mm-thick lead foil (McMaster-Carr, Elmhurst, IL, USA). Two types of markers were constructed: strips (1 mm-wide, cut to length) and dots (between 1 and 4 mm^2).

A candidate ghost crab was first placed into a cold chamber (approximately 5 ^oC) for a few minutes until quiescent. The crab was removed from the chamber and restrained with elastic bands. Strips and dots were attached to the crab's body and appendages use cyanoacrylate adhesive (Loctite 1365882; Henkel Corp, Westlake, OH, USA). Strips were attached to each major segment of all walking legs (dactyls, propodus, carpus and merus) and to the dactyl and pollex of both cheale. Dots were attached to the carapace and to the merus of each walking leg. One dot was placed on the dorsal surface of the carapace on the same side as the minor chela. Two dots were placed on the dorsal surface of the carapace on the same side as the major chela. Each merus of each walking leg was equipped with a number of small dots equal to number of that walking leg (i.e. one dot for the first walking leg, two dots for the second walking leg and so on).

Ghost crabs were allowed at least 6 hours to recover from the marking procedure. Any crabs that exhibited lethargic behavior, appendage loss or damage were disqualified from behavioral experiments.

X-ray Imaging

The artificial beach environment, in either horizontal or vertical configurations, was placed into the same fluoroscope described in Chapter 2 (Figure 4.5C). A ghost crab, equipped with x-ray markers, was placed inside the artificial beach environment and allowed to begin burrowing in a self-directed fashion. Due to imaging constraints, the room dedicated to x-ray imaging was kept completely dark while the crab was burrowing. The x-ray video was captured by a camera (Phantom v9.1, Vision Research, Wayne, NJ, USA). The ghost crab's behavior was continuously remotely monitored. If a crab did not begin burrowing within approximately 30 minutes, the trial

was discontinued. Once a crab began burrowing, videos approximately four minutes in length were captured every eight minutes. The trial ceased once the crabs either burrowed beyond the visible region (approximately 18 cm in diameter) or when the crabs ceased burrowing for at least 30 minutes.

Figure 4.6 shows video still images from both vertical (Figure 4.6A) and horizontal (Figure 4.6B) burrowing trials. All markers, the undisturbed substrate and the crab's burrow were all clearly visible. Videos were analyzed with FIJI (http://fiji.sc) and Cine Viewer (Vision Research, Wayne, NJ, USA).

Figure 4.5

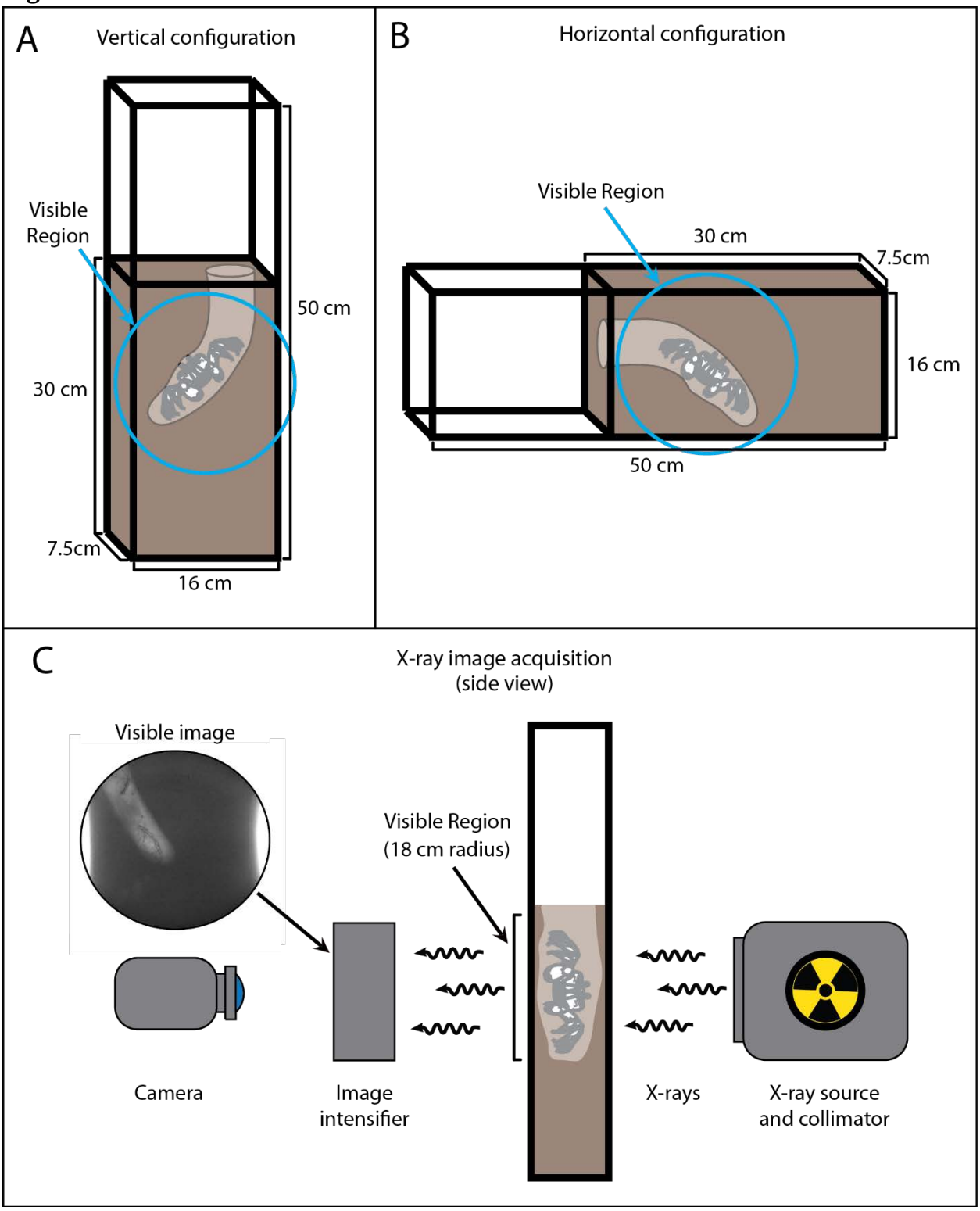
A
Vertical configuration
Visible Region
50 cm
30 cm
7.5cm
16 cm
B
Horizontal configuration
Visible Region
30 cm
7.5cm
16 cm
50 cm
C
X-ray image acquisition
(side view)
Visible image
Visible Region
(18 cm radius)
Camera
Image intensifier
X-rays
X-ray source and collimator

Figure 4.5: Enclosure design and x-ray image acquisition. This system is derived from the system used in Chapter 2, Section 2. **A**: The vertical configuration, where the subject crab is place on top of volume of damp sand (14% water by mass). The enclosure is constructed from aluminum framing, with clear acrylic panels. **B:** The horizontal configuration, where the crab is placed next to a volume of damp sand (14% water by mass). The horizontal enclosure is identical to the vertical enclosure except for the addition of a seal that prevents the subject crab from exiting the enclosure. **C:** Diagram illustrating the function of the x-ray imaging system and its modifications from that described in Chapter 2, Section 2. The x-ray source produces x-rays which pass though the enclosure. The Image intensifier converts the converts the x-rays into a visible image (video still image shown), that is recorded by the camera. This configuration permits a circular visible area, approximately 18 cm in diameter.

Figure 4.6

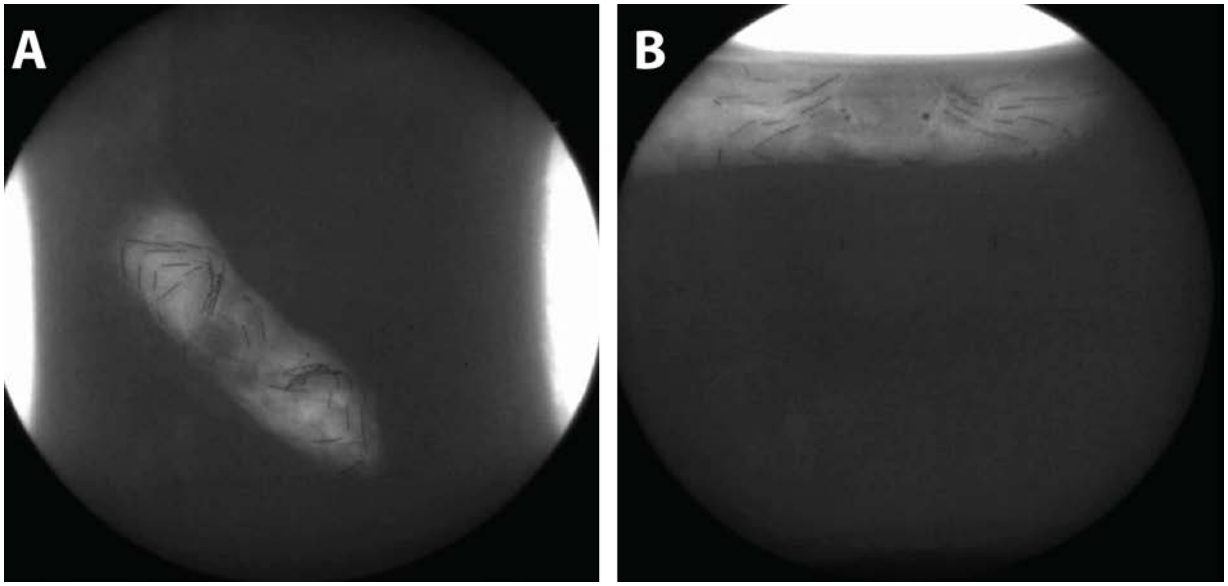

Figure 4.6: Still images from x-ray videos of vertical burrowing (A) and horizontal burrowing (B).

Burrowing Enclosure for Examining Effect of Moisture Content

An artificial beach environment was constructed from aluminum framing (80/20, Inc., Columbia City, IN, USA) and polycarbonate panels (McMaster-Carr, Elmhurst, IL, USA). The apparatus is diagramed in Figure 4.7. The overall dimensions of the environment were 100 cm wide by 110 cm high. The depth could be adjusted to any value between 0 cm and 10 cm using plastic spacers. The depth was adjusted before each trial to 75% of the subject crab's carapace width. Each crab performed at least four independent trials at a randomly-chosen GMC of approximately 2%, 4%, 8% or 15%.

The enclosure was filled with wet granular media to a depth of 100 cm. A wide, flat bar was used to pack the substrate as it was added to the enclosure, ensuring a uniform packing density. A 10 cm high void was intentionally left to provide space for the crab to walk and begin burrowing in a self-directed fashion. The granular media was entirely composed of bead blasting material (uniform glass spheres, 100-200 μm in diameter; Grainger, Inc., Lake Forrest, IL, USA). Distilled water was added to the granular media to reach the required gravimetric moisture content and the mixture was tumbled until uniform in a small cement mixer (Harbor Freight, Calabasas, CA, USA). Samples of the substrate were collected as the enclosure was filled. These samples were weighed, dried and re-weighed, providing a secondary verification of the substrate's moisture content. The substrate was prepared immediately prior to use. Granular media were reused only after being completely dried using a combination of heat lamps and tumble drying. The packing density was measured at 0.49 ± 0.02 and the wet bulk density was 1.32 ± 0.06 g/cm^3. These values are consistent with typical values measured in the field.

Time-lapse Videography

Videos of the ghost crabs were obtained using an infrared time-lapse camera (Brinno TLC200 Pro equipped with IR lens; Brinno, Taipei City, Taiwan) and an infrared spotlight (Phantom Lite; Phantom Lite, LLC, Starrucca, PA, USA) (Figure 4.8). The infrared spotlight was placed on the opposite side of the enclosure as the camera, creating a silhouette of the burrow as it was constructed by the crab (Figure 4.9). After the crab was placed into the enclosure, the spotlight was activated, the room lights were turned off and the camera began capturing one frame per 10 seconds. Crabs were allowed to burrow for 18 hours, at which point the apparatus was dismantled and the crab was recovered.

Time-lapse Video Analysis

Time-lapse videos were analyzed using custom-written MATLAB scripts (MathWorks, Natick, MA, USA). These scripts identified the following burrowing performance metrics by locating the end of the burrow every five minutes:

1) Burrow length, the total distance covered by the burrow. (Figure 4.10A)

2) Maximum depth, the deepest point reached by the burrow at any point (Figure 4.10A).
3) Average burrow extension rate, which is calculated by averaging the extension per unit time for all data points.
4) Maximum burrow extension rate, the highest extension rate from the entire trial (Figure 4.10C)
5) Working ratio, the ratio of time spent actively extending the burrow to the total trial time (Figure 4.10B).

Tracking began when the crab started burrowing and ended after 18 hours or when the crab ceased making measurable progress for one hour.

Figure 4.7

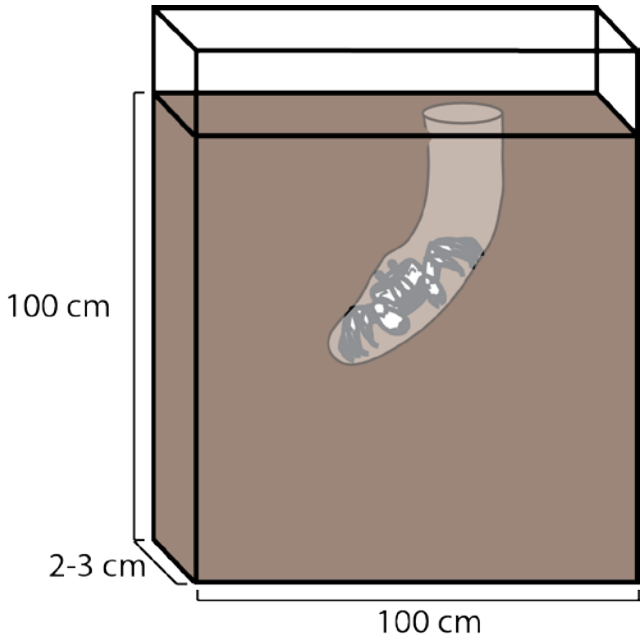

Figure 4.7: Schematic of the enclosure used for time-lapse burrowing studies. The chamber was constructed from an aluminum frame and clear polycarbonate panels. The chamber was filled to a depth of 100 cm with wet bead blasting media (glass spheres 100-200 um in diameter) of known moisture content. A 10 cm tall volume was left unfilled at the top of the chamber. Crabs were inserted into this open area and allowed to begin self-directed burrowing. The width of the enclosure was adjusted for each subject crab to approximately 75% of that crab's carapace width.

Figure 4.8

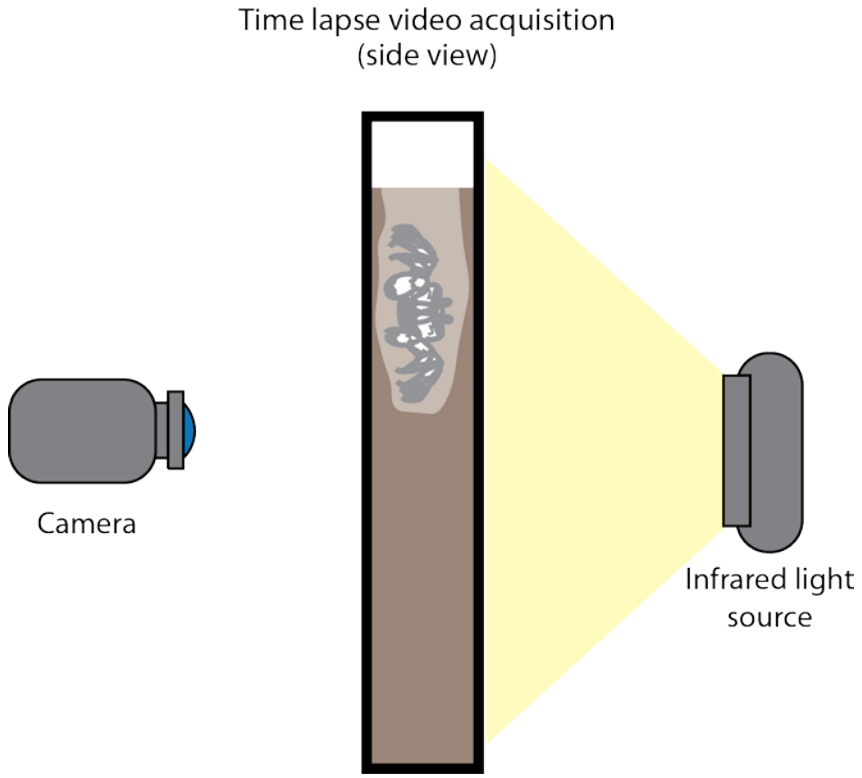

Figure 4.8: Schematic view of the method used to acquire time lapse videos of ghost crab burrowing. An infrared light source projects a beam onto the burrowing enclosure. A camera, equipped with an infrared lens, was placed on the other side of the burrowing enclosure. The camera recorded at 0.1 frames per second. The infrared light could not penetrate the undisturbed substrate but, as the crab burrowed, the light could pass through open areas of the burrow, creating a silhouette of the burrow at that time.

Figure 4.9

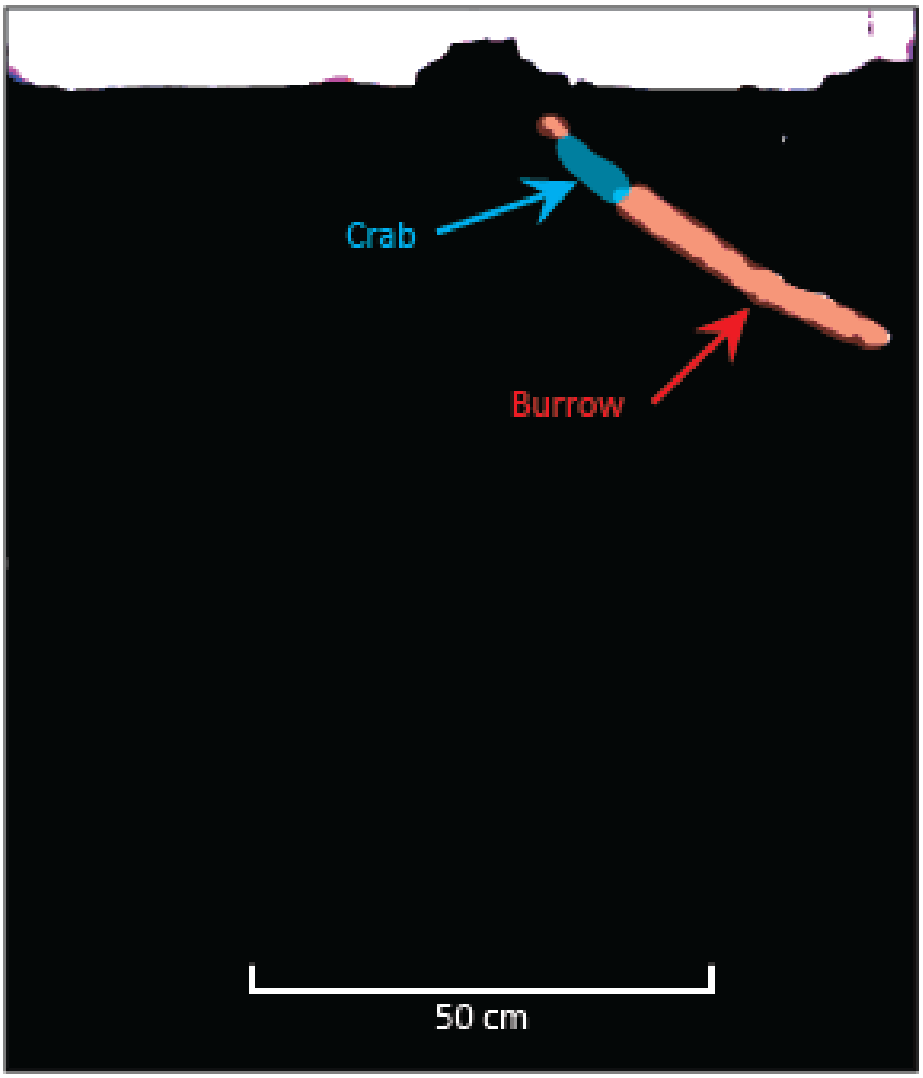

Figure 4.9: A video still image from a time lapse video of a ghost crab burrowing. The black area is undisturbed substrate. The white area is area without substrate. The burrow under construction is highlighted in red. The crab (inside the burrow) is highlighted in blue.

Figure 4.10

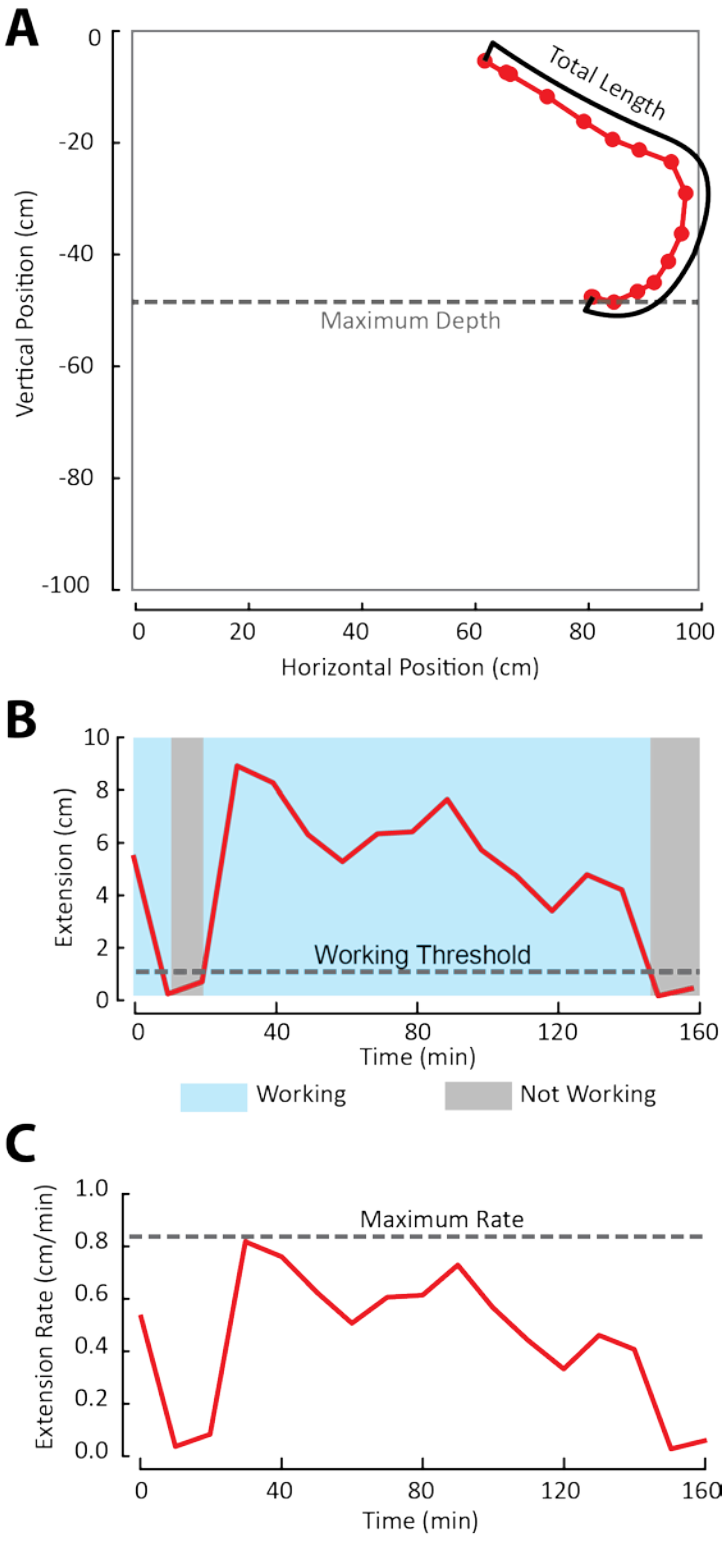
A
Total Length
Maximum Depth
Vertical Position (cm)
0
-20
-40
-60
-80
-100
0
20
40
60
80
100
Horizontal Position (cm)
B
Extension (cm)
10
8
6
4
2
0
Working Threshold
0
40
80
120
160
Time (min)
Working
Not Working
C
Extension Rate (cm/min)
1.0
0.8
0.6
0.4
0.2
0.0
Maximum Rate
0
40
80
120
160
Time (min)

Figure 4.10: Definitions of burrowing performance metrics used to assess time lapse burrowing videos. **A:** The end of the burrow was located every 5 minutes and its position in the chamber was digitized (red line). The maximum depth is the deepest point beneath the surface that the burrow reached at any time during the trial. The total length is total distance that the crab excavated. **B:** The distance excavated by the crab between two subsequent samples as a function of time (red line). If the crab extended the burrow more than one cm (i.e. "working threshold", the dashed line) between two measurements, the intervening time was noted as "working" (blue area). If the crab extended the burrow less than or equal to one cm, then the intervening time was noted as "not working" instead (grey area). The ratio of working time to the total time is the "working ratio". This is the proportion of time during which crab was actively extending the burrow. **C:** Burrow extension rate as a function of time (red line). The burrow extension rate is the distance the crab extended the burrow between two subsequent measurements, divided by the time between those two measurements. The maximum burrow extension rate (dashed line) is the highest extension rate observed at any point during the trial. The average burrow extension rate is average extension rate for the entire trial.

4.3 Results and Discussion

Burrowing Preferences and Environmental Conditions

In general, ghost crab burrowing in the Rachel Carson Reserve will encounter burrowing substrates that change with both location and depth. Four vertical transects were constructed (one in each sub-environment) and three independent measurements of all substrate properties were made at depth increments of 10 cm, for a total of 63 substrate properties measurements. The compressive strength (Figure 4.11), shear strength (Figure 4.12) and GMC (Figure 4.13) all vary substantially between sub-environments. Burrowing ghost crabs will encounter compressive strengths of 0.25 – 1.25 kgf/cm^2, shear strengths of 0 – 1.0 kgf/cm^2, GMC of 3 – 23% and saturation depths between 25 and 85 cm. Substrate bulk density and packing density were also measured. Bulk density (wet) was 1.1 – 1.7 g/cm^3. Packing density was between 0.4 and 0.6.

Small increases in depth can have large effects on the substrate properties. For example, a depth increase of only 10 cm can reduce compressive strength by a factor of four (Figure 4.11). In inter-dune and dune environments, the compressive strength at or near the surface can be approximately five times the lowest measured compressive strength in those sub-environments. Marsh-like and high tide sub-environments, however, are characterized by consistently low compressive strength.

The shear strength can also vary substantially (Figure 4.12). For example, the shear strength in the high tide line can vary up to four times the smallest value in that sub-environment. Notably, the shear strength of the substrate appears to collapse as the depth approaches the saturation depth. This observation corresponds with experimental studies of wet granular media, where cohesive forces were found rise with increasing moisture content before collapsing as the material approaches saturation (Mitari & Nori, 2006).

The GMC of each sub-environment increases with depth, though the rate of increase varies between each sub-environment (Figure 4.13). The saturation depth occurs when the GMC exceeds approximately 20%. Saturation depth is a critical feature of each sub-environment, varying from 25 cm (marsh-like) to 85 cm (Dune). This depth represents a hard limit on the maximum depth of a ghost crab's burrow as the burrow will flood and the walls will collapse, potentially drowning the crab (Milne & Milne, 1946).

Three independent surface transects were made in each of the sub-environments (nine total). A total of 204 burrows were counted over approximately 1000 m^2 of the reserve. Ghost crabs were found to inhabit all four of the sub-environments, as shown in Figure 4.14. Burrow density varied between approximately 0.075 and 0.14 burrows per m^2. The average burrow diameter was typically 25 to 30 mm.

No significant difference in burrow density between the sub-environments (ANOVA $F(3,11) = 1.1772$, $p = 0.3627$). Nor was a significant difference observed in average burrow diameter between sub-environment types (ANOVA $F(3,200) = 0.71$, $p = 0.5471$).

It is clear the substrate properties of the ghost crabs' natural habitat vary substantially with location and depth. However, the crabs did not demonstrate a clear preference for one sub-environment type over another. Furthermore, no significant difference in burrow diameter was observed between environment types. This suggests that ghost crabs, regardless of body size, possess robust burrowing strategies that allow them to burrow throughout the beach environment. Crab may still have preferences for burrowing in one environment over another. For example, certain burrow locations may confer additional resistance to desiccation or protection from predators (Chakrabarti, 1981). However, these results suggest that any observed differences are more likely due to behavioral effects, rather than mechanical interaction with the substrate.

Figure 4.11

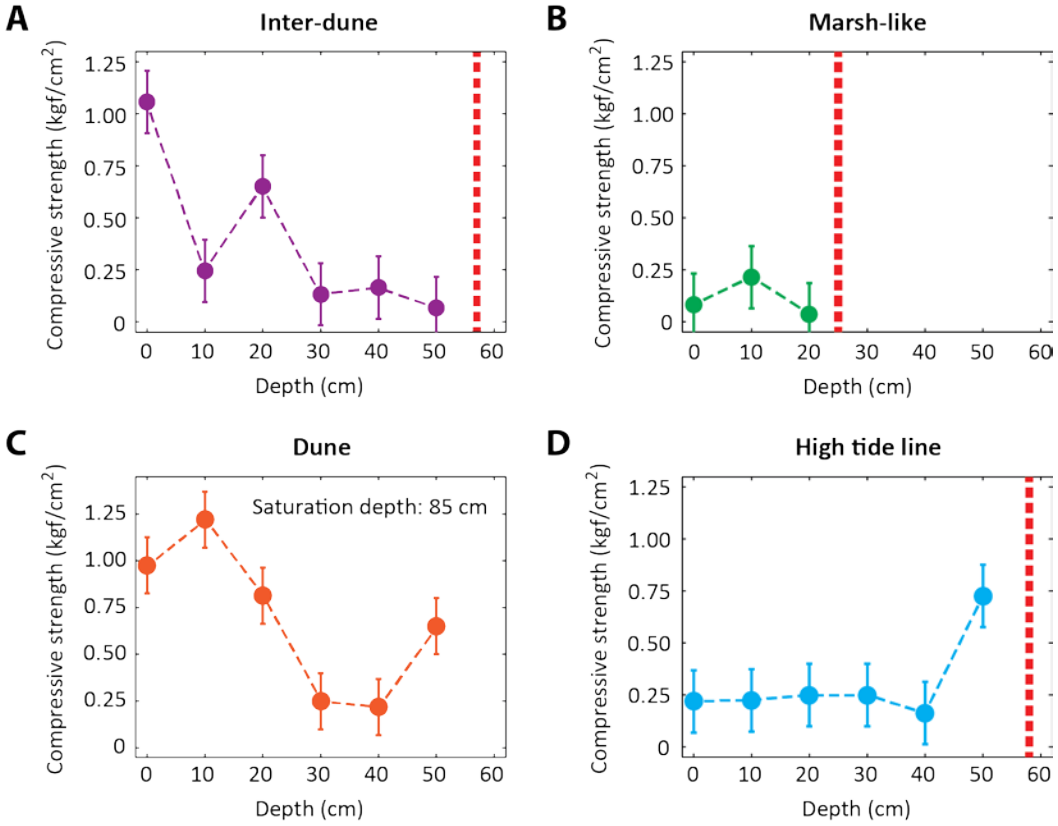

Figure 4.11: Substrate compressive strength as a function of depth. The compressive strength is the pressure (in kgf/cm^2) required to insert a spring-loaded penetrometer tester 5 mm into the substrate. Red dashed lines indicate the depth at which the substrate is completely saturated with water, entering the slurry state. It is not possible for the ghost crabs to dig past this point. Error bars indicate propagated measurement uncertainty (incorporating both inherent instrument error and the variation of subsequent measurements). **A:** Substrate compressive strength for the inter-dune region. The saturation depth was approximately 67 cm. **B:** Substrate compressive strength for the marsh-like region. The saturation depth was approximately 25 cm. **C:** Substrate compressive strength for the dune region. The saturation depth was approximately 85 cm (not shown on this graph). **D:** Substrate compressive strength for the high-tide line. The saturation depth was approximately 58 cm.

Figure 4.12

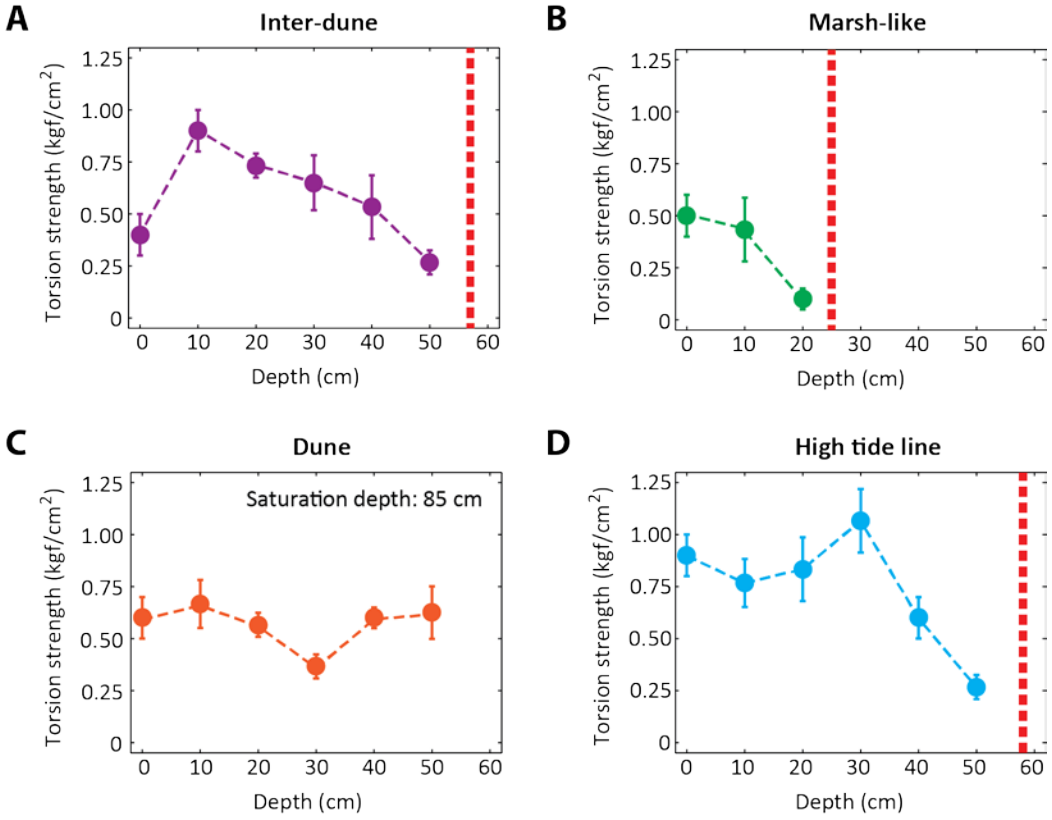

Figure 4.12: Substrate torsion strength as a function of depth. The torsion strength is the pressure (in kgf/cm^2) required to shear away a circular area of the substrate using a spring-loaded sheer strength tester. Red dashed lines indicate the depth at which the substrate is completely saturated with water, entering the slurry state. It is not possible for the ghost crabs to dig past this point. Error bars indicate propagated measurement uncertainty (incorporating both inherent instrument error and the variation of subsequent measurements) **A:** Substrate torsion strength for the inter-dune region. The saturation depth was approximately 67 cm. **B:** Substrate torsion strength for the marsh-like region. The saturation depth was approximately 25 cm. **C:** Substrate torsion strength for the dune region. The saturation depth was approximately 85 cm (not shown on this graph). **D:** Substrate torsion strength for the high-tide line. The saturation depth was approximately 58 cm.

Figure 4.13

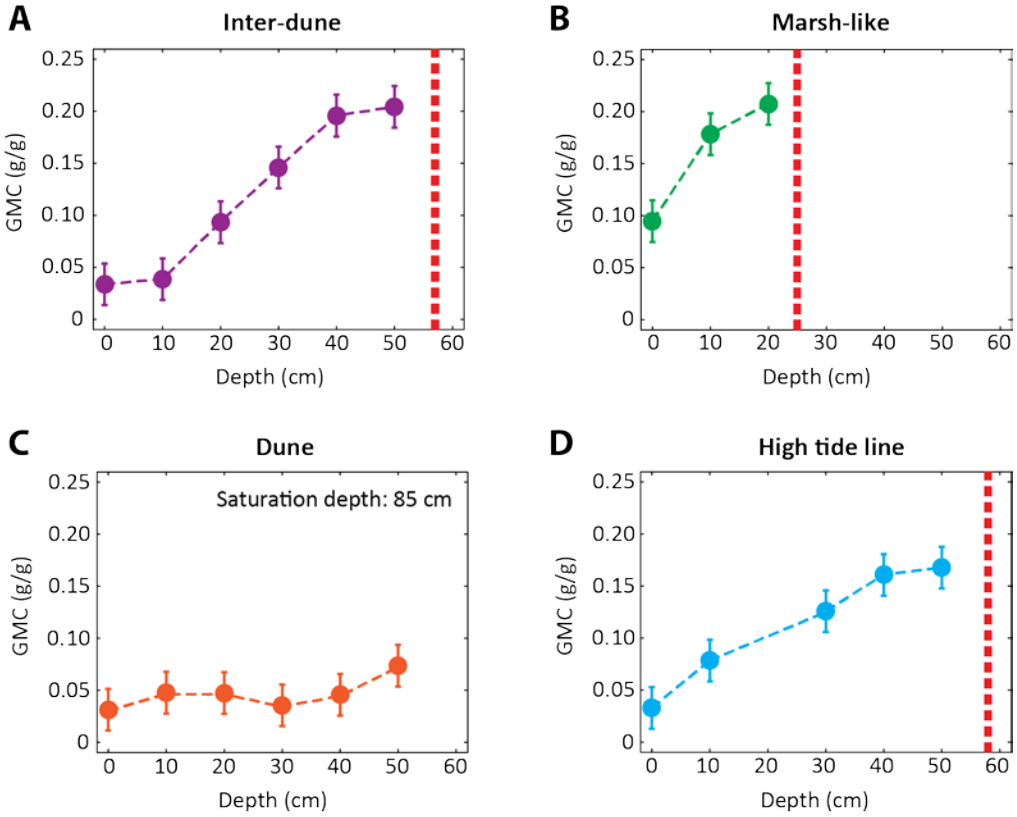

Figure 4.13: Substrate gravitational moisture content (GMC) as a function of depth. The GMC is the ratio of water in a substrate sample to the total mass of that sample. Red dashed lines indicate the depth at which the substrate is completely saturated with water, entering the slurry state. It is not possible for the ghost crabs to dig past this point. Error bars indicate propagated measurement uncertainty (incorporating both inherent instrument error and the variation of subsequent measurements) **A:** GMC for the inter-dune region. The saturation depth was approximately 67 cm. **B:** GMC for the marsh-like region. The saturation depth was approximately 25 cm. **C:** GMC for the dune region. The saturation depth was approximately 85 cm (not shown on this graph). **D:** GMC for the high-tide line. The saturation depth was approximately 58 cm.

Figure 4.14

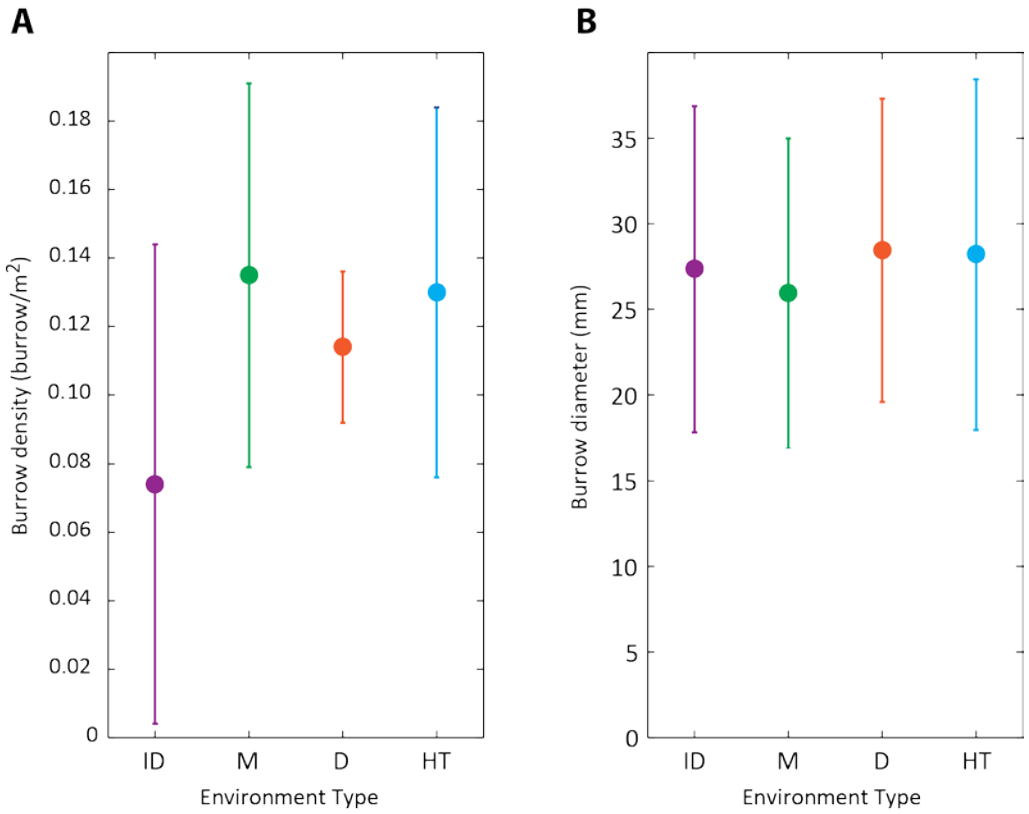

Figure 4.14: Burrow density and burrow sizes for the four environment types. **ID:** inter-dune, **M:** marsh-like, **D:** dune, **HT:** high tide. A total of 204 burrows were counted across all transects. For ID, M and HT environment types, the total area of each transect was 112 m^2. For D environment types, the area varied between 96 and 182 m^2. No significant difference was observed in either burrow density or burrow diameter in any of the environments studied. **A:** The number of ghost crab burrows (of any size) per square meter in each environment type. Error bars indicate the standard deviation of the total number of burrows in a single transect. **B:** The average burrow entrance diameter for each environment type. Error bars indicate the standard deviation of the burrow size for all transects in that environment type.

Burrow Casting

A total of 23 burrows were collected from the field site. Example burrow casts are shown in Figure 4.15. Of these burrows, 48% had a branching structure, producing a Y-shaped structure. The longest burrow excavated was 104 cm long. The deepest burrow extended 80 cm below the surface. Resident crabs were recovered for 17 of the 23 burrows collected.

Notably, large obstacles, such as shells or plant material, were frequently found embedded in the walls of the burrow. In most cases, the burrow continued past this obstacle, demonstrating that ghost crabs can navigate around impenetrable obstacles while burrowing. In other cases, the obstacle occurred at the end of a burrow or branch, as shown in Figure 4.16. This suggests that large hard obstacles may represent one of the principle limits on ghost crab burrowing.

A significant correlation between the carapace width of the resident crab and the diameter of the burrow (Figure 4.17; $n = 17$; $R^2 = 0.844$). This corresponds with previous findings in related ghost crabs (Chan et al., 2006). Ghost crabs may build burrows that are closely related to their body size to minimize the amount of material they must transport. Additionally, small burrow diameters may exclude larger crabs from invading the burrows of smaller crabs, protecting the smaller crab from predation and from losing its energetic investment in the burrow.

No correlation was found between burrow length (Figure 4.18; $n = 17$; $r^2 = 0.108$), burrow depth (Figure 4.19; $n = 17$; $r^2 = 0.002$) and burrow structure (Figure 4.20; $n = 17$; T-test: $p= 0.1203$). While these results cannot address the specific behaviors used to construct a burrow or the comparative energetic costs, they do suggest that ghost crabs of all sizes can produce comparable burrows.

Measurements of the compressive strength were not associated with the burrows' maximum depth (Figure 4.21A; $n = 23$; Paired t-test: $p = 0.96$). Nor was compressive strength associated with the burrows' maximum depth (Figure 4.21B; $n = 23$; Paired t-test: $p = 0.87$). The range of shear and compressive strength measurements were not outside the range measured in during vertical transects. Similar to the results discussed in the previous section, this suggests that ghost crabs are able to burrow through the entire range of conditions. However, these results cannot state whether the crabs adopt alternate or compensatory burrowing behaviors in response to the substrate properties.

GMC, unlike compressive and shear strength, was associated with the maximum burrow depth (Figure 4.21C; $n = 23$; Paired t-test: $p < 0.01$). This relationship is likely due in part to the general increase in moisture content with depth, as discussed in the previous section. However, no burrow was found to extend into substrate with a GMC exceeding approximately 22% and only two burrows out of 23 were found to extend beyond 19.3% GMC (Figure 4.22). This is very likely due to the collapse of substrate cohesion as the moisture content approaches saturation (Mitari & Nori, 2006). However, crabs do not necessarily continue burrowing until they reach the saturation depth. Only two burrows out of 23 extend beyond a depth of 58 cm. While the forces required to burrow have been shown to increase with depth (Sharpe, et al., 2012; Winter,

et al., 2012), it is difficult to estimate how burrowing forces change with depth in ghost crab burrows since burrows necessarily create a new air/substrate interface.

Overall, the only burrow feature significantly correlated with ghost crab size is burrow diameter. All other features (length, depth and branching structure) are equivalent for ghost crabs with 15 – 50 mm carapace widths. This suggests that the hypothesis stated in the introduction, that smaller ghost crabs produce different structures, should be generally rejected. The effect of body size on burrowing strategy, however, cannot be rejected yet. It is possible that smaller ghost crabs maintain this overall performance by adopting compensatory strategies. The performance envelope of ghost crab burrowing appears primarily determined by burrow depth and moisture content. Crabs burrow between depths of approximately 0 cm and 60 cm and between moisture contents of 4% and 18%. Excluding subterranean obstacles (e.g. shells), ghost crabs are able to burrow in the entire range of substrate shear and compressive strengths present in their habitat.

Figure 4.15

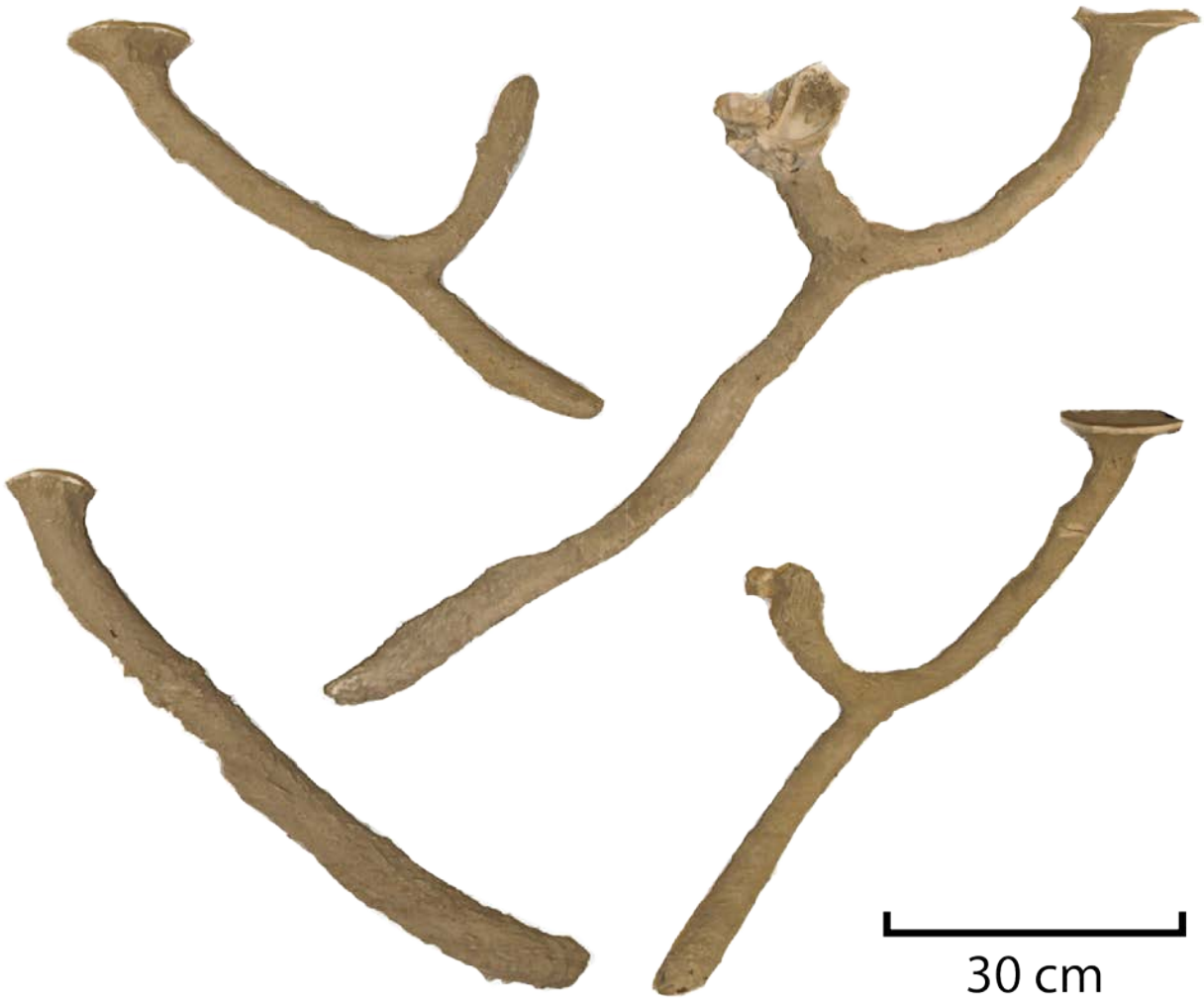

Figure 4.15: Images of four burrow casts obtained in filed data collection.

Figure 4.16

Figure 4.16: An oyster shell embedded in a burrow cast. While burrowing, ghost crabs encounter many obstacles, including shells, stones and plant fibers. Small obstacles may be transported out of the burrow by a ghost crab but larger obstacles may require the crab to change their burrowing strategy or path.

Figure 4.17

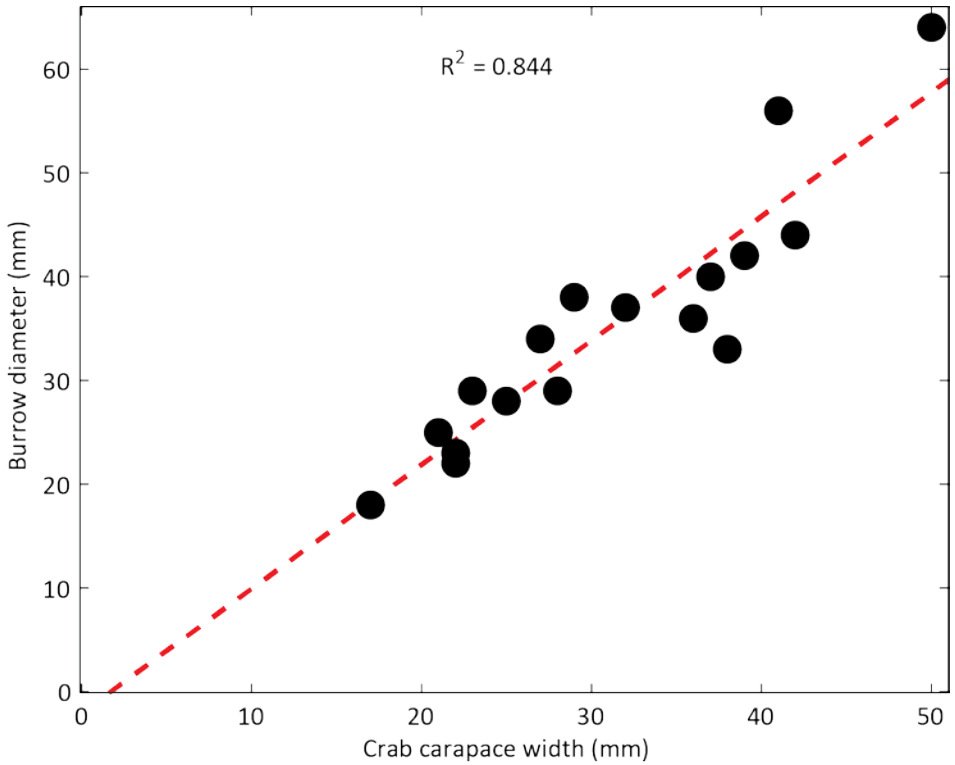

Figure 4.17: Crab carapace width vs. the same crab's burrow diameter. The diameter of a crab's burrow is linearly correlated with the crab's body size.

Figure 4.18

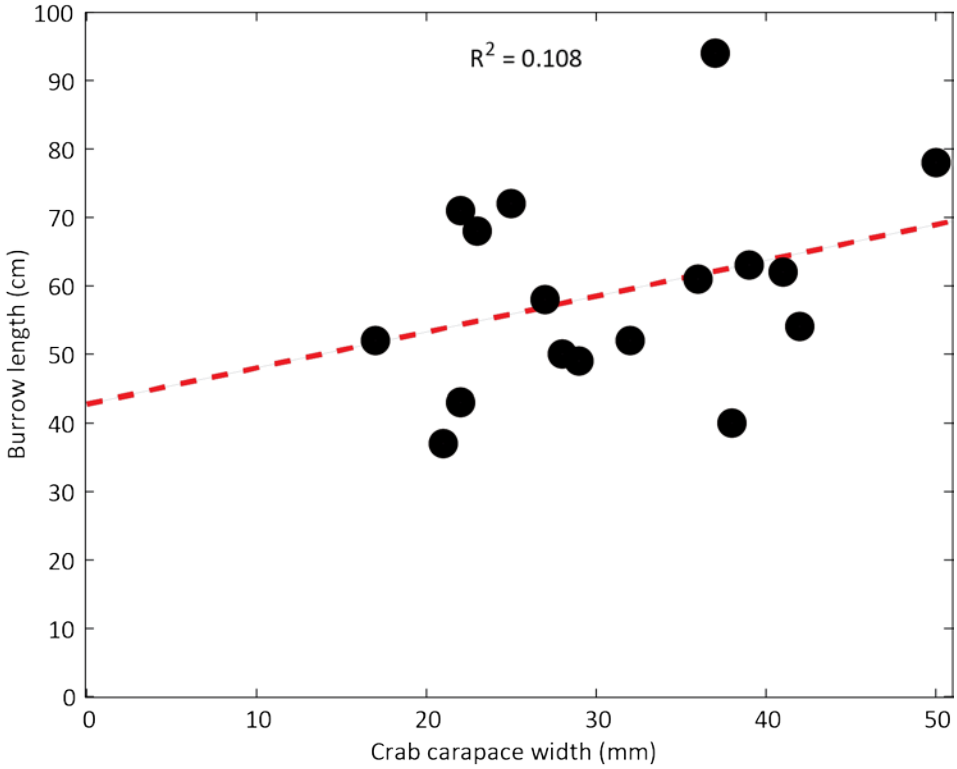

Figure 4.18: Burrow length as a function of crab size. Crab carapace width was not an accurate predictor of the burrow length.

Figure 4.19

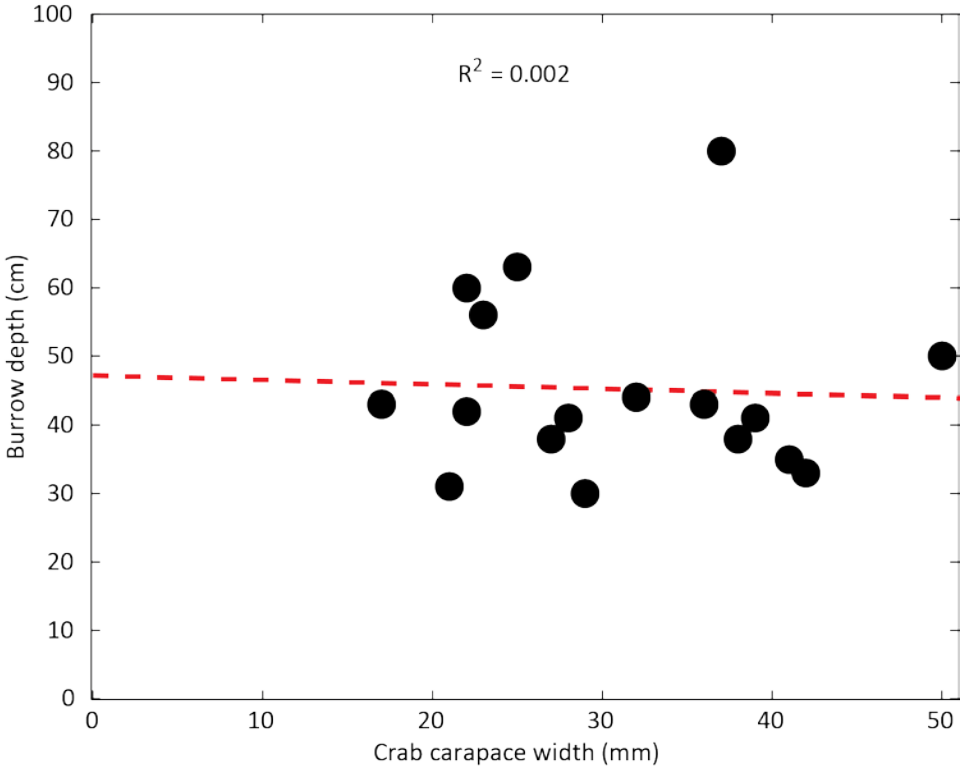

Figure 4.19: Burrow depth as a function of crab size. Crab carapace width was not an accurate predictor of the burrow depth.

Figure 4.20

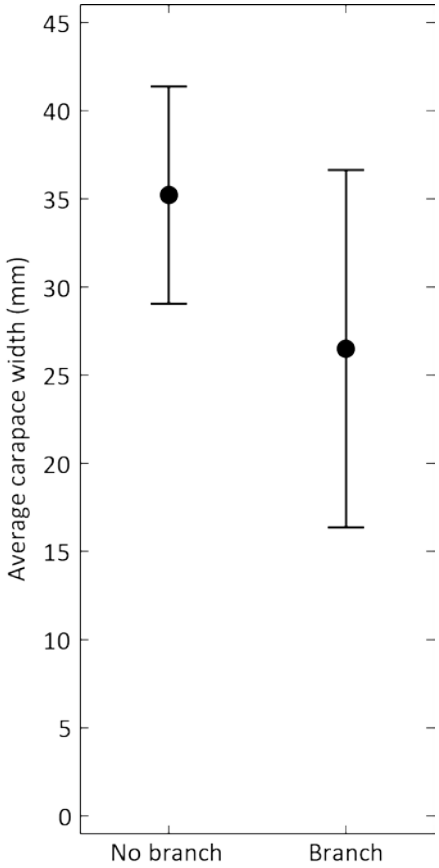

Figure 4.20: The average crab size for all burrows with branches and without branches. Error bars indicate the standard deviation of these populations. No significant difference was observed, meaning large and small crabs were equally likely to inhabit branching burrows

Figure 4.21

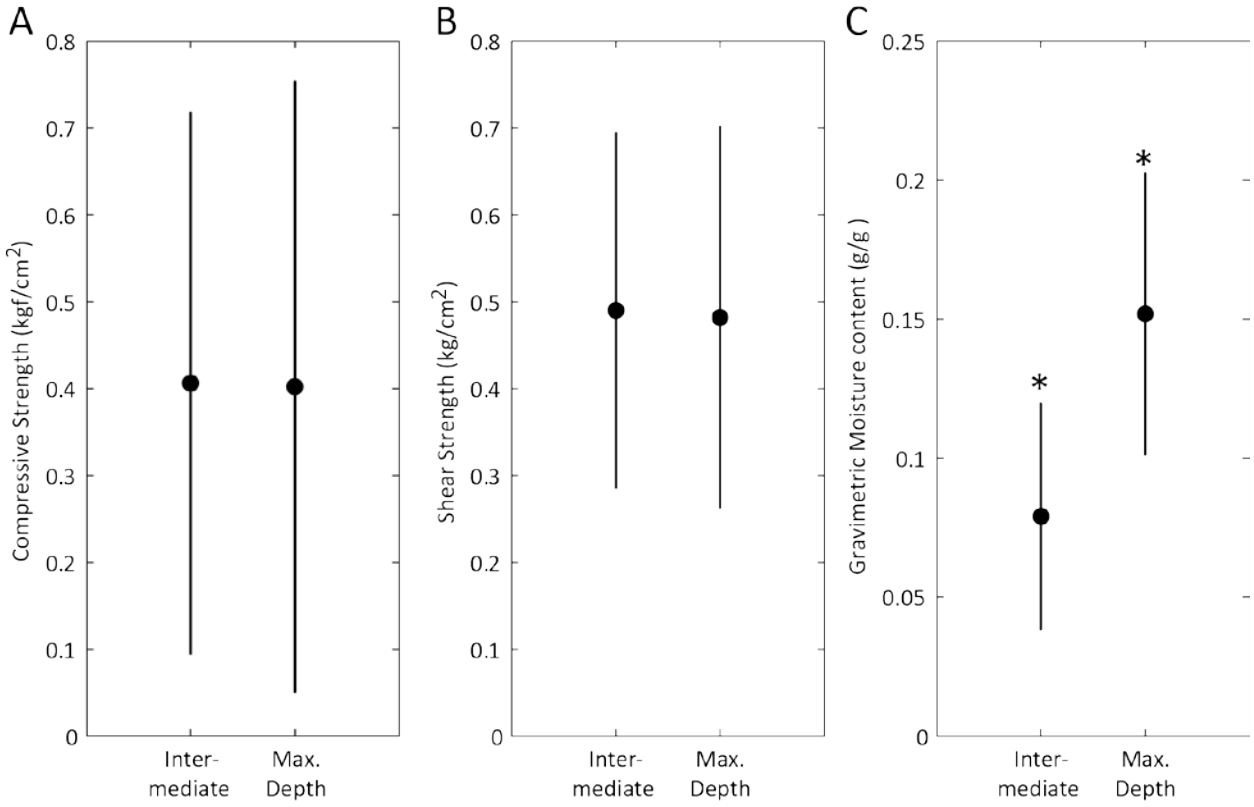

Figure 4.21: Mechanical properties of the substrate near excavated burrows. As the burrow casts were excavated, the compressive strength, shear strength and gravimetric moisture content were sampled at 10 cm depth and the burrow's maximum depth. A third measurement was taken at one-half of the burrow's maximum depth. Dots represent the average values for all values at intermediate (10 cm depth and on-half maximum depth) and maximum depths. Error bars indicate the standard deviation. **A:** Compressive strength. No significant difference was observed between intermediate values and the value at the burrow's maximum depth. **B:** Shear strength. No significant difference was observed between intermediate values and the value at the burrow's maximum depth. **C:** Gravimetric moisture content. The GMC was significantly greater at the burrow's maximum depth.

Figure 4.22

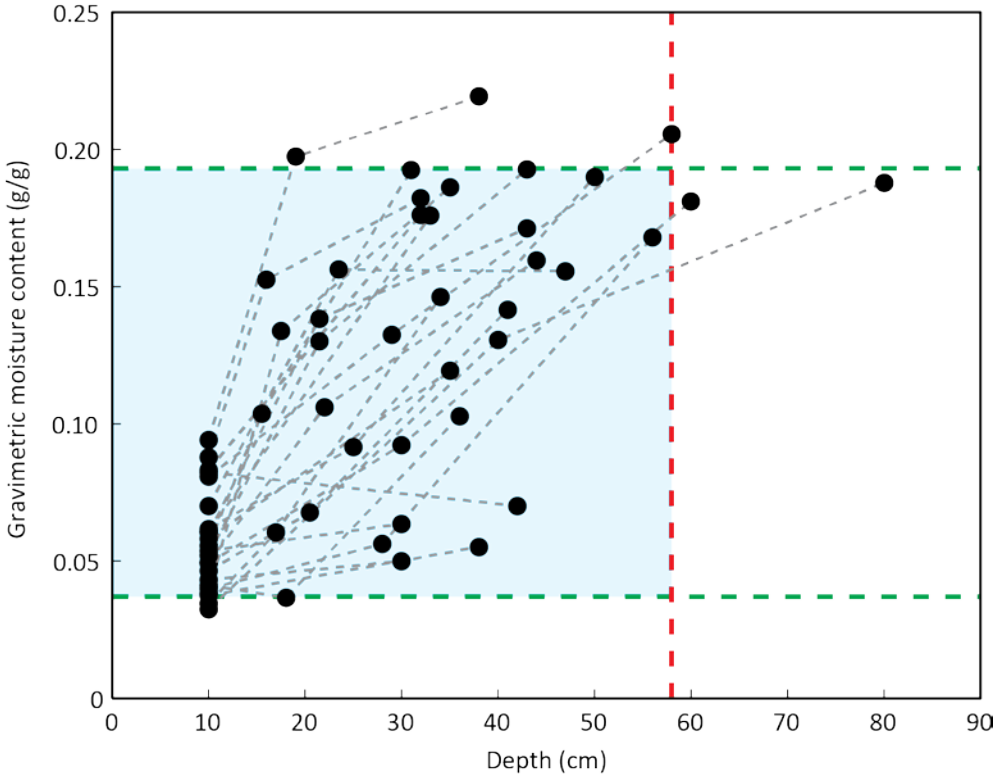

Figure 4.22: Gravimetric moisture content (GMC) as a function of burrow depth for all the excavated burrows. As the burrow was excavated, the GMC was sampled at 10 cm depth, one-half of the maximum depth of the burrow and the maximum burrow depth. Grey dashed lines indicate samples from a single burrow. The blue shaded area indicates the crabs' typical burrowing space. 90% of the observed burrow depths and GMC lie within this area. Specifically, 90% of the excavated burrows had a maximum depth of less than 58 cm (red dashed line) and 90% of the excavated collected GMC samples were between 3.7% and 19.3% (green lines). Generally, the moisture content increases with depth. At GMC above about 20%, substrate cohesion begins to collapse (Monaenkova et al., 2013). Since burrows are rarely observed extending into substrate with GMC > 20%, regardless of depth, GMC may be one of the major environmental conditions limiting burrowing performance.

Horizontal vs. Vertical Burrowing

Four crabs were presented with both horizontal and vertical trials. Each subject performed one horizontal trial and one vertical trial.

Ghost crabs demonstrated the ability to produce burrows in both horizontal and vertical conditions. Notably, horizontally burrowing ghost crabs were able to extend their burrows significantly faster than vertically burrowing crabs (Figure 4.23; $n = 23$; Paired t-test: $p < 0.001$). The average horizontal burrow extension rate was approximately three times the vertical burrow extension rate. In general, the burrowing behavior in horizontal and vertical conditions appeared equivalent. All ghost crabs demonstrated the same excavation cycle structure described in Chapter 2. All excavation behaviors, including hook-and-pull, scratch digging and body rotation, were observed from all crabs in horizontal and vertical conditions. Transportation and manipulation behaviors were also equally present.

It is interesting that body rotations were observed in both horizontal and vertical burrowing. While a vertically burrowing crab may have no preferred orientation within the burrow since the direction of gravity is close to the principal axis of the burrow, horizontally burrowing crabs appeared to prefer a 'right-side-up' orientation within the burrow while walking. During excavation, however, horizontally burrowing crabs used body rotations to change their orientation with respect to gravity, lending some credence to the hypothesis that body rotations are important to ghost crab burrowing either by stabilizing the burrow walls or by expanding the available workspace.

Burrowing behavior was quantified using the same metrics developed to measure inter-individual variation in Chapter 2. These metrics specifically included:

1) Excavation cycles per time
2) Total time spent performing hook-and-pull behaviors during an excavation cycle
3) The number of hook-and-pull behaviors per excavation cycle

Consistent with the results presented in Chapter 2, no individual effects were observed, permitting data for all individuals to be pooled.

No significant difference was observed between horizontal and vertical conditions for either hook-and-pull duration (Figure 4.23B; $n = 128$; Paired t-test: $p = 0.36$) or the number of hook-and-pulls per excavation cycle (Figure 4.23C; $n = 23$; Paired t-test: $p = 0.32$). The results suggest that the basic burrowing behavior remains unchanged even though horizontally burrowing crabs are able to extend their burrows significantly faster. This suggests that ghost crab burrowing performance responds to changing substrate conditions but that the basic motion pattern may be generally stereotyped.

However, the number of complete excavation cycles per minute significantly increased in the horizontal condition (Figure 4.23D; $n = 23$; t-test: $p < 0.01$). This is primarily because crabs reduced the amount of time they spent being inactive. Reduced inactivity may be related to lower

energetic costs of burrowing due to reduced substrate transportation costs. In the horizontal condition, the gravitational potential energy of the transported substrate is near-constant, whereas the vertical condition requires the gravitational potential energy to be increased during transportation. By substantially reducing transportation costs, crabs may be able to maintain a higher burrow extension rate, while keeping the average power output the same.

However, higher horizontal burrow extension rates may also be due to behavioral motivation or the substrate properties. Because ghost crabs produce burrows for protection from predators and environmental stresses (Milne & Milne, 1946) and the protection conferred by a burrow is related to the burrow's depth (Chan et al., 2006), horizontally burrowing crabs may have increased their burrow extension rate in an effort to compensate for reduced protection. The substrate's material properties may also be responsible for reducing the burrow extension rate with depth. The forces required to burrow have been shown to increase with depth for animals moving within a sandy substrate (Sharpe et al., 2012; Winter et al., 2012). It is unknown, however, how ghost crab burrowing forces change with depth due to the complex nature of the substrate and animal/substrate interaction (Ding et al., 2010). Resolving which of these possibilities (energetic, behavioral and/or material) explains the observed difference in performance will require additional experiments. Energetic studies (similar to those employed by Vleck (1979)) and empirical models of animal/substrate interactions (Li, et al., 2013) may be particularly valuable.

Figure 4.23

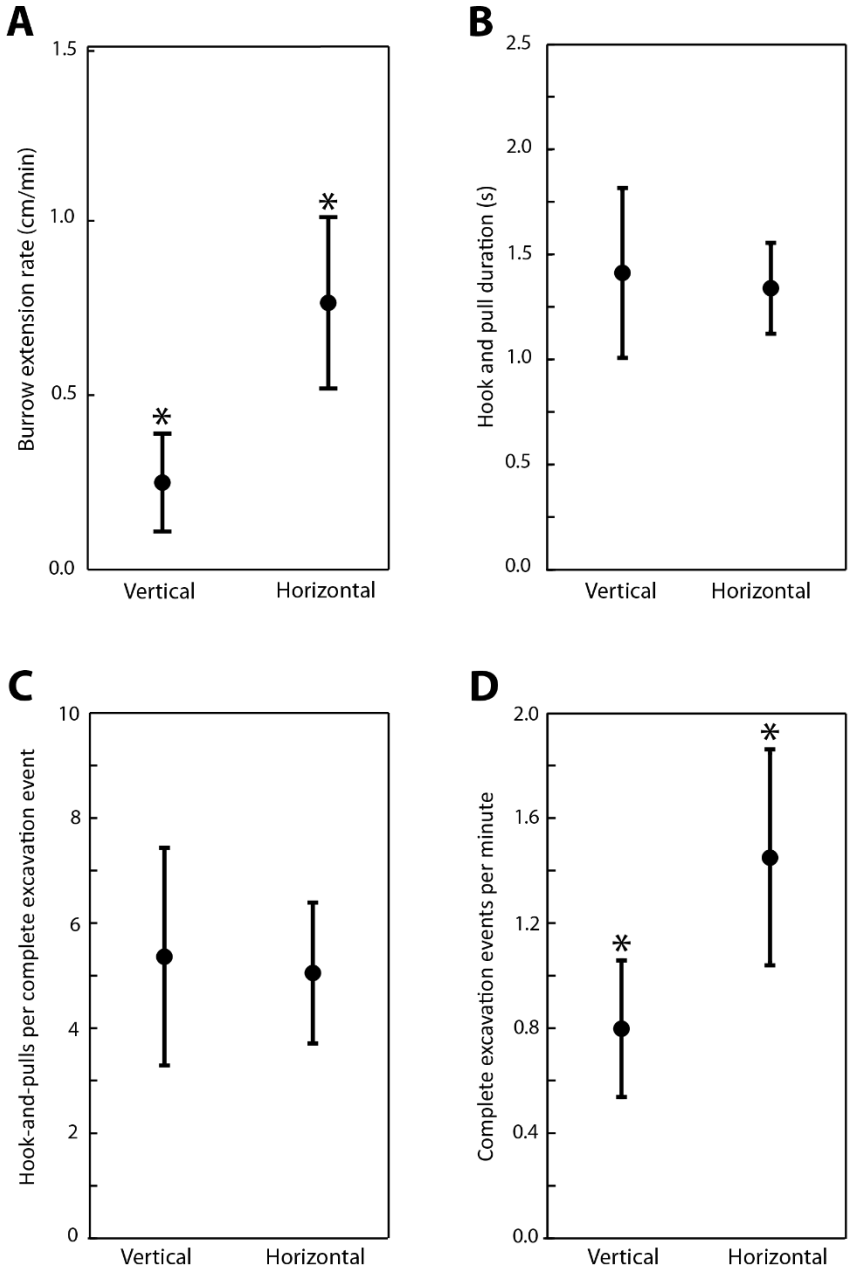
A
Burrow extension rate (cm/min)
1.5
1.0
0.5
0.0
*
*
Vertical
Horizontal
B
Hook and pull duration (s)
2.5
2.0
1.5
1.0
0.5
0.0
Vertical
Horizontal
C
Hook-and-pulls per complete excavation event
10
8
6
4
2
0
Vertical
Horizontal
D
Complete excavation events per minute
2.0
1.6
1.2
0.8
0.4
0.0
*
*
Vertical
Horizontal

Figure 4.23: Burrowing performance in horizontal and vertical conditions. As no significant individual effects were observed, results from all individuals were pooled. **A:** The average burrow extension rate (in cm per minute) for horizontal and vertical conditions. Error bars indicate the standard deviation. The observed horizontal burrow extension rate was significantly faster than the vertical burrow extension rate. **B:** The average duration of a hook-and-pull in horizontal and vertical conditions. Error bars indicate the standard deviation. No significant difference was observed. This suggests that ghost crabs do not maintain the faster burrow extension rates by collecting material faster. **C:** The average number of hook-and-pulls per excavation event for horizontal and vertical conditions. Error bars indicate the standard deviation. No significant difference was observed. This suggests that ghost crabs do not maintain the faster burrow extension rates by collecting more material per excavation event. **D:** The average number of complete excavation events per minute for horizontal and vertical conditions. Error bars indicate the standard deviation. The number of excavation events per minute was significantly faster in the horizontal condition. This suggests that ghost crabs maintain a higher burrow extension rate by reducing resting/inactive time.

Figure 4.24

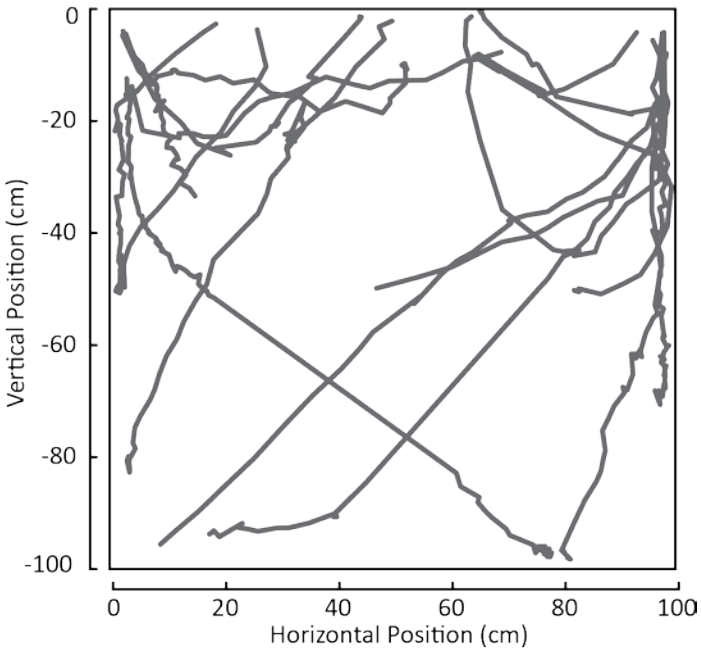

Figure 4.24: Burrow trajectories for all individuals and all trials. Crabs were able to access all areas of the burrowing enclosure by burrowing.

Effect of Moisture Content on Burrowing Performance

The ghost crabs demonstrated the ability to burrow inside the enclosure, producing 17 burrows in total and reaching nearly every part of the enclosure (Figure 4.24). The sum of all burrow lengths was approximately 14 m. Total burrowing time was approximately 136 hours. Each crab performed at least four trials in a substrate with a randomly-chosen GMC of either 2%, 4%, 8% of 15%. All observed burrows had a non-branching structure, contrasting with field studies showing that 48% of ghost crab burrows are Y-shaped. All data were pooled as no individual effects were observed.

No correlation was observed between any of the metrics and the substrate moisture content (Figure 4.25). Linear models of substrate moisture content's effect on burrowing performance were did not accurately predict the observed results (maximum depth $r^2 = 0.093$; total length $r^2 = 0.017$; average extension rate $r^2 = 0.009$; maximum extension rate $r^2 = 0.005$; working ratio $r^2 = 0.047$). Second-order polynomial models, approximating the hypothesized relationship between performance and moisture content illustrated in figure 4.2, were also unable to predict the observed results (maximum depth $r^2 = 0.152$; total length $r^2 = 0.065$; average extension rate $r^2 = 0.019$; maximum extension rate $r^2 = 0.007$; working ratio $r^2 = 0.059$).

Instead, the ghost crabs maintained equivalent performance across the entire range of experimental moisture contents. This suggests that ghost crabs are substrate generalists that can burrow effectively in a range of conditions. While the variability in the crabs' burrowing performance was very high and it is possible that ghost crab performance may be influenced by behavioral or motivational effects, these results support rejection of the hypotheses that burrow depth, burrow length, burrow extension rate or the working ratio are related to the substrate's moisture contents between 3% and 15% GMC.

Follow-up studies, examining the crab's burrowing habits in three dimensions and further quantifying the kinematics and kinetics of ghost crab burrowing, may offer more insight into how burrowing performance corresponds to the substrate's material properties and the mechanics of any potential compensatory mechanisms. Ghost crabs may be able to employ compensatory mechanisms that allow them to maintain burrowing performance over a wide range of substrate conditions. Potential compensatory mechanisms may include (but are not limited to) altered burrowing strategies or modified burrowing kinematics/kinetics.

Figure 4.25

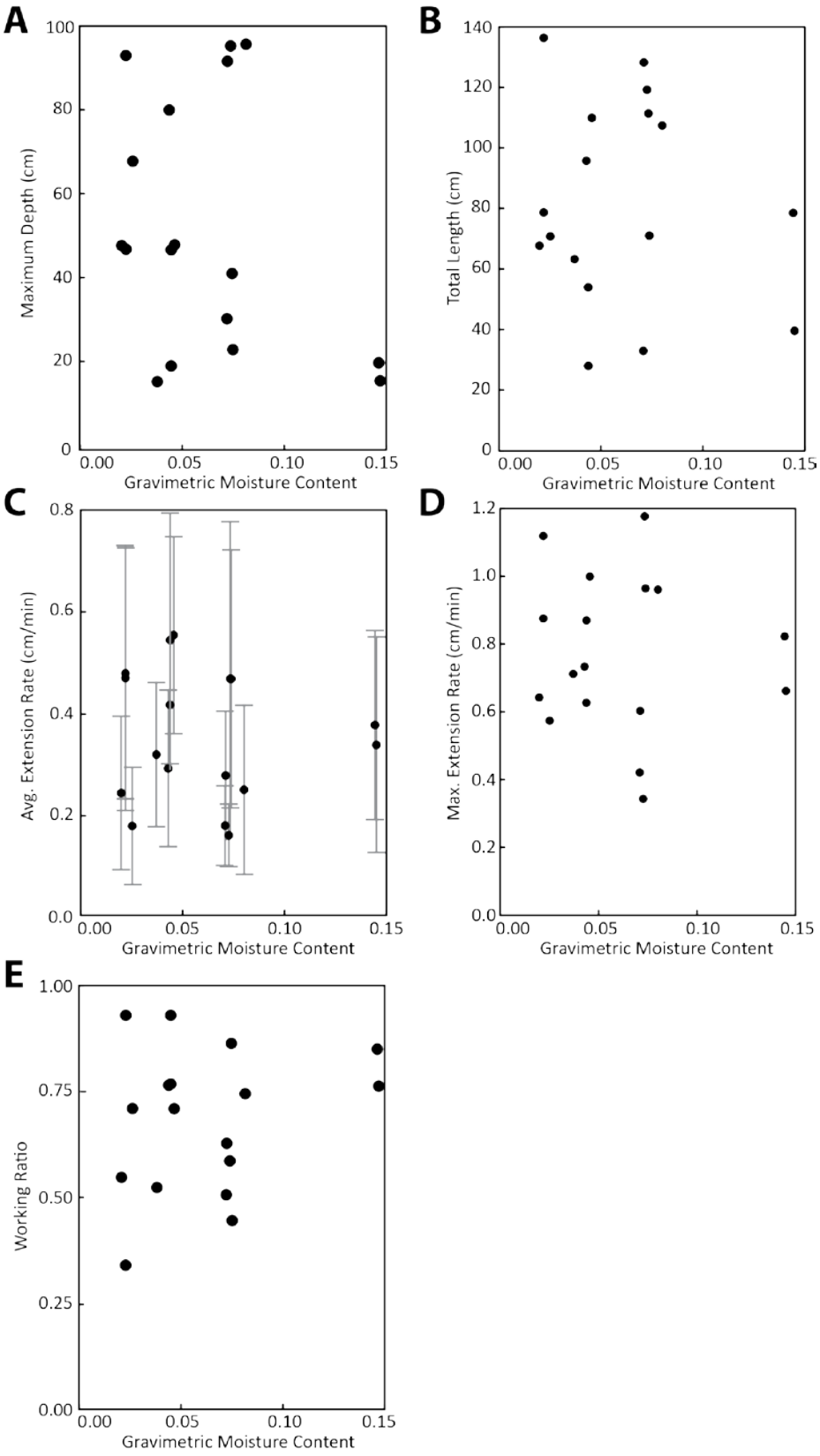
A
Maximum Depth (cm)
Gravimetric Moisture Content
B
Total Length (cm)
Gravimetric Moisture Content
C
Avg. Extension Rate (cm/min)
Gravimetric Moisture Content
D
Max. Extension Rate (cm/min)
Gravimetric Moisture Content
E
Working Ratio
Gravimetric Moisture Content

Figure 4.25: Burrowing performance metric for the time lapse studies. Each point represents the value for one trial. As no significant individual effects were observed, results from all individuals were been pooled. **A:** Maximum depth as a function of gravimetric moisture content (GMC). **B:** Total burrow length as a function of GMC. **C:** Average burrow extension rate as a function of GMC. Error bars indicate the standard deviation of burrow extension rate for that trial. **D:** The maximum burrow extension rate as a function of GMC. **E:** The working ratio (the ratio of time spent actively extending burrow to total trial time) as a function of GMC. For all metrics measured here, no correlation was detected, suggesting the crabs may be able to maintain consistent burrowing performance across a range of substrate conditions. This, in turn, suggests (but does not prove) that crabs may be employing compensatory mechanisms.

4.4 Conclusions

Burrowing Preferences and Environmental Conditions

Ghost crabs burrow in a highly variable environment where the properties of the substrate can change substantially with both depth and location (Figures 4.11, 4.12, 4.13). Despite this variation, ghost crabs demonstrated the ability to burrow throughout the beach environment studied here. No correlation between environment type and burrow density (Figure 4.14A) or burrow diameter (Figure 4.14B) was found. This suggests rejection of the general hypothesis that ghost crabs prefer to burrow in a certain substrate due to that substrate's material properties.

Burrow Casting

Burrow casts show that burrow diameter is significantly correlated with ghost crab body size (Figure 4.17), confirming the hypothesis that burrow diameter is related to ghost crab size. This is similar to findings in related crabs (Chan et al., 2006). This may be explained by an attempt to minimize the energetic costs of burrowing since the costs of substrate transportation are related to the burrow diameter. Additionally, small burrows may protect the resident crab from larger crabs entering the burrow. The other measured burrow structure properties (burrow length, burrow depth and burrow structure) were not correlated with crab body size, however (Figures 4.18, 4.19 and 4.20). It appears that crabs of all sizes are capable of constructing generally equivalent burrows, suggesting rejection of the hypothesis that burrow structure (excluding burrow diameter) can be predicted by ghost crab size.

The only substrate that appears to limit ghost crab burrowing is substrate moisture content (Figure 4.21); sufficiently high moisture contents collapse the substrate's cohesive forces (Mitari & Nori, 2006) and prevent crabs from extending the open structure of the burrow further. Thus, the crabs' typical performance envelope is bounded by moisture contents of 4% to 18% GMC and depths between 0 cm and 60 cm (Figure 4.22).

While it is possible that ghost crabs can continue burrowing within saturated substrates as demonstrated by other beach dwelling animals including the mole crabs (Trueman, 1970) and razor clams (Winter, et.al., 2012), this appears unlikely. The burrowing behavior described in Chapter 2 would not function because ghost crab burrowing falls into a quasi-static domain (Hosoi & Goldman, 2015) that relies on the existence of a semi-permanent void and submerged ghost crabs will generally drown (Milne & Milne, 1946).

Horizontal vs. Vertical Burrowing

Ghost crabs burrow horizontally approximately three times faster than vertically (Figure 4.23A). This confirms the hypothesis that burrowing performance changes between horizontal and vertical conditions. However, the overall burrowing strategies remain consistent between the two conditions. Observations showed that the same overall excavation cycle structure and the excavation strategies were the same. No significant difference was observed between the number or rate of hook-and-pull behaviors within an excavation cycle (Figures 4.23B and 4.23C). This suggests rejection of the hypothesis that burrowing strategies change between horizontal and vertical conditions if substrate properties are otherwise constant. Instead, the increased burrow extension rate appears to be primarily due to reduced resting times (Figure 4.23D).

Overall, these results suggest that ghost crab burrowing performance does change between horizontal conditions. This, in turn, suggests that crabs may maintaining a power output target rather than a performance (e.g. burrow extension rate) target. However, the basic burrowing strategies of the ghost crabs remain the same.

Effect of Moisture Content on Burrowing Performance

Longer-term experiments examining burrowing performance and substrate moisture content also found that the crabs were able to maintain equivalent performance across the entire range of moisture contents examined (Figure 4.25). This suggests rejection of the general hypothesis that burrowing performance is correlated with substrate moisture content and the corresponding cohesive forces.

The specific mechanisms that allow the crabs to maintain performance across a range of moisture contents are, however, unknown. While comparing horizontal and vertical burrowing suggests that ghost crab burrowing may be generally stereotyped, it is possible that ghost crabs adopt

modified strategies or employ compensatory mechanisms. Alternatively, the burrow strategies described in Chapter 2 may be inherently robust to changing substrate conditions, similar to locomotion strategies observed in other running arthropods (Sponberg & Full, 2008). This represents a new hypothesis that could be tested by further quantifying burrowing kinematics and kinetics in an even greater variety of substrate conditions.

Broader Conclusions

Overall, ghost crabs appear to be substrate generalists on the sandy shore. This contrasts with substrate specialists, such as the mole crab (Trueman, 1970). While the specialist mole crabs are able to burrow quickly, up to 0.5 body lengths per second, they have highly specialized appendages (Faulkes, 2012) for burrowing in very wet sand and cannot move quickly on the surface (Trueman, 1970). The ghost crabs are much slower burrowers, moving through the substrate at approximately 0.1 body lengths per minute, but they have demonstrated the ability to burrow in a variable substrates.

Potentially similar tradeoffs have been observed in bivalves, where substrate generalists maintained consistent but moderate performance in many different substrates while specialists demonstrated high performance in a specific material and very low performance in others (Alexander et al., 1993). Thus, ghost crabs may represent the generalist end of a tradeoff between performance and multifunctionality.

This suggests that ghost crab burrowing may be a particularly valuable source of bio-inspiration for legged robots that require the ability to burrow or manipulate the substrate. Combining the findings reported here with existing work on locomotion on granular media (Li et al., 2013; Qian et al., 2015), may lead to a more complete understanding of granular media interactions and potentially facilitate robots with both running and burrowing capabilities. For example, robotic platforms like RHex (Saranli, et al., 2001), may be equipped with modified legs and additional degrees of freedom enabling rapid locomotion over granular media (Qian et al., 2015) and substrate manipulation using the strategies described in Chapter 2.

Chapter 5

Hurdling Behaviors of the Ghost Crab

The previous chapters detailed the burrowing strategies used by the ghost crab, *Ocypode quadrata*. Burrowing, however, represents only one of the crabs' many capabilities, which also include rapid running and climbing in a highly variable environment. Notably, ghost crabs can also use locomotor (walking legs) and manipulating (chelae) appendages in concert during behaviors such as prey capture or climbing.

The crabs' combined use of locomotor and manipulating appendages to achieve a goal represents a biological instance of self-manipulation (Johnson, 2014). Examining how ghost crabs use their chelae and walking legs together may offer substantial insight into appendage multifunctionality and mobile manipulation by demonstrating how different appendage sets can be used to together to enable functions or behaviors that are not possible with either set alone. In particular, ghost crabs were observed in field studies negotiating many barriers in their environment effectively using a deliberative, controlled hurdling strategy.

Summary

Ghost crabs are natural climbers that demonstrate the ability to climb in both confined (e.g. burrows) and open (e.g. dunes) areas. This chapter presents a novel climbing behavior in ghost crabs, termed hurdling, where crabs climbed over rigid vertical barriers of varying heights. Specifically, this chapter examines how hurdling strategies changed with obstacle height, how success rates changed with obstacle height, and whether the chelae are required for any components of hurdling. Crabs employed their walking legs and chelae together while hurdling. Three distinct climbing strategies were observed. For low obstacles, crabs simply raised their hip height and stepped over the obstacle but otherwise maintained a typical walking gait. For medium-sized hurdles, crabs grasped the top of the obstacle with their walking legs and lift their bodies over without using their chelae substantially. Tall hurdles were associated with combined use of both the walking legs and chelae. In this behavior, the crabs initially climbed up the obstacle with their walking legs alone. As the crab approached the top of the obstacle, the chela

on the ascending side was used to grasp the top of the obstacle as the crab moved its body to the other side of the barrier. To determine if the chelae are required for climbing high hurdles, a follow-up experiment was performed. First, ghost crabs were presented with a 100 mm high barrier and allowed to ascend normally. Then, each ghost crab's chelae were restrained so they could not grasp the obstacle and a 100 mm hurdle was re-presented. Climbing success rates for all individuals decreased from 100% in the control condition to 0% in the restrained-chelae condition, suggesting that the chelae are required for climbing tall obstacles. A quasi-static model of ghost crab hurdling suggest that the chelae are required because they allow crabs to overcome torque and range-of-motion limitations. Overall, hurdling represents a multifunctional, self-manipulation behavior where both locomotor and manipulating appendages are required.

5.1 Introduction

In addition to being capable runners (Herreid & Full, 1988) and burrowers, ghost crabs are skilled climbers. They readily demonstrate the ability to climb in a variety of circumstances, including the within confines of a burrow and in the open, heterogeneous beach environment as recent field studies have revealed directly. Despite lacking any obvious morphological adaptations to climbing (Hafemann & Hubbard, 1969), ghost crabs are able to navigate even vertical obstacles including the entrances to their burrows, debris, vegetation, rocks and even dune scarps.

Many animals demonstrate the ability to climb, using a variety of mechanisms including friction (Cartmill, 1974), interlocking (Gorb et al., 2002), suction (Alberch, 1981), wet adhesion (Hanna & Barnes, 1991) and dry adhesion (Autumn et al., 2006). Arthropods in particular possess a wide variety of specialized climbing structures, which may be used individually or together (Chapman, 1982). For example, ants possess both interlocking claws and wet adhesive pads (Federle, et al., 2002). Employing multiple adhesive mechanisms, in a range of size scales, increases the effectiveness of climbing on varied terrain (Gillies et al., 2014).

Ghost crabs, however, lack the specialized climbing structures commonly observed in other arthropods. Ghost crabs do not have interlocking spines like cockroaches (Roth & Willis, 1952) or the ability to create adhesive forces using fluids or dry adhesives. Instead, ghost crabs climb using their relatively unspecialized walking legs and chelae.

This combined use of locomotor and manipulating appendages to achieve a goal represents a biological instance of dexterous mobile manipulation, a field of extensive study in robotics (Bicchi & Kumar, 2000; Okamura, et al., 2000). Mobile robots, however, often employ the locomotor and manipulating systems independently (Srinivasa et al., 2010). That is, a robot's legs or wheels are used only to move its body and its manipulator(s) generally work while its body remains stationary. Recently, however, a new paradigm called self-manipulation has emerged (Johnson, 2014). Self-manipulation addresses any activity that alters a robot's configuration, integrating all aspects of a robot's motion and interaction with the environment,

thus providing a framework for understanding dual-use appendages capable of both locomotion and manipulation.

This chapter specifically examines self-manipulation in ghost crabs by investigating a novel climbing behavior, termed hurdling, where a crab's chelae and walking legs are employed together to climb over tall vertical obstacles. Behavioral experiments were first conducted to identify the mechanisms used by hurdling ghost crabs. These studies identified appendage use and climbing strategies for a range of obstacle heights. The following specific questions were addressed:

1) What strategies and appendages do ghost crabs use to climb over vertical obstacles?
2) Do these strategies change with obstacle height?
3) Does the rate of failure increase with obstacle height?

General observations of climbing ghost crabs suggest that ghost crabs will demonstrate a suite of hurdling behaviors. Prior studies studying obstacle climbing in cockroaches (Ritzmann, et al., 2004) suggests that ghost crabs might use modified walking gaits for low obstacles and transition to specialized climbing postures for higher obstacles.

Ghost crabs' chelae might also be expected to play a role in hurdling. While climbing by grasping is common in vertebrates, especially primates (Ashton & Oxnard, 1964), many arthropods (e.g. beetles, spiders, decapods, etc.) also possess grasping structures (Dollar, 2001). Mantids, scorpions and crustaceans are of particular note because they possess both grasping structures and the ability to employ them dexterously (Corrette, 1990; Warner, 1977). However, these animals have not been generally documented as using these appendages for climbing. Instead, most crustaceans, including the ghost crabs, have only been shown to use their grasping appendages (chelae) for prey manipulation (Elner & Campbell, 1981) and intraspecific competition (Hyatt & Salmon, 1977).

To understand how the chelae are involved in hurdling, the following questions were addressed:

1) Are hurdling strategies dependent on the chelae?
2) Does the rate of failure change when the chelae are disabled?
3) If the chelae are found to increase hurdling performance, through what mechanism(s) do the chelae contribute?

The general lack of grasping-based climbing behaviors in arthropods (Dollar, 2001) suggests that the chelae should not play a major role in hurdling. As discussed in Chapter 2, however, ghost crabs use their chelae dexterously while burrowing, both to assist with substrate transportation and locomotion within the burrow. This suggests that hurdling performance may be increased by employing the chelae.

The results of these experiments may provide new insights into self-manipulation and animal multifunctionality by demonstrating how relatively simple, unspecialized manipulating and locomotor appendages can be employed in concert to enable a behavior that is impossible with either set alone.

5.2 Materials and Methods

Animals

Ghost crabs, *Ocypode quadrata*, were either purchased from a commercial vendor (Gulf Specimen Marine Lab, Panacea, FL, USA) that captured wild ghost crabs on the Gulf Coast of Florida, USA or captured at the Rachael Carson Marine Reserve (Beaufort, NC, USA). The crabs were housed individually in ventilated plastic containers, approximately 60 cm long, 45 cm wide and 20 cm tall. A 50 ml dish was filled with fresh sea water substitute (Instant Ocean, Blacksburg, VA, USA) and changed every 1-2 days. The crabs were provided with a diet of 1-3 live, medium-sized crickets (LSA Animal Car Facility, Berkeley, CA, USA) each day. Uneaten crickets were removed within 24 hours. The crabs were maintained at approximately 23 ^{o}C continuously. Artificial light maintained a day:night cycle of approximately 12 hrs:12 hrs. Only complete, healthy crabs were used for behavioral trials. Any crab that was missing an appendage or that exhibited lethargic behavior was removed from the experimental cohort.

Data for the initial experiments examining how hurdling strategies change with obstacle height came from eight crabs (carapace width: 32 - 38 mm; mass: 20 – 32 g). Data for the chelae restraint experiments came from five crabs, with a carapace width of 30 - 36 mm and a body mass of 21 - 29 g.

Enclosure Design

Ghost crabs were placed into an experimental enclosure, approximately 50 cm long, 20 cm wide and 30 cm tall (Figure 5.1A). The enclosure was constructed from clear acrylic panels (McMaster-Carr, Elmhurst, IL, USA) and aluminum struts (80/20, Inc., Columbia City, IN, USA). All of the wall panels except for the front were coated in non-reflective black spray paint. The floor was covered with non-reflective black cloth tape.

Figure 5.1

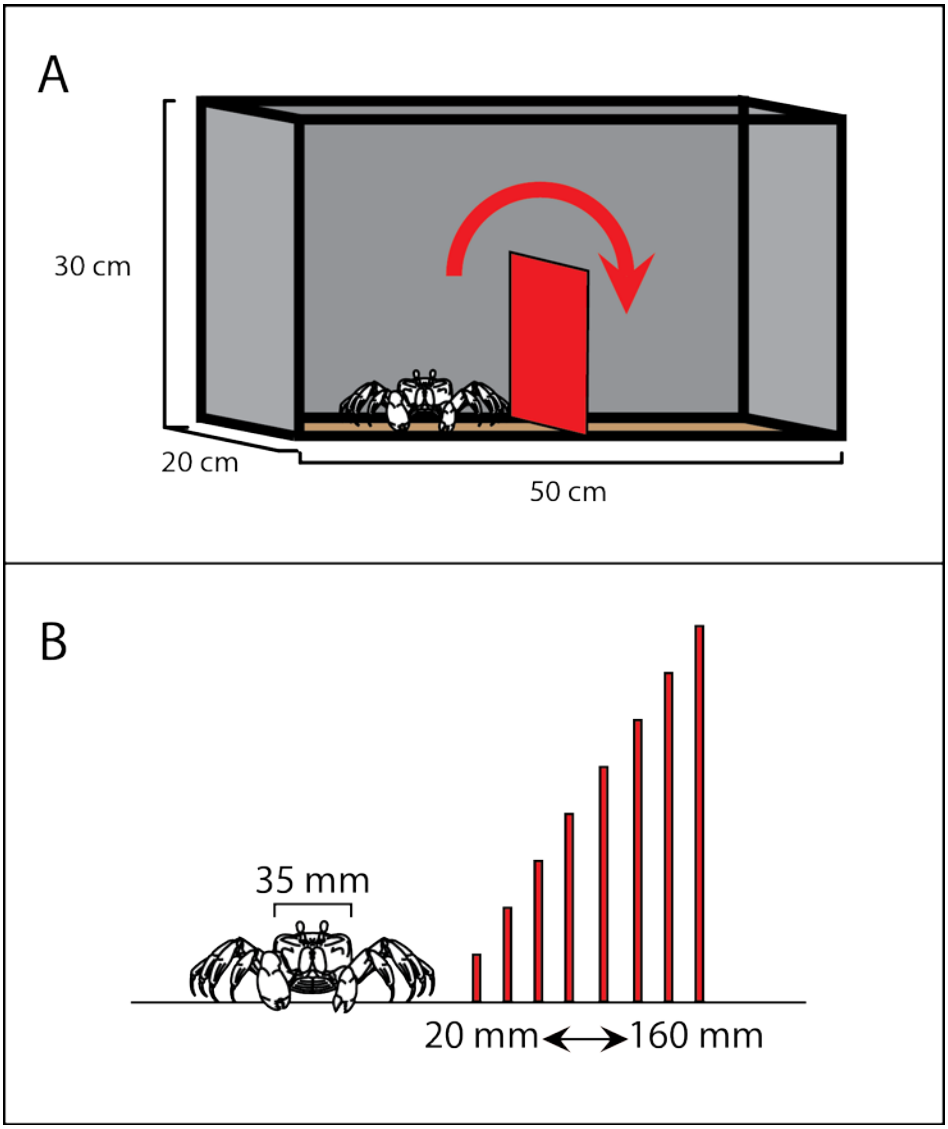

Figure 5.1: Enclosure and obstacle design for hurdling experiments. **A:** The enclosure used for all hurdling experiments. The obstacle (red), was placed in a slot and secured using tape. The crab was placed on the starting side of the enclosure and allowed to climb over the obstacle (red arrow). **B:** The obstacles presented to the crabs. Obstacles ranged in height from 20 mm to 160 mm in 20mm increments. A crab of average carapace width is shown for scale (drawing to scale).

Obstacle Design

Hurdles were constructed from 3.1 mm thick acrylic and inserted into a slot in the center of the enclosure, creating a fence-like obstacle. The face of the obstacle was covered in fine-grained sandpaper. This surface provided high friction but was too fine to permit crabs to interlock with the surface. Considering that ghost crabs lack adhesive structures (e.g. arolia) and that interlocking is not possible, it is unlikely that adhesive forces contributed to the behaviors described here.

Obstacles ranged in height from 20 mm to 160 mm (Figure 5.1B). Obstacles for the chelae restraint experiments were uniformly 100 mm high. In terms of the crabs' typical dimensions, these obstacles ranged from 2x to 16x their typical hip height and between 6% and 100% of their maximum leg span.

Videography

The crabs' behavior was recorded with an array of eight infrared cameras equipped with integrated infrared lighting (Optitrack Prime 17W; NaturalPoint, Inc., Corvallis, OR, USA). Each camera recorded from a different angle at 120 frames per second.

Experimental Procedure

An obstacle was first inserted into the center of the experimental enclosure and the obstacle was inspected for stability. Any ability for the obstacle to move was removed using tape and shims applied outside the enclosure. A crab was then placed on the starting side of the barrier and allowed a period of at least one minute to acclimate to the environment, after which video recording was started. The crabs were encouraged to leave the starting area and climb the burrow by waving a small flag or gently touching the tips of their legs. No substantial or assistive forces were applied to the crab once it began climbing the obstacle.

The crabs were allowed to climb the obstacle using self-determined strategies. A success was defined as the crab moving its body from the starting side of the hurdle to the ending side using any strategy or combination of strategies. A failure was defined as any trial where the ghost crab fell from the obstacle, voluntarily retreated from the obstacle after initiating climbing, or ceased climbing (failing to make further progress) up the obstacle for one minute. Each crab made five consecutive attempts at a given obstacle height. Obstacle heights were presented in a random order. If a crab exhibited 0% success rate at a given obstacle height, a higher obstacle was not presented.

Figure 5.2

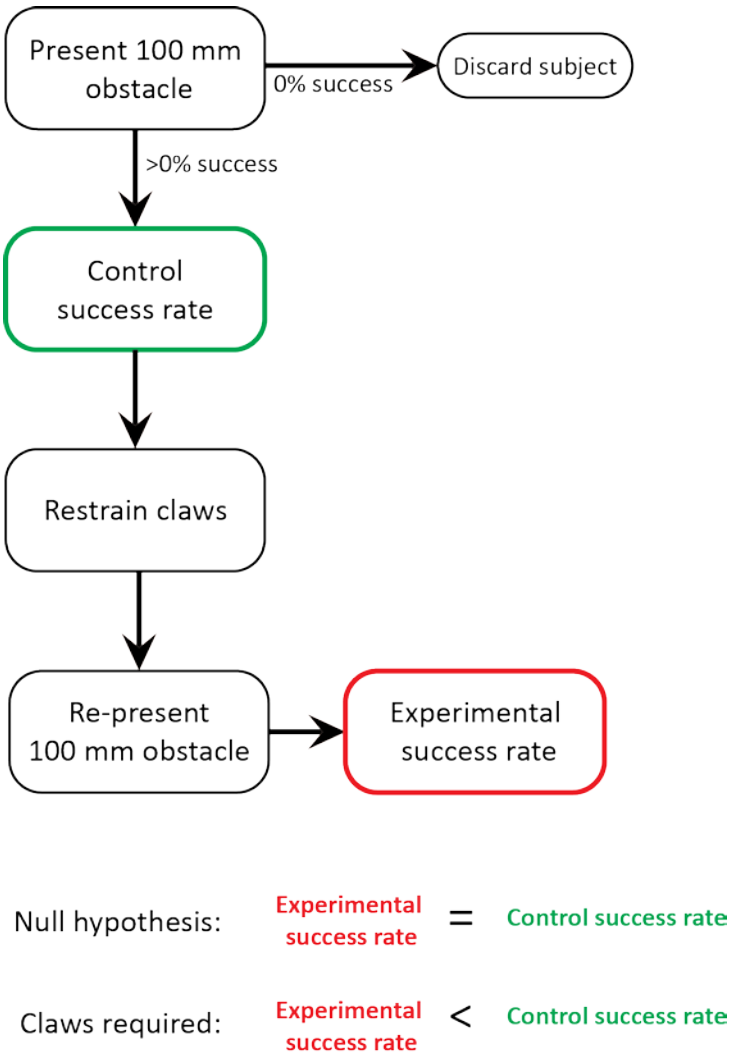

Figure 5.2: Schematic diagram of claw restraint experiments. Crabs were first presented with a 100 mm-high obstacle. Any crab that was unable to successfully climb the 100 mm obstacle in at least one trial was removed from the experiment. The unaltered crab's initial success rate was the control success rate. Then, the crab's claws were restrained using cyanoacrylate adhesive and the crabs were presented with the same 100 mm-high obstacle. The altered crab's success rate was the experimental rate. These rates were compared to test one of two hypotheses. If success rates were not statistically different, then the claw restraint manipulation had no effect on success rate, implying that the legs and claw climbing strategy is not required for climbing high obstacles. However, if the experimental success rate were statistically lower than the control rate, then the use of claws is either required or increases that chance of success.

Figure 5.3

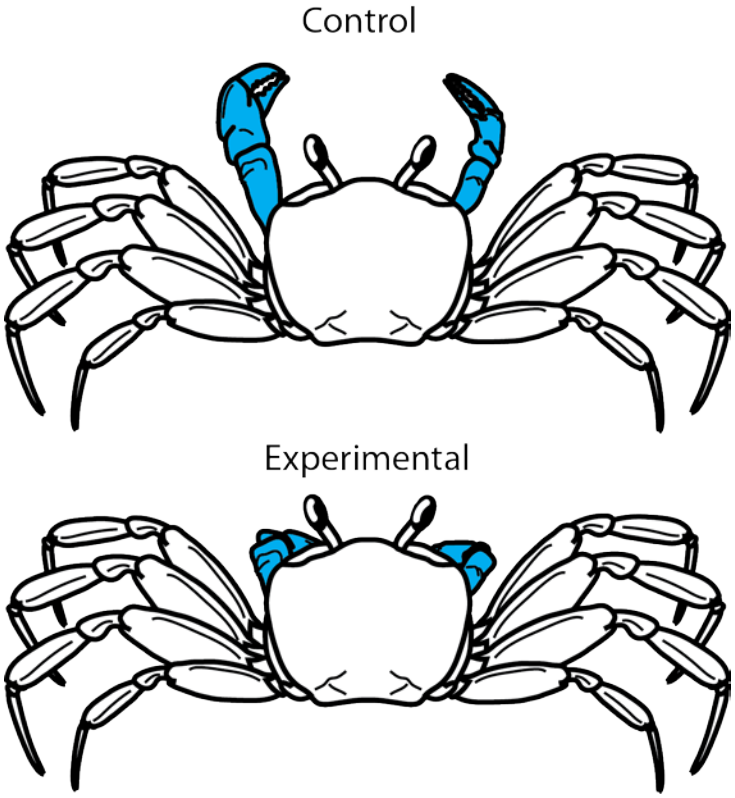

Figure 5.3: The claw restraint method used in this series of experiments. In the control condition, the crab is unrestrained. In the experimental condition, the crab's chelae are attached to the crab's body using cyanoacrylate adhesive. Specifically, the chelae are first attached to the merus and the adhesive is allowed to cure. Then, the chela/merus is attached to the front of the carapace. The experimental condition is a natural configuration of the crab's appendages, typically adopted in confined spaces such as a burrow.

Chelae Restraint

For experiments examining the role of the chelae in hurdling, a modified experimental procedure was used.

Unaltered ghost crabs were first presented with a 100 mm high obstacle. After performing five climbing trials, the crabs' chelae were restrained and the 100 mm obstacle was then re-presented for another five climbing trials. The success rates and strategies were then compared, with each crab acting as its own control. This experiment is diagrammed in Figure 5.2.

The crabs' chelae were restrained by attaching the chela to the merus and carapace on both sides using cyanoacrylate adhesive (Loctite 1365882; Henkel Corp, Westlake, OH, USA). This manipulation, illustrated in Figure 5.3, prevented the crabs from actively applying any forces to the obstacle with their chelae. This method was chosen over inducing autotomy since it is less traumatic for the animals and recreates a natural posture that is observed when the crabs move in confined spaces (e.g. burrows).

To apply the restraints, a candidate ghost crab was first placed into a cold chamber (approximately 5 ^{o}C) for a few minutes until quiescent. Cyanoacrylate adhesive was then applied to the chelae. Curing time was accelerated by applying a small amount of sodium bicarbonate (Arm & Hammer; Church & Dwight Co., Inc., Princeton, NJ, USA). Ghost crabs were allowed at least six hours to recover from the procedure. Any crabs that exhibited lethargic behavior, restricted movement (except in the manipulated degrees-of-freedom), appendage loss or damage were disqualified.

5.3 Results and Discussion

A total of 310 hurdling events were recorded from eight individuals. Each crab performed five trials at each height for a typical total of 40 trials. Two crabs were not presented the 160 mm obstacle (one because it demonstrated 0% success at 140 mm and the other due to unrelated experimental limitations). These individuals each performed 35 trials.

Overall, crabs demonstrated the ability to climb obstacles between 20 mm and 160 mm with varying strategies and success rates. Depending on obstacle height, the crabs used either the walking legs and chelae together or the walking legs alone. All crabs demonstrated the same three general climbing strategies: hip raise, legs only and legs with chelae assist.

Notably, none of these strategies involved dynamic or inertial behaviors, such as jumping. Instead, the crabs ascended the obstacles in a deliberate and controlled fashion.

Hip Raise Strategy

The hip raise strategy was associated exclusively with low obstacle heights, predominately 20 mm or approximately two times the crabs' normal hip height. This behavior, diagramed in Figure 5.4, is characterized by the crabs simply raising their hip height while otherwise maintaining a normal walking gait. This raised posture allowed the crabs to step over the obstacle without making substantial contact with the hurdle. Due to the limited contact made with the obstacle, the hip raise strategy does not require any forces to be applied to the obstacle.

Legs Only strategy

For medium-height obstacles, predominately 40 mm high or approximately four times the crabs' typical hip height, the crabs adopted a strategy where they hooked the top of the obstacle with their walking legs. This behavior is illustrated in Figure 5.5. Crabs initially ascended the obstacle by "walking" up it with the walking legs. When crabs climbed high enough, they hooked the top of the hurdle with the walking legs and pulled their bodies across the barrier. The crabs did not make substantial contact with the hurdle with either chela during any phase of the legs only strategy.

Legs with Chela Assist Strategy

For tall obstacles, more than 60 mm or approximately six times the crabs' typical hip height, the crabs employed both their walking legs and chelae for climbing. This behavior is diagramed in Figure 5.6. The crabs initially ascended the obstacle using their walking legs, similar to the legs only strategy described previously. Once the crabs reached the top of the barrier, they contracted their walking legs and drew their bodies to the top of the hurdle. The crabs then grabbed the top of the obstacle with the ascending chela, either by pinching or grasping the obstacle between the dactyl and pollex or by hooking the entire chela over the top of the hurdle. The chela and walking legs were then used together to move the body to the other side of the barrier. The crabs made substantial contact with the chelae in 100% of successful climbing trials for hurdles 80 mm and higher, suggesting that the chelae may be critical to the climbing over tall hurdles.

Figure 5.4

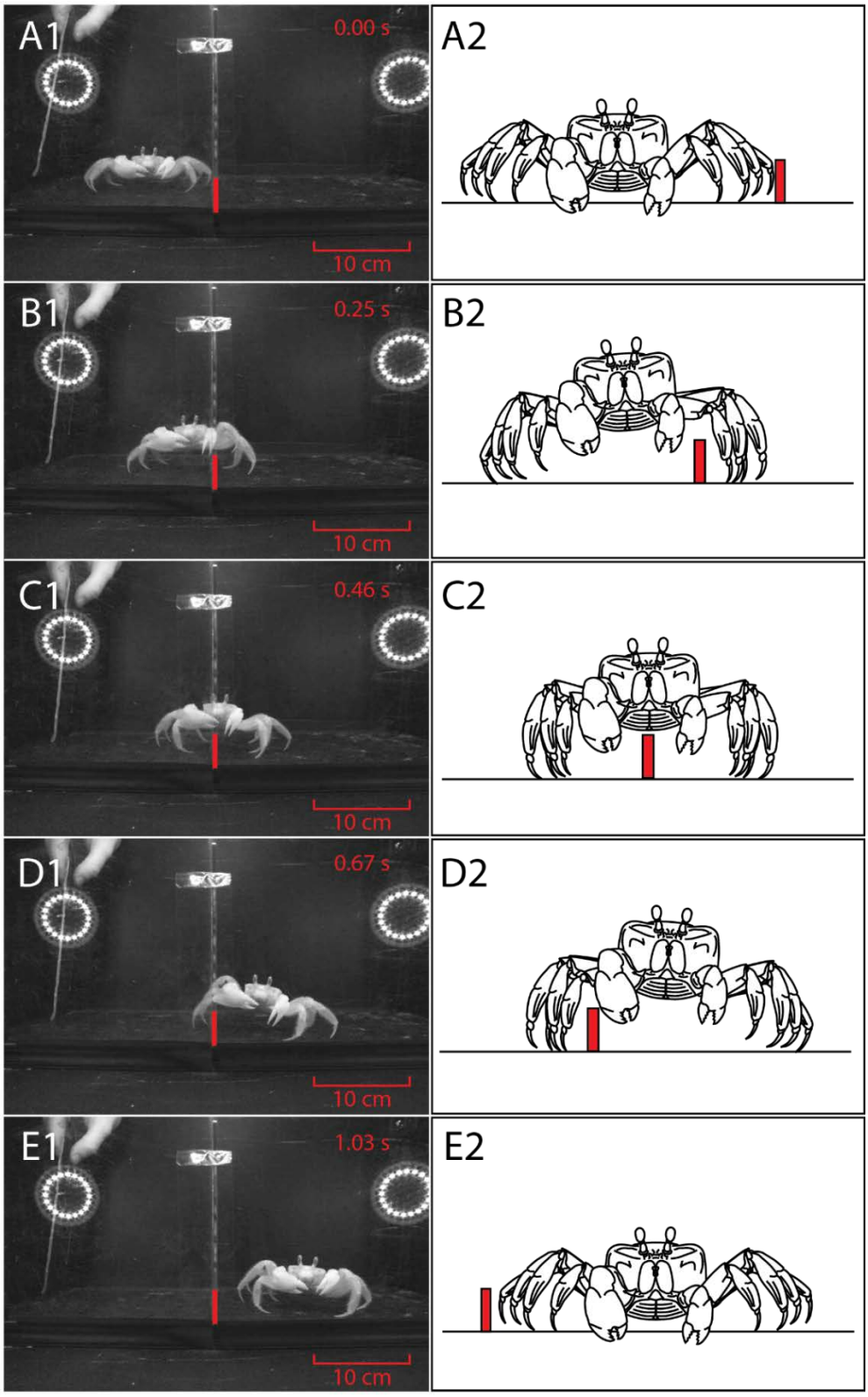
A1
0.00 s
10 cm
A2
B1
0.25 s
10 cm
B2
C1
0.46 s
10 cm
C2
D1
0.67 s
10 cm
D2
E1
1.03 s
10 cm
E2

Figure 5.4: Low hurdling (“hip raise”) strategy, which is distinguished by the crab simply raising its hip height while walking over the obstacle. Crabs made only incidental contact with the barrier. Video still images (left) and diagrams (right). Obstacle (20 mm height), shown in red. The white circles in the images in the left column are reflections from the infrared lights. These lights were not visible to the crabs. Video timestamps are in the upper right corner of the images in the left column. **A1/2:** The crab approaches the obstacle. **B1/2:** The crab increases its hip height by straightening its legs while stepping over the obstacle. **C1/2:** The crab continues to use a walking gait with a raised hip height. The crab’s body and/or chelae may make incidental contact with the obstacle but this contact does not appear to be required or generate significant forces. **D1/2:** As the crab clears the obstacle, it begins to lower its hip height. **E1/2:** After the crab has cleared the obstacle, it reduces hip height back to normal and resumes its typical walking gait.

Figure 5.5

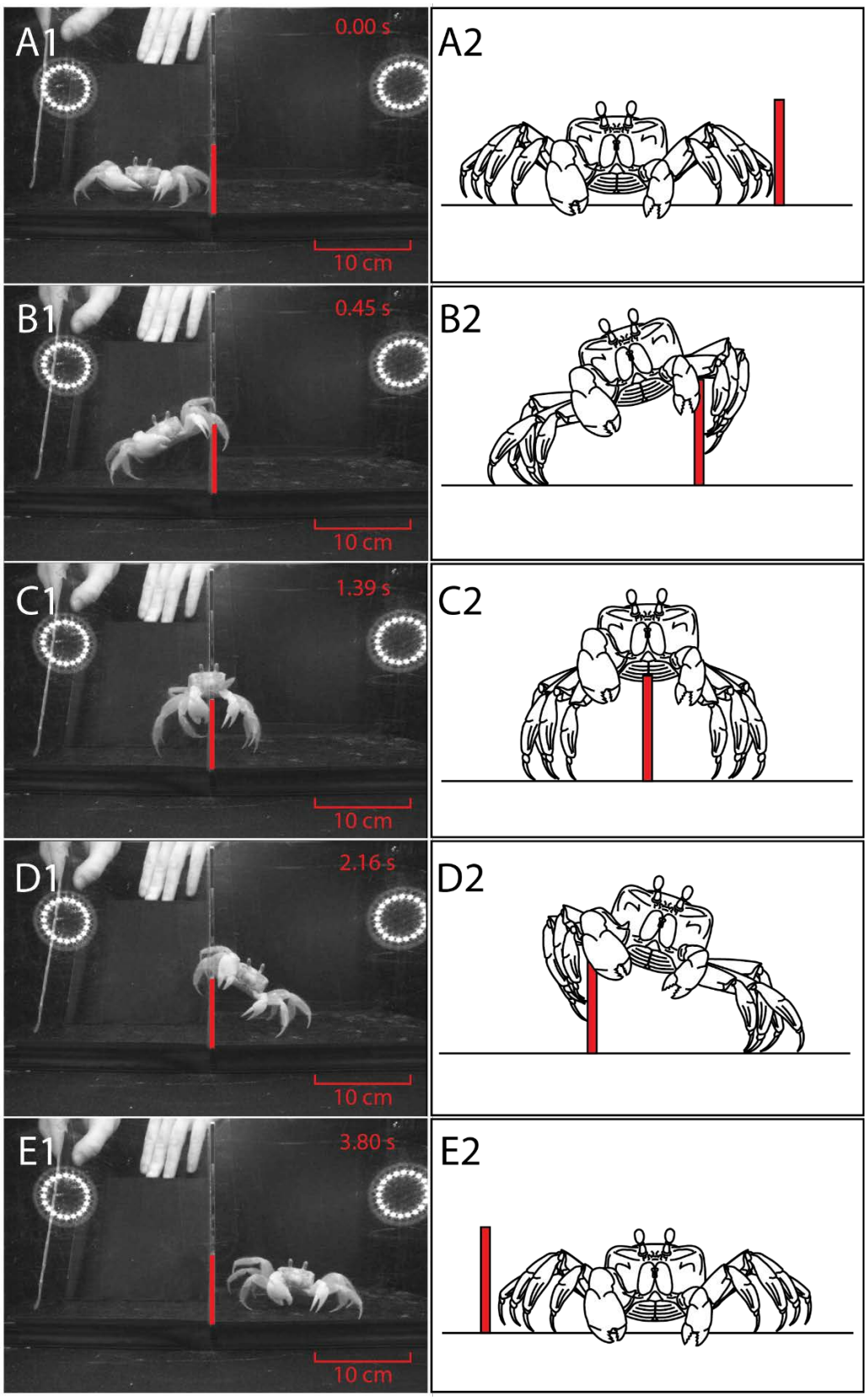
A1
0.00 s
10 cm
A2
B1
0.45 s
10 cm
B2
C1
1.39 s
10 cm
C2
D1
2.16 s
10 cm
D2
E1
3.80 s
10 cm
E2

Figure 5.5: Medium (legs only) hurdling strategy. As in the low hurdling strategy, the crabs were able to reach the ground with both sets of legs from the top of the obstacle. However, the medium strategy differed from the low strategy in that the medium strategy involved substantial contact with the obstacle, by grabbing the obstacle with the walking legs. Video still images (left) and diagrams (right). Obstacle (40 mm height), shown in red. The white circles in the images in the left column are reflections from the infrared lights. These lights were not visible to the crabs. Video timestamps are in the upper right corner of the images in the left column. **A1/2:** The crab approaches the obstacle. **B1/2:** The crab reaches its leading walking legs over the obstacle and grasps the obstacle. The crab's body is drawn towards the obstacle so that the obstacle is at the joint between the merus and carapace on the leading side. **C1/2:** The crab reaches the ground with both sets of walking legs, balancing its body on the top of the obstacle. The crab is able to make substantial contact with the ground on both sides of the obstacles. **D1/2:** The crab lowers its body while lifting its trailing walking legs, so that the obstacle is between the merus/carapace and merus/carpus joint. **E1/2:** The crab lowers it body back to the typical walking height and releases the obstacle, resuming its typical walking gait.

Figure 5.6

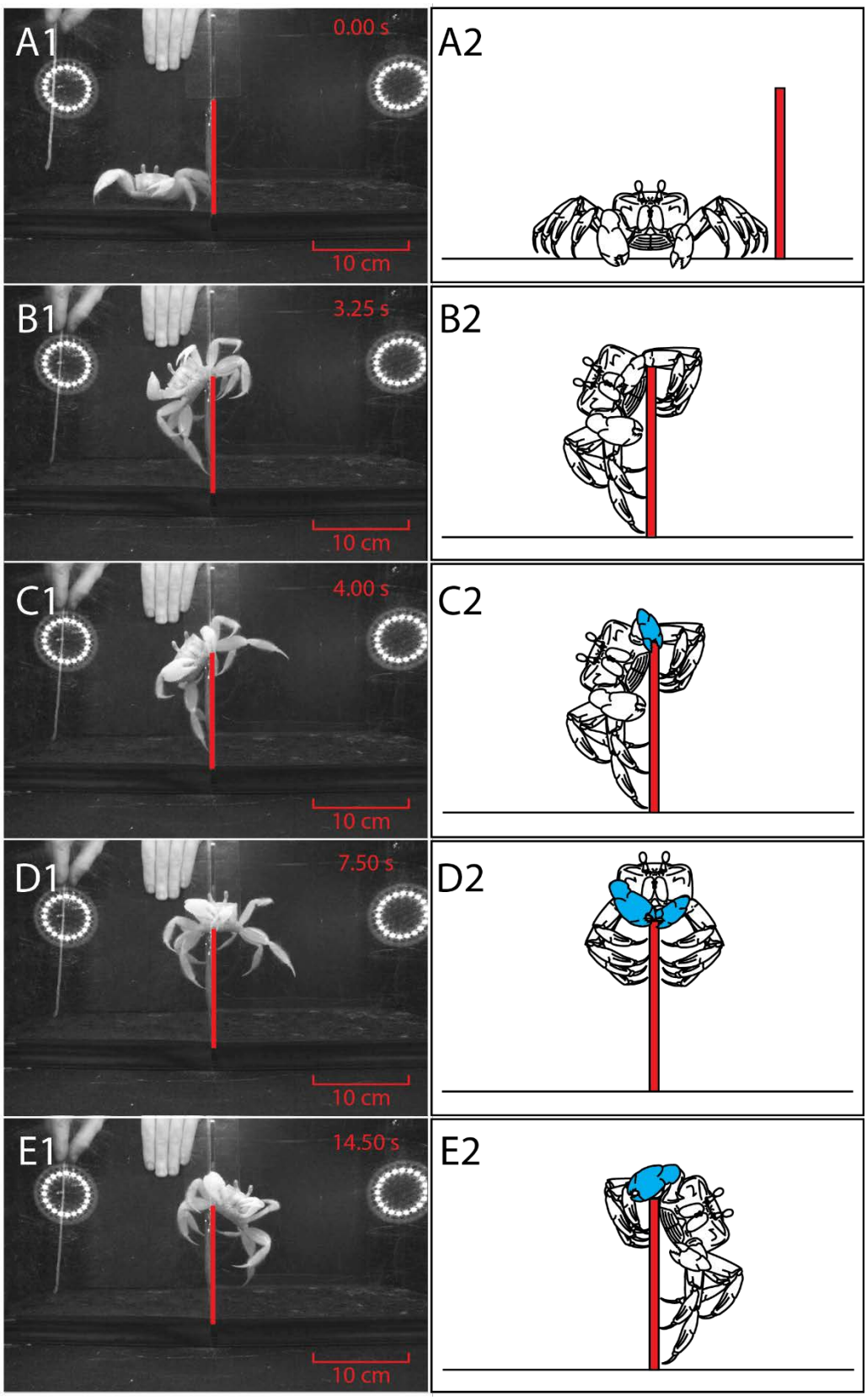
A1
0.00 s
10 cm
A2
B1
3.25 s
10 cm
B2
C1
4.00 s
10 cm
C2
D1
7.50 s
10 cm
D2
E1
14.50 s
10 cm
E2

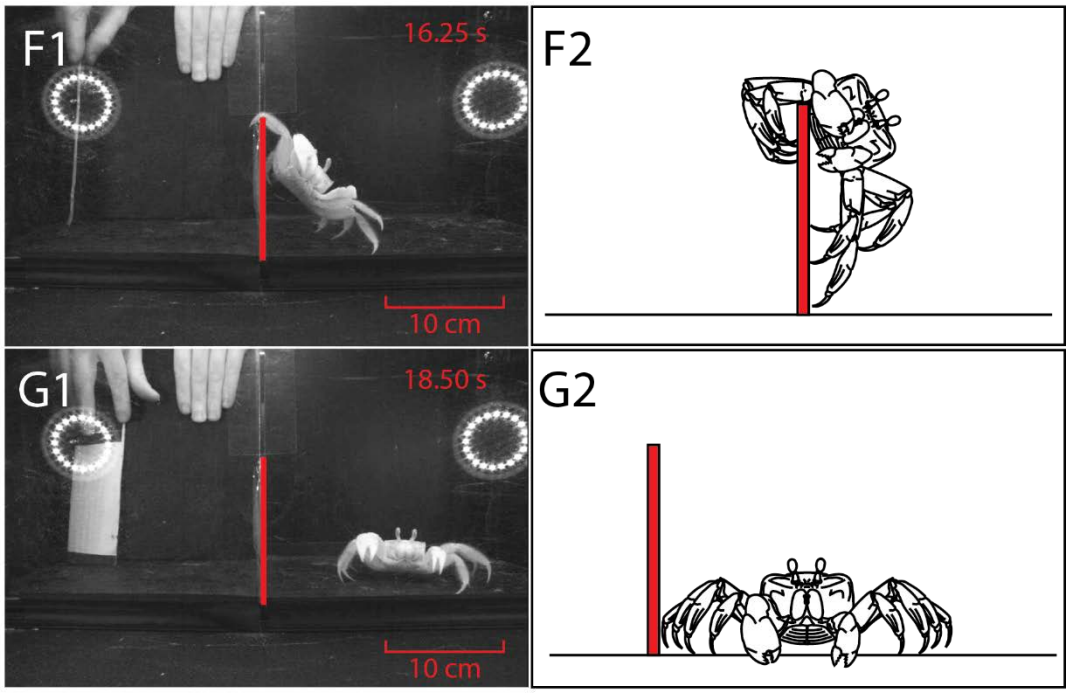

Figure 5.6: High hurdling strategy. In contrast with the low and medium strategies, the high strategy involves grasping the obstacle with the chelae. Crabs may grasp the obstacle with the dactyl/pollex (i.e. pinching) or hook the entire chela over the obstacle. Video still images (left) and diagrams (right). Obstacle (100 mm height), shown in red. The white circles in the images in the left column are reflections from the infrared lights. These lights were not visible to the crabs. Video timestamps are in the upper right corner of the images in the left column. **A1/2:** The crab approaches the obstacle. **B1/2:** The crab climbs up the obstacle using the leading legs. As the crab reaches the top of the obstacle, it reaches over the obstacle and draws its body towards the obstacle, placing the obstacle at the joint between the merus and carapace. **C1/2:** The crab grasps the obstacle with the leading chela, either by pinching with the dactyl/pollex or by draping the entire chela over the obstacle (highlighted in blue). **D1/2:** Pulling with the leading legs and chela, the crab pulls its body on top of the obstacle. The crab maintains balance with both sets of walking legs and the chelae (highlighted in blue). **E1/2:** The crab lowers its body on the other side of the obstacle using the trailing legs and chela (highlighted in blue). **F1/2:** Once the crab can make contact with the ground with its leading legs, it releases its trailing chela from the obstacle and begins to walk the leading legs away from the obstacle while continuing to lower itself with its trailing legs. **G1/2:** Once the crab has reached the bottom of the obstacle, it resumes it typical walking gait.

Success Rate and Obstacle Height

For obstacles ranging from 20 mm to 120 mm (2x to 12x typical resting hip height; between 6% and 75% of their typical maximum leg span), success was consistently high, as shown in Figure 5.7. All tested crabs were able to climb obstacles up to 60 mm with 100% success and seven of eight crabs maintained a success rate of 60% or more up to obstacle heights of 140 mm. Success rates began to drop at 140 mm obstacle height. Failure most frequently occurred when the crab did not successfully grasp the top of the hurdle and voluntarily retreated. Notably, many crabs were able to successfully climb the highest obstacle of 160 mm, with an average success rate of approximately 42%. In particular, one crab exhibited a 100% success rate at 160 mm obstacle height.

Strategies and Obstacle Height

Ghost crab hurdling strategies were related to the height of the obstacle, as shown in Figure 5.8. Low obstacles, 20 mm to 40 mm in height were generally traversed using the hip raise strategy. This behavior was predominantly confined to the lowest obstacle height, however. Only 8% of 40 mm obstacle trials were accomplished with hip raising. The remaining 92% of 40 mm height trials saw the ghost crabs successfully climb the obstacle using the legs only strategy. The legs only strategy also had a relatively narrow range of applicable heights, from 20 mm to 60 mm. At 20 mm, only a single trial (out of 40 total trials) was accomplished with the legs only strategy. At 60 mm height, only 20% of all trials were accomplished using only the legs. The legs with chela assist strategy was successfully applied to the widest range of obstacle heights, being present in the vast majority of successful trials at 60 mm obstacle height and above. For obstacles 80 mm and higher, both the legs and chelae were used in 100% of successful trials.

Chelae Restraint Results

Five unaltered ghost crabs were presented with a 100 mm high obstacle. All individuals demonstrated a control success rate of 100%. However, after the crabs' chelae were restrained and the 100 mm obstacle was re-presented, the success rate for all individuals dropped to 0%. As per the experiment diagrammed in Figure 5.2, this strongly suggests that the chelae are required for climbing high obstacles.

In successful (i.e. control) trials, the ghost crabs demonstrated the legs with chela assist strategy discussed previously (Figure 5.6). This is consistent with prior experiments (Figure 5.8). When crabs with restrained chelae attempted to climb the obstacle, they appeared to try the same hurdling strategy. Restrained crabs were able to successfully perform the first phase of the ascent, where they walked up the obstacle and hooked the top of the barrier with their walking legs. However, once the restrained crabs had fully contracted their walking legs on the ascending

side, they stopped making any substantial progress (Figure 5.9). Typically, restrained crabs would voluntarily retreat from the obstacle 30 s to 60 s after reaching this point.

Consistent with the previous experiments, the crabs did not demonstrate dynamic or inertial climbing behaviors. No individual, in either control or chelae-restrained conditions, ascended the obstacle by running and/or jumping.

Unfortunately, all attempts to remove the chelae restraint following the experiment failed. Thus, a crab could not be returned to the control state to further verify that the ability to climb high hurdles returned with normal chelae function. However, it appears unlikely that some part of the experimental procedure unrelated to the chelae restraint was the source of the observed results. All restrained crabs appeared to maintain their typical health and motivational states, surviving for several weeks following this experiment. Despite this, the role of the chelae in high hurdling could be further examined with a reversible chelae restraint method. This chapter's findings suggest the hypothesis that normal climbing ability should return once the restraint is removed.

Figure 5.7

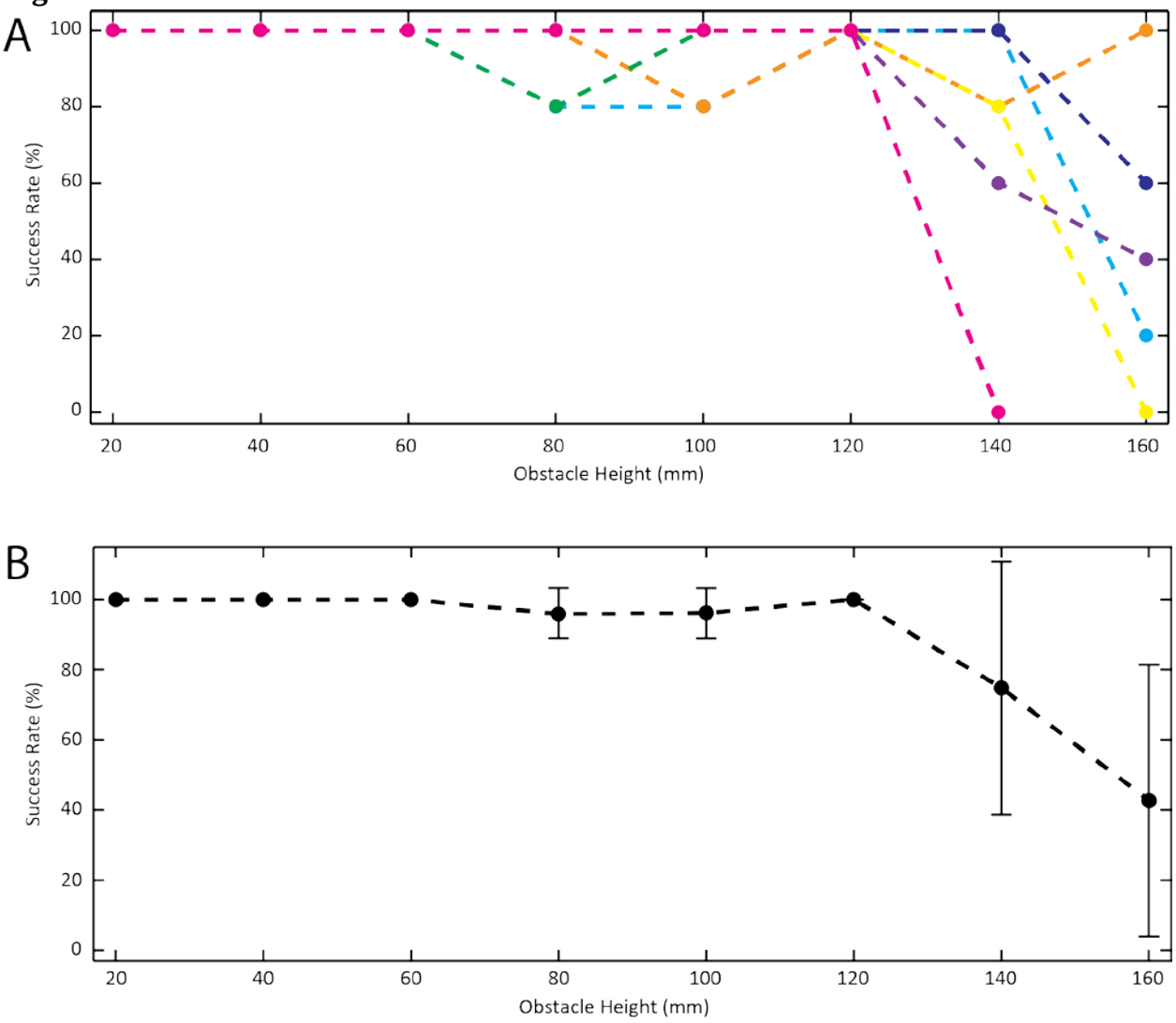

Figure 5.7: Climbing success rate as a function of obstacle height. A success is defined as the crab moving from one side of the obstacle to the other using any strategy. Success rate is defined as the number of successful trials divided by the total number of trials at that obstacle height. Eight crabs were tested with a range of obstacles between 20 mm and 160 mm. All crabs were approximately the same size (carapace width of approximately 35 mm, maximum leg span of approximately 160 mm). **A:** Success rates for all individual crabs. Each color indicates one individual (five trials per individual at each height). **B:** The average success rate for all crabs (all individual success rates pooled). Error bars indicate one standard deviation. Up to 120 mm obstacle height, the average ghost crab will succeed effectively every time. Above 120 mm obstacle height, the typical success rate declined substantially, though success remained possible, even though the obstacle was approximately equal to the crab's maximum leg span

Figure 5.8

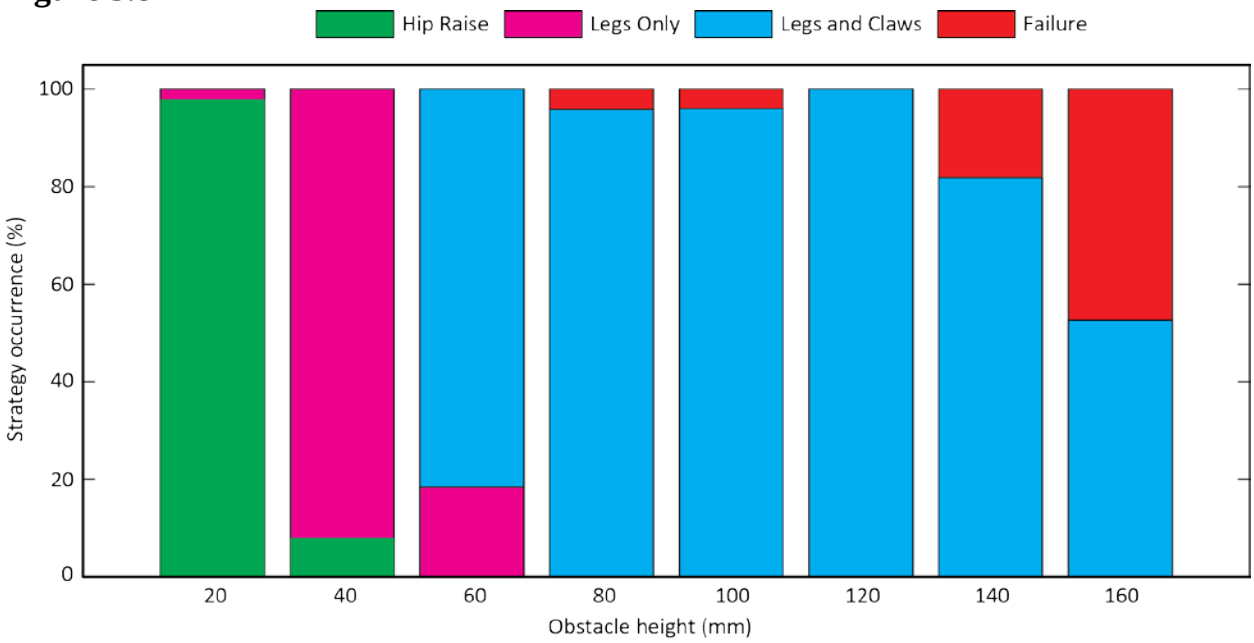

Figure 5.8: Climbing strategies as a function of obstacle height. All trials from all individuals pooled. Each vertical bar for heights 20 – 140 mm represents 40 total trials (five trials each from eight individuals). The vertical bar for 160 mm represents 30 trials (five trials each from six individuals). Failures shown in red, all other colors indicate successful trials. Crabs used the hip raise strategy (green) predominately for the lowest obstacles. As obstacle height increased, crabs switched to the legs only strategy (magenta) and then to legs and claws (cyan). For obstacles ≥80 mm, crabs exclusively employed the legs and claws strategy in successful trials, with decreasing success rates above 120 mm obstacle height.

Figure 5.9

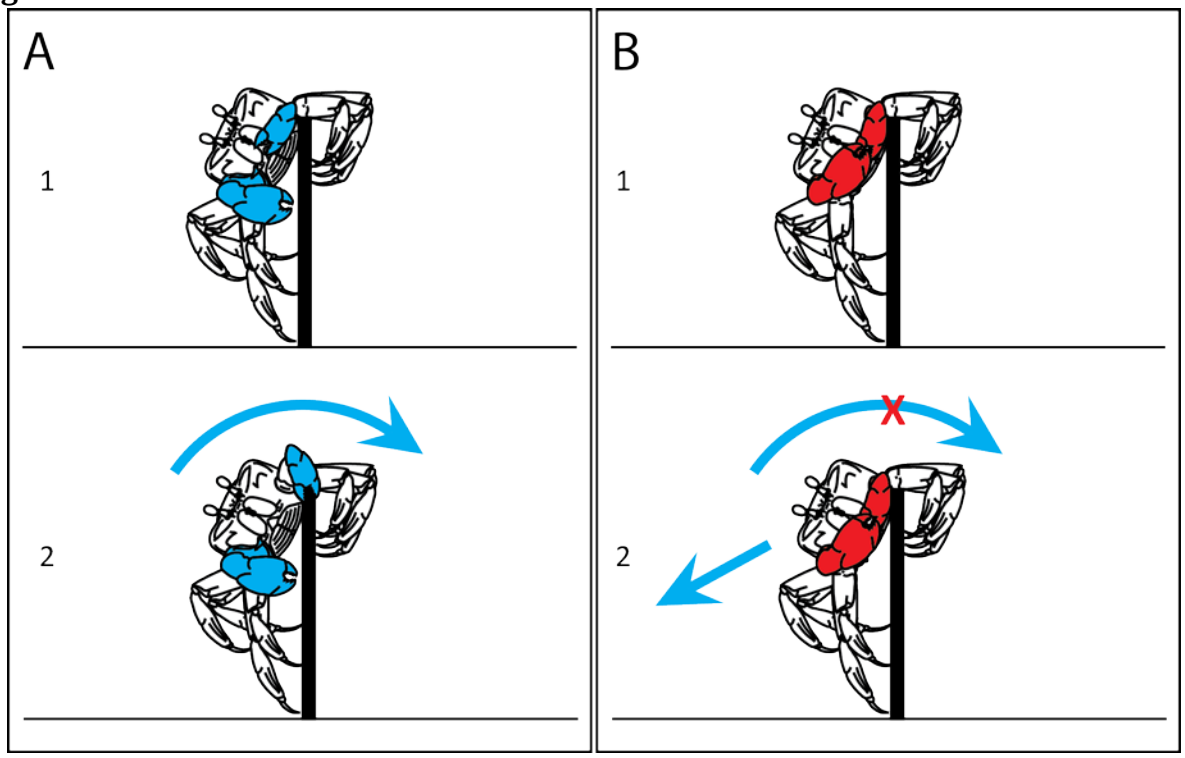

Figure 5.9: A: The mechanism that crabs use to climb the obstacle in the control experiments. After the crab draws its body to the top of the obstacle with its legs, it grasps the top of the obstacle using either by pinching or by draping the entire chela over the obstacle. Then, the crab moves its body to the other side of the obstacle and descends. **B:** The mechanism of failure in restrained climbing trials. As in the control condition, the crabs draw their bodies to the top of the obstacle using their legs. However, they cannot move their chelae, due to the restraint manipulation. At this point, the modified crabs ceased climbing, though they continued to pull with and reposition their legs. The trials always ended with the crab either: 1) aborting the ascent and descending or 2) falling.

5.4 Quasi-Static Model

The experimental results detailed in section 4.3 strongly suggest that a ghost crab's chelae are required for climbing tall hurdles. However, these results cannot indicate the mechanism behind this requirement. To explain how the chelae affect hurdling behaviors, a quasi-static model was developed, modeling the different phases of hurdling. Simplified models, such as that developed here, have a demonstrated value to explaining biomechanical phenomena (Mongeau et al., 2012), particularly where the forces, controlled values and internal logic of a behavior are difficult to assess experimentally. The results of this model indicate one potential mechanism through which chelae use can facilitate hurdling behavior.

Model Derivation

This model divides the hurdling behavior into two principal phases: the initial ascent and the secondary ascent. The initial ascent covers the first part of the hurdling behavior where the crab "walks" up the obstacle, with the aim of hooking the top of the barrier with the tips of the walking legs. The initial ascent is primarily characterized by vertical motion of the carapace. The secondary ascent is defined as the second part of the hurdling behavior where the crab has ascended to the point where the merus/carapace joint is at the top of the obstacle. The secondary phase is primarily characterized by rotation of the body about the top of the obstacle.

Both phases make the same simplifying assumptions. The crabs' body and legs are modelled as a two-dimensional structure. The body is approximated as a uniform rectangular structure, with the center-of-mass located at the geometric center of the rectangle. Each crab's eight legs are approximated as two thin, massless structures of three segments each, connected with simple pin joints. While these approximations substantially reduce the complexity of the ghost crabs' appendages, such simplifications have been proven sufficient in prior biomechanical models, leading to new insights into the fundamental physical mechanisms that enable certain behaviors (Full & Koditschek, 1999).

This model further assumes that ghost crab climbing can be approximated as quasi-static, meaning that each phase of the model assumes that dynamic and inertial effects do not contribute to the behavior. This is supported by the generally slow, stable movement demonstrated by hurdling ghost crabs; no crab was observed to employ dynamic motion (e.g. jumping) while hurdling. All symbol definitions can be found in Table 5.1.

Table 5.1

Symbol	Description
F_W	Force produced by body weight
F_d	Force applied at lower contact point
F_u	Force applied at upper contact point
F_{U2}	Second force applied by upper leg (normal to obstacle)
F_{U2}	Third force applied by upper leg (friction between ascending dactyl and obstacle)
τ_w	Torque produced by F_w
τ_d	Torque produced by F_d
τ_u	Torque produced by F_u
τ_{U2}	Torque produced by F_{U2}
τ_{U3}	Torque produced by F_{U3}
τ_c	Torque produced by ascending chela
$\theta_{d\text{-}u}$	Angle between ground and line connecting lower and upper contact points during initial ascent
$\theta_{d\text{-}COM}$	Angle between ground and line connecting lower contact point and COM during initial ascent
$\varphi_{u\text{-}body}$	Angle between body and obstacle during secondary ascent
$\varphi_{u\text{-}COM}$	Angle between obstacle and line connecting point of rotation and COM during secondary ascent
ψ	Angle between obstacle and line connecting F_{U3}'s contact point and point of rotation during secondary ascent
α	Angular span of the merus/carapace joint
β	Angular span of the merus/carpus joint
γ	Angular span between propodus/dactyl joint
$l_{d\text{-}COM}$	Distance between lower point of contact and COM
$l_{u\text{-}COM}$	Distance between upper point of contact and COM
$l_{d\text{-}u}$	Distance between lower and upper contact points
$l_{d\text{-}u,\,max}$	Maximum distance between lower and upper contact points, maximum leg span
l_d	Distance between lower contact point and lower carapace/merus joint.
l_{U3}	Vertical distance between second upper point of contact and point of rotation
w_c	Carapace width
w_o	Obstacle width
h	Obstacle/ascent height
a	Height of COM above bottom of body
d	Horizontal distance between lower point of contact and COM during initial ascent
c_f	Coefficient of friction between dactyl and obstacle
c_l	Ratio of maximum leg length to carapace width

Table 5.1: Symbol definitions for the model presented here

Morphometrics

This model relies in part on the crabs' typical dimensions and range of motion. These values were obtained by measuring five freshly dead individuals and averaging the results. The individuals chosen for measurement were within the same range of sizes/weights as those individuals discussed in section 4.3. Body dimensions were measured directly using calipers or a ruler. A crab's COM was assumed to be at the geometric center of the carapace. The ranges of motion for leg joints were measured by moving a joint through its entire range of motion and measuring the maximum angular span with a goniometer. The results of these measurements are presented in Table 5.2.

Table 5.2

Symbol	Description	Measured Values
w_c	Carapace width	36 ± 3 mm
a	Height of COM above bottom of body	18 ± 2 mm
c_l	Ratio of maximum leg length to carapace width	1.9 ± 0.1
α	Angular span of the merus/carapace joint	145 ± 10 º
β	Angular span of the merus/carpus joint	100 ± 10 º
γ	Angular span between propodus/dactyl joint	100 ± 10 º

Table 5.2: Average morphometric measurements, used to inform the quasi-static model. Average values are reported ± s.d. (n = 5).

Initial Ascent

The initial ascent (video still image: Figure 5.10A) is diagramed in Figure 5.10B. For a given height of ascent, *h*, the crab's body weight, F_W, is supported by the vertical component of a force, F_d, applied by the ground at the contact point between the lower leg and the ground.

$$F_{d,y} = F_w$$

The force applied on the ascending leg, F_u, is assumed to be perpendicular to obstacle and is balanced the horizontal component of F_d:

$$F_{d,x} = F_u$$

The quasi-static condition also stipulates that the torques produced by F_w, F_d, and F_u must all sum to zero. The point of rotation is defined as the point of contact between the lower leg and the ground.

$$\tau_w + \tau_d + \tau_u = 0$$

Since the distance between the point of rotation and F_d point of contact is zero, τ_d is also equal to zero. This simplifies the torque balance equation:

$$\tau_w = \tau_u$$

These torques may be expressed in terms of the forces and geometry. $\theta_{d\text{-}u}$ is the angle between the ground and a line from the lower and upper points of contact. $\theta_{d\text{-}COM}$ is defined as the angle between the ground and lower point of contact and the crab's center-of-mass (COM). $l_{d\text{-}COM}$ and $l_{d\text{-}u}$ are the distances between the lower point of contact and the center-of-mass and the upper point of contact, respectively. Thus, the following expressions of τ_w and τ_u are possible:

$$\tau_w = F_w l_{d-COM} \sin\theta_{d-COM}$$

$$\tau_u = F_u l_{d-u} \cos\theta_{d-u}$$

The crab's legs have many possible configurations, even in this simplified two-dimensional model. However, a crab will maximize the height to which it can climb by fully extending its legs. In this condition, $l_{d\text{-}u}$ becomes $l_{d\text{-}u,\,max}$:

$$l_{d-u,max} = w_c + 2c_l w_c$$

c_l is the ratio of maximum leg length to carapace width, w_c, which is typically 1.9 (Table 4.2). This permits τ_u to be expressed in terms of the crab's geometry and forces:

$$\tau_u = F_u l_{d-u,max} \cos\sqrt{1 - \left(h/l_{d-u,max}\right)^2}$$

The maximum reach condition also permits only a single value of $l_{d\text{-}COM}$ and θ_{COM}, which can both be expressed in terms of the crab's geometry by including, a, the shortest distance between the COM and the bottom of the body:

$$l_{d-COM} = \sqrt{\left(\frac{l_{d-u,max}}{2}\right)^2 + a^2}$$

$$\theta_{d-COM} = \sin^{-1}(h/l_{d-COM}) + \tan^{-1}(2a/l_{d-COM})$$

These, in turn, can be used to express τ_w in terms of the crab's forces and geometry:

$$\tau_w = F_w \sin[\sin^{-1}(h/l_{d-COM}) + \tan^{-1}(2a/l_{d-COM})] \sqrt{\left(\frac{l_{d-COM}}{2}\right)^2 + a^2}$$

As $\theta_{d\text{-}COM}$ approaches 90°, the torque produced by the crab's body weight also approaches zero. Once $\theta_{d\text{-}COM}$ moves beyond 90°, however, the torque will increase again, though the torque will not be in the opposite direction. Balancing τ_w in this state requires F_u to be directed into the obstacle. Since crabs do not have the ability to create adhesive forces, this means the torques can no longer be balanced and the crabs will fall away from the obstacle.

This condition can be simply expressed in terms of d, the horizontal distance between the lower contact point and the COM. As long as $d > 0$, the crab's center-of-mass will be between the lower and upper contact points, allowing the torques to be balanced and maintaining the quasi-static condition. Once $d < 0$, the crab's center-of-mass is outside the statically stable zone and the crab will fall away from the wall. *d* can be expressed as follows:

$$d = l_{d-COM} \cos \theta_{d-COM}$$

This expression can be expanded in terms of the crab's geometry:

$$d = \cos[\sin^{-1}(h/l_{d-COM}) + \tan^{-1}(2a/l_{d-COM})] \sqrt{\left(\frac{l_{d-COM}}{2}\right)^2 + a^2}$$

Figure 5.10C shows how *d*, changes with obstacle height for a crab of typical carapace width for the crabs discussed in section 4.3. These results suggest that a typical crab should be able to climb obstacles up to a maximum height of approximately 170 mm, corresponding with observed behavior. In practice, it is unlikely that crabs can attain their theoretical maximum height since transitioning from the primary to the secondary ascent requires that the ghost crabs grasp the top of the obstacle with the dactyls of the walking legs.

Figure 5.10

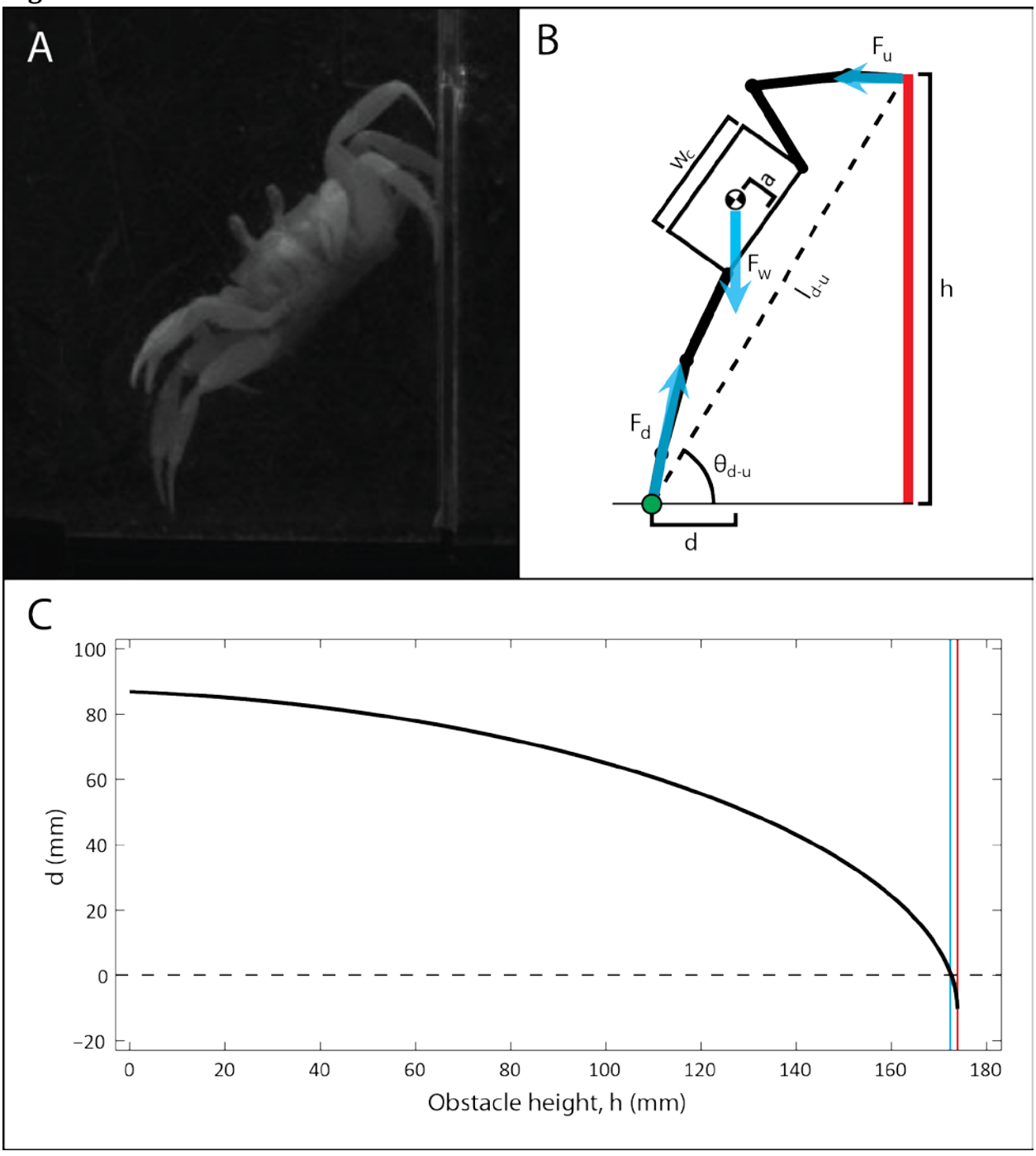
A
B
F_u
w_c
a
F_w
l_{d-u}
h
F_d
θ_{d-u}
d
C
100
80
60
40
20
0
−20
d (mm)
0
20
40
60
80
100
120
140
160
180
Obstacle height, h (mm)

Figure 5.10: A quasi-static model of a crab's initial ascent, where the crab climbs up the barrier using only the walking legs. Variable are defined in Table 4.1. **A:** a video still image of the initial ascent. **B:** A simplified diagram indicating the geometry and forces of the crab's initial ascent. The green circle indicates the axis of rotation for all torques (assumed to be a pin joint). **C:** A graph of d as a function of obstacle height, h, for a crab with a 36.2 mm carapace width (the average of the individuals used in the manipulation experiments presented here). This graph assumes that the crab will employ its maximum leg span (approximately 4.8x the crab's carapace width), which maximizes the achievable obstacle height for a given d. As the obstacle height increases, d decreases. When $d = 0$ (blue line), the crab's body weight switches from producing a clockwise torque to producing a counterclockwise torque, which would rotate the crab away from the obstacle. To counteract this torque, the crab must apply an attachment force with the ascending leg. Since the crabs cannot do this, the blue line represents a theoretical maximum obstacle height. The red line represents the crab's maximum leg span. If the crabs could apply attachment forces with the ascending leg, then they might attain this slightly higher obstacle height. Beyond this height, it is impossible for the crab to touch the top of the obstacle in any quasi-static configuration. This prediction is consistent with the behavior observed. Crabs are theoretically capable of climbing obstacles beyond 160 mm, though, as the obstacle height moves beyond 140 mm, the crabs must stretch farther and farther, while approaching the unstable equilibrium at $d = 0$.

Secondary Ascent

The secondary ascent (video still image: Figure 5.11A) is diagramed in Figure 5.11B. At this point, the crab is no longer in contact with the ground, but is entirely supported by the obstacle. This model assumes that ascending leg only exerts forces at the upper contact point. While crabs demonstrated the ability to touch the obstacle with the ascending dactyls, producing a second ascending contact point, the only forces a crab can produce at this point will counteract the forces required to ascend the obstacle. Thus, this model disregards any forces exerted by the ascending dactyls, assuming that the crab will avoid being counterproductive.

The crab's body weight, F_w, is now supported by the vertical component of a contact force between the carapace/merus joint on the ascending side:

$$F_{u,y} = F_w$$

The lower leg also produces a contact force on the barrier, which is assumed to be normal to the obstacle's surface. This force is balanced by the horizontal component of the ascending side's contact force:

$$F_{u,x} = F_d$$

Similar to the initial ascent, the torques produced by these forces must sum to zero. The point of rotation is defined as the upper contact point.

$$\tau_w + \tau_d + \tau_u = 0$$

Since the distance between the point of rotation and F_u point of contact is zero, τ_u is also equal to zero. This simplifies the torque balance equation:

$$\tau_w = \tau_d$$

These torques can be expressed in terms of the bodyweight and lower contact forces (F_w and F_d respectively), the distances at which these forces are applied ($l_{u\text{-}COM}$, the distance between the upper contact point and the crab's center-of-mass, and $l_{d\text{-}u}$, the distance between the upper and lower contact points) and the angle between the obstacle and the crab's center-of-mass, $\varphi_{u\text{-}COM}$:

$$\tau_w = F_w l_{u-COM} \sin \varphi_{u-COM}$$

$$\tau_d = F_d l_{d-u}$$

τ_d does not require an angular term because the F_d is always perpendicular to the $l_{d\text{-}u}$.

$l_{u\text{-}COM}$ is related to the crab's carapace width, w_c, and the height of the crab's center-of-mass above the bottom of the carapace, a:

$$l_{u-COM} = \sqrt{\left(\frac{w_c}{2}\right)^2 + a^2}$$

$\varphi_{u\text{-}COM}$ can also be expressed in terms of w_c, a, and the angle between the crab's body, $\varphi_{u\text{-}body}$:

$$\varphi_{u-COM} = \varphi_{u-body} + \tan^{-1}\left(\frac{2a}{w_c}\right)$$

The distance between the upper and lower contact points can be expressed in terms of $\varphi_{u\text{-}body}$, w_c and the distance between the lower contact point and the lower leg/carapace joint, l_d

$$l_{d-u} = w_c \cos\varphi_{u-body} + \sqrt{{l_d}^2 - \left(w_c \sin\varphi_{u-body}\right)^2}$$

These expressions, combined with the simplified torque balance equation allow ratio of F_d to F_w to be expressed as a function of l_d and $\varphi_{u\text{-}body}$:

$$\frac{F_d}{F_w} = \frac{\sin\left(\varphi_{u-body} + \tan^{-1}(2a/w_c)\right)\sqrt{\left(\frac{w_c}{2}\right)^2 + a^2}}{w_c \cos\varphi_{u-body} + \sqrt{{l_d}^2 - \left(w_c \sin\varphi_{u-body}\right)^2}}$$

If there are no limitations on the crab's range of motion, l_d can have any value between w_c and $c_l w_c$, where c_l is the ratio of maximum leg length to carapace width, which is typically 1.9 (Table 5.2). The ratio of F_d to F_W is plotted (Figure 5.11C) for a crab of typical carapace width for the crabs studied in sections 5.3. When $\varphi_{u\text{-}body}$ reaches 90°, the crab can trivially transition to the other side of the obstacle by exerting any horizontal force with the ascending leg.

As figure 5.11C indicates, the force requirements for reaching $\varphi_{u\text{-}body} = 90^o$ are relatively low, being approximately one-third of the crab's body mass. This suggests that ghost crabs should be able to climb over the obstacle using only their walking legs. Since this does not correspond with the experimental results in section 5.3, another biomechanical limitation seems likely.

Figure 5.11

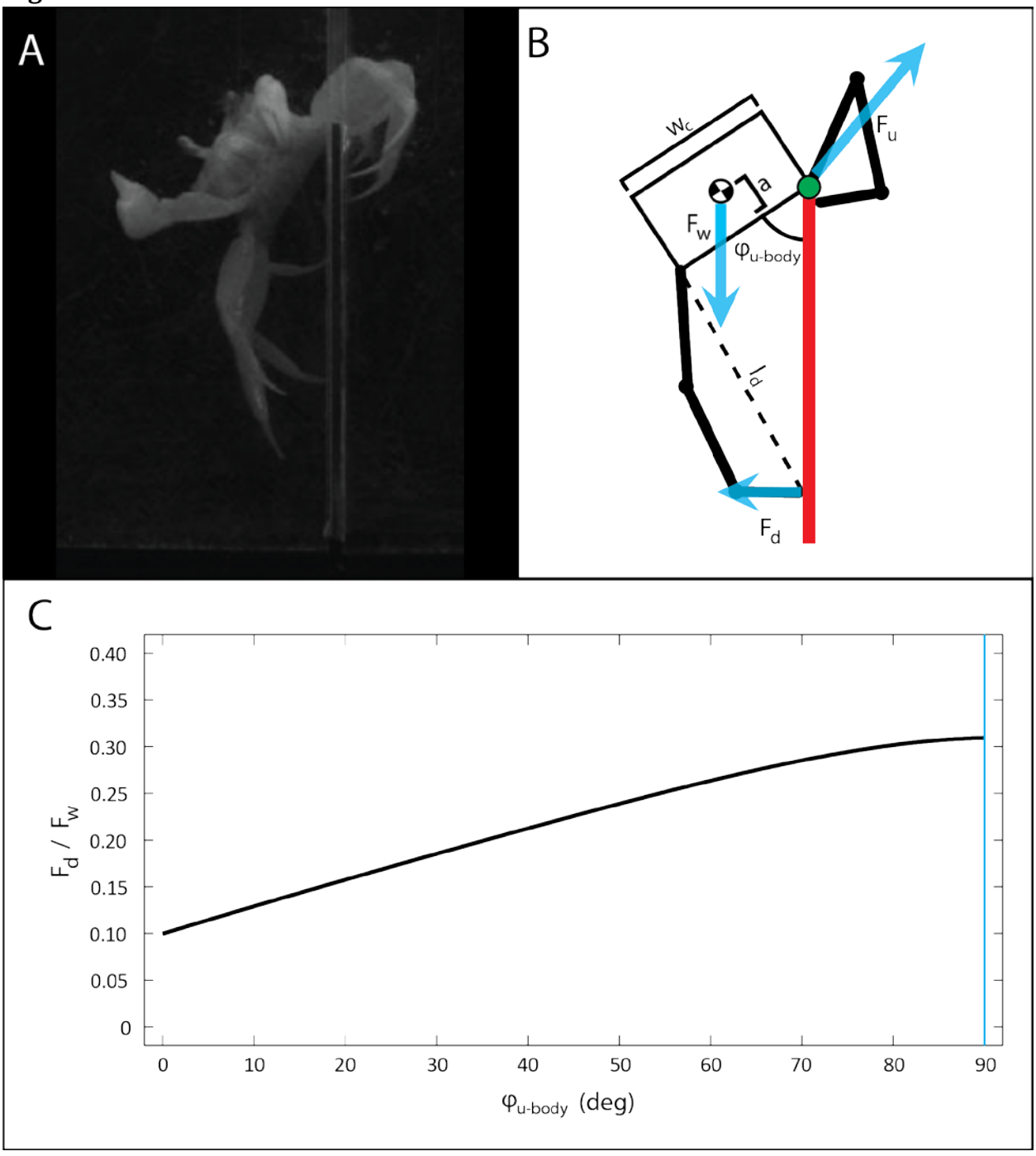
A
B
w_c
F_u
a
F_w
$\varphi_{u\text{-}body}$
l_d
F_d
C
F_d / F_w
0.40
0.35
0.30
0.25
0.20
0.15
0.10
0.05
0
0
10
20
30
40
50
60
70
80
90
$\varphi_{u\text{-}body}$ (deg)

Figure 5.11: A quasi-static model of a crab's ascent after it has secured itself to the top of the obstacle. **A:** a video still image of the secondary ascent. **B:** A simplified diagram indicating the geometry and forces of the crab's secondary ascent. The green circle indicates the axis of rotation for all torques (assumed to be a pin joint). Variables are defined in Table 4.1. **C:** The ratio between F_d and F_w as a function of $\varphi_{u\text{-}body}$, assuming that the crab minimizes F_d by extending the lower leg as much as possible ($l_d \approx 1.9\ w_c$). The crab's carapace width was assumed to be 36 mm, a typical value for the individuals used in prior climbing studies. To pivot about the axis of rotation, F_d/F_w must exceed the value indicated at each value of $\varphi_{u\text{-}body}$. When $\varphi_{u\text{-}body} = 90^o$ (blue line), the crab's carapace is entirely above the obstacle, a condition where the ascending leg can trivially translate the carapace to the other side of the obstacle. This quasi-static model indicates that the crab should be able to achieve $\varphi_{u\text{-}body} = 90^o$ by exerting a force greater than approximately 0.3 times the crab's body weight, strongly suggesting that a crab should be able to ascend without using its chelae to assist. This contradicts observed behavior, indicating that there is another constraint limiting the crabs' ability to climb high obstacles.

Range of Motion Limitations

The quasi-static model predicts that ghost crabs should be able to climb over high hurdles with only their walking legs. However, this contradicts experimental results, suggesting that another limitation exists.

The most likely limitation concerns the crab's range of motion. If the crab is unable to maintain contact with the lower legs at some point, then this violates the assumption that the distance between the lower contact point and the lower leg/carapace joint, l_d, can have any value between the carapace width and the maximum leg length.

Figure 5.12A details the angular range-of-motion for each principal degree of freedom in a typical ghost crab, as determined by morphometric measurements. A ghost crab's leg has three primary degrees of freedom relevant to the quasi-static model presented here: the vertical merus/carapace joint, α, which has a range of approximately 145^o, the merus/carpus joint, β, which has a range of approximately 100^o, and the propodus/dactyl joint, γ, which also has a range of approximately 100^o. Ghost crabs have two additional degrees of freedom: the carpus/propodus joint and the horizontal merus/carapace joint. The former has a limited ability to affect the climbing behavior, since it has a very limited range of motion (approximately $\pm 5^o$) and operates only perpendicular to the plane of this illustration. The horizontal merus/carapace joint also operates perpendicular to the plane of this illustration, though the range of motion is quite substantial ($\pm 30^o$). While this degree of freedom can assist with climbing behaviors by allowing the crab to find alternate and more advantageous footings, it cannot increase the maximum theoretical performance used in this quasi-static model.

When the crab reaches the top of the obstacle, the crab's ability to maintain contact with the lower leg is limited by the range of motion in the merus/carapace joint and the overall length of the carpus, propodus and dactyl (Figure 5.12B). When the angle between the crab's body and the obstacle exceeds 70.5^o, there is no configuration of the lower leg that permits the crab to maintain contact with the barrier.

Figure 5.12

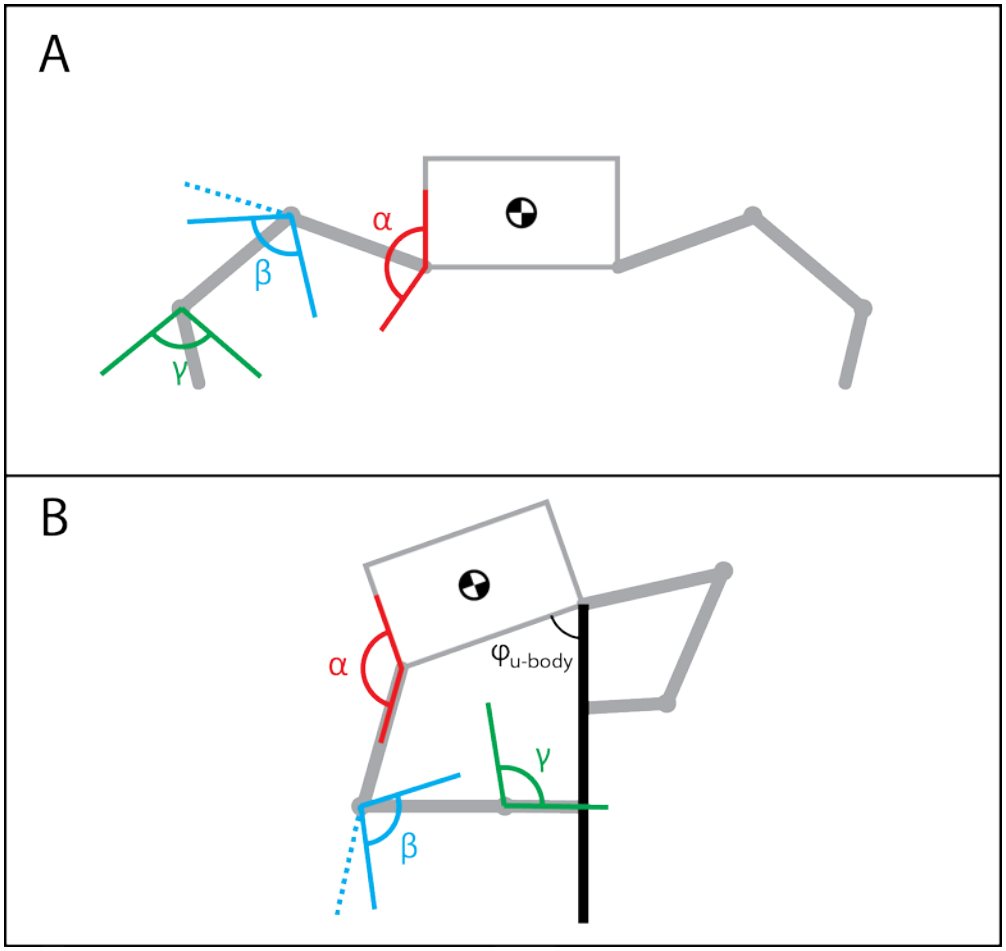

Figure 5.12: The ghost crab's range of motion. The crab's leg segments are to scale with the representation of the carapace. **A:** A ghost crab's leg has three primary degrees of freedom relevant to the quasi-static model presented here. **α** is the vertical merus/carapace joint, which has a range of approximately 145°. **β** is the merus/carpus joint, which has a range of approximately 100°. **γ** is the propodus/dactyl joint, which also has a range of approximately 100°. **B:** The maximum values of $\varphi_{u\text{-}body}$ attainable while maintaining contact with the lower leg. Beyond $\varphi_{u\text{-}body} = 70.5°$, the crab cannot reach the obstacle with its lower leg in any configuration.

Chelae Overcome Torque Limitations

If the crab cannot maintain contact with the lower leg, then the torque produced by the crab's body weight, τ_w, must be opposed by another torque to maintain the quasi-static assumption. It is not possible for the force at the upper contact point to oppose τ_w because the distance between the point of rotation and point of contact is zero. A second contact force, F_{U2}, created by the dactyls on the ascending leg is also unable to counteract τ_w because any value of F_{U2} will produce a torque in the same direction as τ_w (Figure 5.13A).

If the second ascending contact force, F_{U2}, also facilitates a frictional force, F_{U3} (Figure 5.13B), then it is possible for the crab to create a torque that opposes τ_w. The torque produced by the frictional force, F_{U3}, depends on the barrier having a non-zero thickness (Figure 5.13C). For a given obstacle width, w_o, and vertical distance between the top of the obstacle and the contact point, l_{U3}, the torque created by F_{U3} is:

$$\tau_{U3} = \frac{F_{U3}\left({l_{U3}}^2 + {w_o}^2\right)(w_o/l_{U3})}{\sqrt{(w_o/l_{U3})^2 + 1}}$$

When the ratio of w_o to l_{U3} is small (as it is in the hurdling behavior), this torque will approach zero, limiting the crab's ability to maintain a quasi-statically stable state.

Furthermore, the frictional force, F_{U3}, is proportional to the magnitude of the normal force, F_{U2}. Increasing τ_{U3} by increasing F_{U3} means that the crab must also increase F_{U2} which produces a counter-productive torque in the same direction as τ_w. For the frictional torque to be effective, the ratio of τ_{U3} to τ_{U2} must be greater than 1. In terms of w_o, l_{U3} and F_{U2}, these torques can be expressed as follows:

$$\tau_{U3} = \frac{c_f F_{U2}\left({l_{U3}}^2 + {w_o}^2\right)(w_o/l_{U3})}{\sqrt{(w_o/l_{U3})^2 + 1}}$$

$$\tau_{U2} = \frac{F_{U2}\left({l_{U3}}^2 + {w_o}^2\right)\left(\frac{\pi}{2} - w_o/l_{U3}\right)}{\sqrt{\left(\frac{\pi}{2} - w_o/l_{U3}\right)^2 + 1}}$$

c_f is the coefficient of friction between the dactyl and the obstacle. The ratio of these two torques is:

$$\frac{\tau_{U3}}{\tau_{U2}} = \frac{c_f\left(\frac{w_o}{l_{U3}}\right)\sqrt{\left(\frac{\pi}{2} - \frac{w_o}{l_{U3}}\right)^2 + 1}}{\left(\frac{\pi}{2} - \frac{w_o}{l_{U3}}\right)\sqrt{\left(\frac{w_o}{l_{U3}}\right)^2 + 1}}$$

For small values of w_o/l_{U3} (i.e. 0.1, dimensions consistent with the results discussed in section 4.3), this resolves to approximately:

$$\frac{\tau_{U3}}{\tau_{U2}} = 0.01c_f$$

For the ratio of τ_{U3} to τ_{U2} to be above 1, the coefficient must be greater than 100, which is highly unlikely.

If, however, the crab directly applies a torque to the top of the obstacle using the ascending chela (Figure 5.13D), then the torque limitation can be trivially resolved, allowing the crab to maintain a quasi-statically stable state regardless of the ability to maintain leg-to-obstacle contact or frictional forces. This analysis may explain the experimental results detailed in section 4.3. The chelae are required for high hurdling because they provide alternate means of producing climbing torques when other mechanisms fail.

Figure 5.13

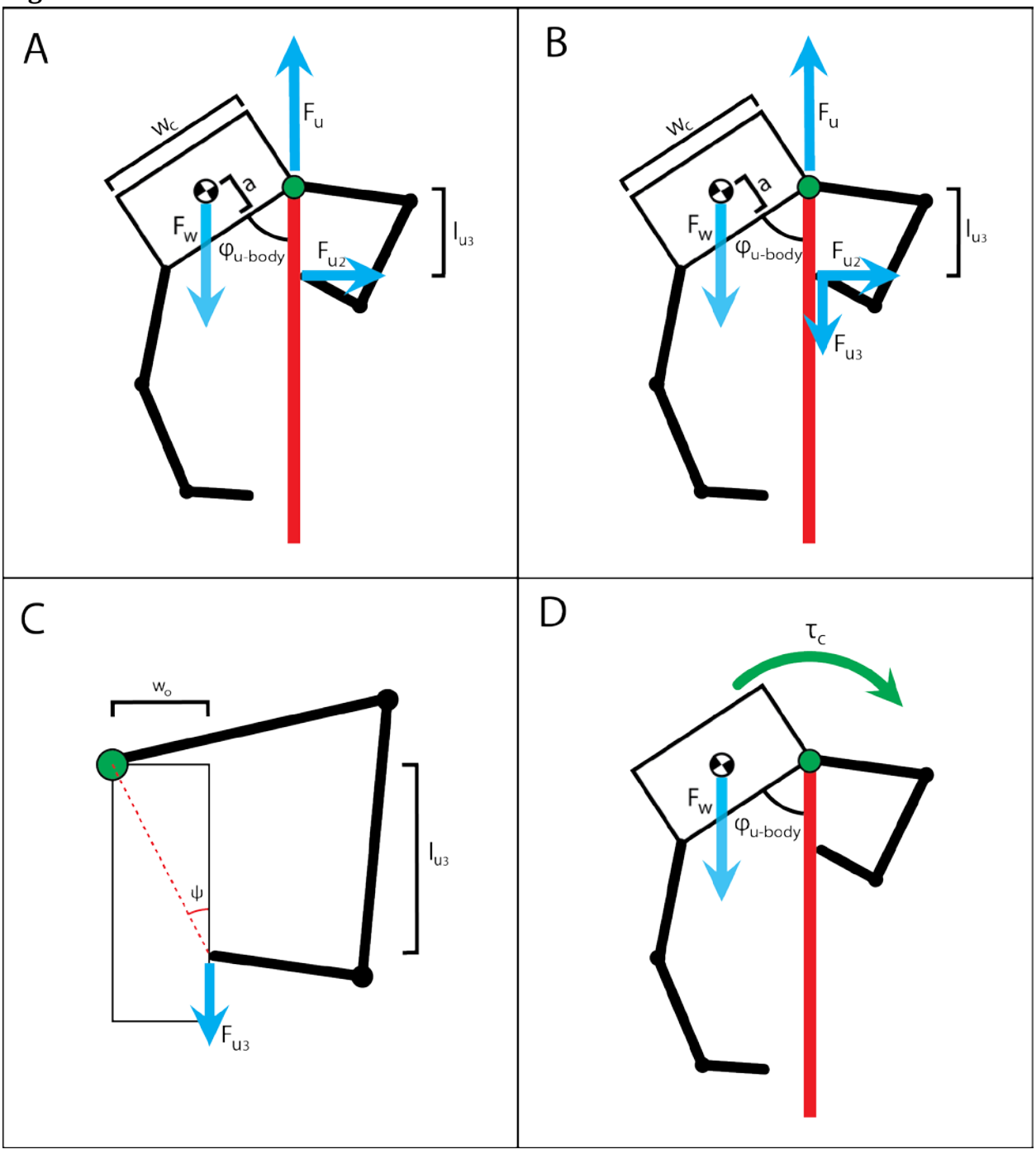
A
w_c
F_u
a
F_w
$\varphi_{u\text{-}body}$
F_{u2}
l_{u3}
B
w_c
F_u
a
F_w
$\varphi_{u\text{-}body}$
F_{u2}
l_{u3}
F_{u3}
C
w_o
l_{u3}
ψ
F_{u3}
D
τ_c
F_w
$\varphi_{u\text{-}body}$

Figure 5.13: Diagrams illustrating quasi-static conditions for configurations where the crab is unable to contact the obstacle. **A:** Once the crab loses contact with the lower leg, the only remaining forces are those from body weight (F_w), contact with the top of the barrier (F_{U1}) and from the normal force from the ascending leg's contact with the barrier (F_{U2}). There is no combination of magnitudes for these forces that will support a static body position. Instead, F_{U2} and F_W produce an un-opposed counter-clockwise torque that will push the crab's center of mass back down the obstacle. **C:** A force parallel to the barrier produced by the ascending leg (F_{U3}) may potentially produce a statically stable condition. However, this is unlikely. For instance, if F_{U3} is produced by static friction, then this F_{U3} is proportional to F_{U2} which, in turn, torques the crab back down the obstacle. **C:** Even if the crab could produce F_{U3} without also producing a counter-productive F_{U2} (e.g. using an asperity), the geometry of the obstacle means only a small fraction of F_{U3} translates into a torque to counteract that created by F_W. For a typical geometrical configuration and assuming that $F_{U2} = 0$, F_{U3} must be equal to approximately 7.5 times the crab's body weight, F_W, to produce a statically stable condition. **D:** If the crab can apply a torque directly to the pivot point by using its chelae, however, it becomes trivial to produce a statically stable condition F_{U2}, and F_{U3} could be equal to 0. Thus, this quasi-static model potentially explains why prior experimental results strongly suggested that the chelae are required for climbing high obstacles.

Assumptions and Limitations

The key assumption of this model is that hurdling can be approximated as a quasi-static behavior. Crabs do not run or jump as part of the hurdling behavior. They used the deliberate, controlled behavior observed in the field when not executing an escape behavior. However, many animals do employ dynamic behaviors while interacting with obstacles (Bertram, et al., 1999; Mongeau et al., 2012). Since ghost crabs have demonstrated the ability to perform high-speed dynamic behaviors, such as jumping and running (Blickhan & Full, 1987), it is possible that the crabs could use similar dynamic behaviors to facilitate hurdling or related behaviors. Although chelae-restrained ghost crabs did not demonstrate such dynamic behaviors when the ability to climb quasi-statically was removed, this does not preclude the possibility that dynamic climbing strategies may exist in ghost crabs.

This model also makes several simplifying assumptions about the geometry of ghost crab hurdling. The contact points of eight legs are reduced to two contact points confined to a two-dimensional plane. In practice, ghost crabs have dexterous legs that make contact with the obstacle at multiple points in three dimensions. Multiple points of contact could help crabs recover from slipping while climbing. If the crab loses one point of contact, the others may be able compensate and allow the crab to avoid falling in a similar fashion to the redundancy observed in geckos (Autumn et al., 2006). Additionally, lateral motion (i.e. out of the two-dimensional plane used to approximate hurdling by this model) may allow the crabs to find alternate or more stable footing while climbing, improving crabs' ability to climb heterogeneous structures.

Finally, this model only permits forces to arise from contact with the ground and the obstacle. However, the crabs' multi-legged design permits them to maintain contact with the barrier while searching for alternate contact points. If the crabs make contact with another surface, then they may be able to employ alternate climbing strategies. In particular, crabs could avoid employing their chelae during the secondary ascent if another surface is within the lower legs' range of motion.

5.5 Conclusions

Ghost crab hurdling represents a multifunctional climbing behavior. The walking legs and chelae are used in concert to enable a behavior that is not possible with either appendage set alone. The crabs use self-manipulation to dexterously interact with the obstacle and successfully cross barriers up to 16 times their normal hip height without requiring additional kinetic energy from running or leaping.

Ghost crabs demonstrated three distinct hurdling behaviors: hip raise (Figure 5.4), legs only (Figure 5.5) and legs with chela assist (Figure 5.6). The first two strategies required only the walking legs. The legs with chela assist strategy, however, involved both the walking legs and chelae. The crabs used all of their appendages to grasp or interact with the obstacle.

The strategy of choice was related to obstacle height (Figure 5.8), consistent with expectations from both field observations and prior studies in climbing cockroaches (Ritzmann et al., 2004). For low obstacles, hip raises were preferred. As obstacle height increased, crabs transitioned from the hip raise strategy to the legs only strategy and finally to the legs with chela assist strategy. The crabs' success rates were remarkably high across a wide range of obstacle heights (Figure 5.7). Crabs were able to maintain >80% success for obstacles up to 120 mm high (approximately 75% of the crabs' maximum leg span). Success rates began to decrease substantially above this height, however, with crabs primarily failing when they were unable to hook the top of the obstacle with their walking legs.

Chelae restraint experiments clearly demonstrate that the chelae are required for the legs with chela assist hurdling strategy (Figure 5.9). Success rates for a 100 mm obstacle were 100% in the control condition (consistent with prior observations illustrated in Figure 5.8), but all individuals decreased to 0% for the same obstacle when the chelae were restrained. While crabs demonstrated the ability to hook the obstacle with their walking legs, they appeared unable to move their bodies across the obstacle.

A quasi-static model suggests that the chelae assist hurdling by providing an alternate means of producing climbing torques (Figure 5.13). While the crabs' walking legs are capable of producing sufficient climbing torques (Figure 5.11), the range of motion is too limited to permit the legs only strategy to function for tall obstacles (Figure 5.12). This represents a novel climbing behavior in arthropods. While many arthropods can climb in a variety of conditions (Chapman, 1982), arthropods with grasping appendages predominately use these appendages exclusively for prey capture and manipulation (Dollar, 2001). Thus, ghost crab hurdling more closely resembles vertebrate self-manipulation/climbing behaviors (Ashton & Oxnard, 1964), rather than climbing with specialized spines or adhesives more typically observed in arthropods (Chapman, 1982).

Future work on ghost crab hurdling could focus on the role of leg span, body size and how self-manipulation permits locomotor transitions. Leg span also appears to be the primary limitation on maximum obstacle height (Figure 5.10). This hypothesis could be tested easily by presenting crabs of different sizes with varying obstacle heights. However, it is possible that hurdling strategies will change with ghost crab size because muscle force and body weight scale differently with body size (Alexander, 2006). It is possible that the hurdling strategies discussed in this chapter are specific to a certain combination of crab sizes or weights. Larger or smaller crabs may adopt alternate strategies accordingly. Finally, the torque limitations encountered in ghost crab hurdling and the self-manipulation used to overcome them may represent a template (Full & Koditschek, 1999) since cockroaches also adopt altered postures at the tops of vertical obstacles (Ritzmann et al., 2004). Further study of ghost crabs and other climbing animals may offer insight into the general principles of climbing transitions, supplementing current climbing templates (Goldman, et al., 2006).

Overall, ghost crab hurdling represents a new source of bio-inspiration for next-generation robots capable of self-manipulation. While current robotic platforms, such as RHex (Saranli et al.,

2001), can use a self-manipulation framework to ballistically leap/climb vertical obstacles (Johnson, 2014), ghost crab hurdling may inspire climbing methods that are more stable, more robust and more adaptable. More generally, these results may inform future studies of both biological and robotic self-manipulation and multifunctionality by providing new insights into locomotion though manipulation. The combined use of manipulating and locomotive appendages will be critical to new robotic technologies (Celine, et al., 2008) that are expected to move within complex terrain, while simultaneously manipulating both themselves and the environment.

Bibliography

Alberch, P. (1981). Convergence and Parallelism in Foot Morphology in the Neotropical Salamander Genus Bolitoglossa. I. Function. *Evolution*, *35*(1), 84–100.

Alexander, R. (2006). *Principles of Animal Locomotion*. Princeton, NJ: Princeton University Press.

Alexander, R., Stanton, R., & Dodd, J. (1993). Influence of sediment grain size on the burrowing of bivalves: correlation with distribution and statigraphic persistence of selected Neogene clams. *Palaios*, *8*, 289–303.

Ansell, A., & Nair, N. (1969). A comparative study of bivalves which bore mainly by mechanical means. *Am. Zoologist*, *9*, 857–868.

Ashton, E., & Oxnard, C. (1964). Locomotion patterns in primates. *Proc. Zool. Soc. Lond.*, *142*, 1–28.

Autumn, K., Hsieh, S., Dudek, D., Chen, J., Chitaphan, C., & Full, R. (2006). The dynamics of vertical running in geckos. *J Exp Biol*, *209*, 260–272.

Bellwood, O. (2002). Occurrence, mechanics and significance of burying behavior in in crabs (Crustacea: Brachyura). *Natural History*, *36*(10).

Bernal, J., & Mason, J. (1960). Packing of spheres: co-ordination of randomly packed spheres. *Nature*, *188*, 910–911.

Bertram, J., Ruina, A., Cannon, C., Chang, Y., & Coleman, M. (1999). A point-mass model of gibbon locomotion. *J Exp Biol*, *202*, 2609–2617.

Bicchi, A., & Kumar, V. (2000). Robotic grasping and contact: a review. *IEEE International Conference on Robotics and Automation*.

Blickhan, R., & Full, R. (1987). Locomotion energetics of the ghost crab: II. Mechanics of the center of mass during walking and running. *Jour. Exp. Biol*, *130*, 155–174.

Brown, A., & Trueman, E. (1991). Burrowing of sandy-beach molluscs in relation to penetrability of the substratum. *Jour. of Molluscan Studies*, *57*, 134–136.

Burrows M, & Hoyle, G. (1973). The mechanism of rapid running in the ghost crab, Ocypode ceratophthalma. *J. Exp. Biol*, *58*, 327–349.

Caine, E. (1974). Feeding of Ovalipes guadulpensis (Saussure)(Decapoda: Brachyura: Portunidae), and morphological adaptations to a burrowing existence. *Biological Bulletin*, *147*(3), 550–559.

Cartmill, M. (1974). Pads and claws in arboreal locomotion. In *Primate Locomotion* (pp. 45–83).

Celine, R., Mondada, F., & Siegwart, R. (2008). What do people expect from robots? *IEEE International Conference on Intelligent Robots and Systems*.

Chakrabarti, A. (1981). Burrow patterns of ocypode ceratophthalma (pallas) and their environmental significance. *Amer. Jour. of Paleontology*, *55*(2), 431–441.

Chan, B., Chan, K., & Leung, P. (2006). Burrow architecture of the ghost crab ocypode ceratophthalma on a sandy shore in Hong Kong. *Hydrobiologia*, *560*, 43–49.

Chapman, R. (1982). The Thorax and Legs. In *The Insects: Structure and Function* (3rd ed.). Cambridge, MA: Harvard University Press.

Che, J., & Dorgan, K. (2010). It's tough to be small: dependence of burrowing kinematics on body size. *Jour. Exp. Biol*, *213*, 1241–1250.

Corrette, B. (1990). Prey Capture in the Praying Mantis Tenodera Aridifolia Sinensis: Coordination of the Capture Sequence and Strike Movements. *Jour. Exp. Biol*, *148*, 147–180.

Ding, Y., Gravish, N., Li, C., Maladen, R., Mazouchova, N., Sharpe, S., … Goldman, D. (2010). Comparative studies reveal principles of movement on and within granular media. *Natural Locomotion in Fluids and on Surfaces: Swimming, Flying and Sliding*.

Dollar, A. (2001). *Arthropod grasping and manipulation: a literature review*. Harvard BioRobotics Laboratory Technical Report.

Dorgan, K. (2015). The biomechanics of burrowing and boring. *Jour. Exp. Biol*, *218*, 176–183.

Dorgan, K., Jumars, P., Johnson, B., & Boudreau, B. (2006). Macrofaunal burrowing: the medium is the message. *Oceanography and Marine Biology*, *44*, 85–121.

Dorgan, K., Jumars, P., Johnson, B., Boudreau, B., & Landis, E. (2005). Burrowing Mechanics: Burrow Extension by Crack Propagation. *Nature*, *433:475*.

Dorgan, K., Lefebvre, S., Stillman, S., & Koehl, M. (2011). Energetics of burrowing by the cirratulid polychaete, Cirriformia moorei. *Jour. Exp. Biol*, *214*, 2202–2214.

Duncan, G. (1986). Burrows of Ocypode quadrata (fabricus) as related to slopes of substrate surfaces. *Jour. of Paleontology*, *60*(2), 384–389.

DuToit, J., Jarvis, J., & Louw, G. (1985). Nutrition and burrowing energetics of the cap mole-rat Georychus capensis. *Oecologia*, *66*(1), 81–87.

Elner, R., & Campbell, A. (1981). Force, Function and Mechanical Advantage in the Chelae of the American Lobster Homarus americanus (Decapoda: Crustacea). *Jour. Zoology*, *193*, 269–286.

Espinoza, D. N., & Santamarina, J. C. (2010). Ant tunneling- a granular media perspective. *Granular Matter*, *12*, 607–616.

Faulkes, Z. (2012). morphological adaptations for digging and burrowing. In L. Watling & M. Thiel (Eds.), *Functional Morphology and Diversity.* Cambridge: Oxford University Press.

Federle, W., Riehle, M., Curtis, A., & Full, R. (2002). An integrative study of insect adhesion: Mechanics and wet adhesion of pretarsal pads in Ants. *Integrative and Comparative Biology*, *42*, 1100–1106.

Full, R. (1987). Locomotion energetics of the ghost crab: I. Metabolic cost and endurance. *J Exp*

Biol, *130*, 137–154.

Full, R., & Koditschek, D. (1999). Templates and anchors: neuromechanical hypotheses of legged locomotion on land. *Jour. Exp. Biol*, *202*(23), 3325–3332.

Gillies, A., Henry, A., Lin, H., Ren, A., Shiuan, K., Fearing, R., & Full, R. (2014). Gecko toe and lamellar shear adhesion on macroscopic, engineered rough surfaces. *J Exp Biol*, *217*, 283–289.

Goldman, D., Chen, T., Dudek, D., & Full, R. (2006). Dynamics of rapid vertical climbing in cockroaches reveals a template. *Jour. Exp. Biol*, *209*, 2990–3000.

Gorb, S., Beutel, R., Gorb, E., Jiao, Y., Kastner, V., Niederegger, S., … Votsch, W. (2002). Structural design and biomechanics of friction-based releasable attachment devices in insects. *Integrative and Comparative Biology2*, *42*, 1127–1139.

Gravish, N., Franklin, S., Hu, D., & Goldman, D. (2012). Entangled granular media. *Phys. Rev. Lett.*, *108*(208001).

Gravish, N., Umbanhowar, P., & Goldman, D. (2010). Force and flow transition in plowed granular media. *Phys. Rev. Let.*, *105*(128301).

Hafemann, D., & Hubbard, J. (1969). On the rapid running of ghost crabs (Ocypode ceratophthalma). *Jour. Exp. Zool.*, *170*, 25–32.

Hanna, G., & Barnes, W. (1991). Adhesion and detachment of the toe pads of tree frogs. *J. Exp. Biol*, *155*, 103–125.

Herreid, C., & Full, R. (1986). Energetics of hermit crabs during locomotion: the cost of carrying a shell. *Jour. Exp. Biol*, *120*, 297–308.

Herreid, C., & Full, R. (1988). Energetics and locomotion. In W. Burggren & B. McMahon (Eds.), *Biology of the Land Crabs* (pp. 333–377). Cambridge University Press.

Hildebrand, M. (1987). Digging of Quadrepeds. In M. H. D. B. K. L. D. Wake. (Ed.), *Functional Vertebrate Morphology* (pp. 89–110). Cambridge, MA: Harvard Press.

Hill, G., & Hunter, R. (1973). Burrows of the ghost crab ocypode quadrata (fabricus) on the barrier islands, south-central texas coast. *Jour. Seimentary Petrology*, *43*(1), 24–30.

Hosoi, A., & Goldman, D. (2015). Beneath our feet: strategies for locomotion in granular media. *Annu. Rev. Fluid Mech.*, *47*, 431–453.

Hunter, D., & Elder, H. (1989). Burrowing dynamics and energy cost of transport in the soft-bodied marine invertebrates Polyphysia crassa and Priapulus caudatus. *Jour. Zoology*, *218*(2), 209–222.

Hyatt, G., & Salmon, M. (1977). Combat in the Fiddler Crabs Uca Pugilator and Uca Pugnax: A Quantitative Analysis. *Behaviour*, *65*, 182–211.

Iagnemma, K., & Dubowsky, S. (2010). *Mobile Robots in Rough Terrain: Estimation, Motion Planning, and Control with application to Planetary Rovers.* Springer Publishing Corp.

Jaeger, H., & Nagel, S. (1992). Physics of the granular state. *Science*, *255*, 1523–1531.

Johnson, A. (2014). *Self-manipulation and dynamic transitions for a legged robot*. Univ. of Pennsylvania.

Jones, C., Lawton, J., & Shachak, M. (1997). Positive and negative effects of organisms as physical ecosystem engineers. *Ecology*, *78*, 1946–1957.

Jung, S., Winter, A., & Hosoi, A. (2011). Dynamics of digging in wet soil. *Int. Jour. Non-Linear Mech.*, *46*, 602–606.

Kram, R. (2000). Muscular force or work: what determine the metabolic energy cost of running. *Excercise and Sport Sciences Review*, *28*(3), 138–144.

Li, C., Umbanhower, P., Komsuoglu, D., Koditschek, D. E., & Goldman, D. (2009). Sensitive dependence of the motion of a legged robot on granular media. *Proc. Nat. Acad. Sci.*, *106*(9), 3029–3034.

Li, C., Zhang, T., & Goldman, D. (2013). A terradynamics of legged locomotion on granular media. *Science*, *339*(1408).

Maladen, R., Ding, Y., Li, C., & Goldman, D. (2009). Undulatory swimming in sand: subsurface locomotion of the sandfish lizard. *Science*, *325*(314).

Mazouchova, N., Gravish, N., Savu, A., & Goldman, D. (2010). Utilization of granular solidification during terrestrial locomotion of hatchling sea turtles. *Biol. Lett.*, *6*(3), 398.

Milne, L., & Milne, M. (1946). Notes on the behavior of the ghost crab. *The American Naturalist*, (792), 362–380.

Mitari, N., & Nori, F. (2006). Wet granular materials. *Advances in Physics*, *55*(1-2), 1–45.

Monaenkova, D., Gravish, N., Goodisman, M., & Goldman, D. (2013). Effect of moisture content on nest construction activity of fire ants. *Society of Integrative and Comparitive Biology*.

Mongeau, J., McRae, B., Jusufi, A., Birkmeyer, P., Hoover, A., Fearing, R., & Full, R. (2012). Rapid inversion: Running animals and robots swing like a pendulum under ledges. *PLoS One*, *7*(6).

Nel, R., McLachlan, A., & Winter, D. (1999). The effect of sand particle size on the burrowing ability of the beach mysid Gastrosaccus psammodytes Tattersall. *Estuarine Coastal and Shelf Science*, *48*, 599–604.

Okamura, A., Smaby, N., & Cutkosky, M. (2000). An overview of dexterous manipulation. *IEEE International Conference on Robotics and Automation*, *1*, 255–262.

Qian, F., Zhang, T., Korff, W., Umbanhowar, P., Full, R., & Goldman, D. (2015). Principles of appendage design in robots and animals determining terradynamics performance on flowable ground. *Bioinspiration & Biomimetics*, *10*.

Ritzmann, R., Quinn, R., & Fischer, M. (2004). Convergent evolution and locomotion through

complex terrain by insects, vertebrates and robots. *Arthropod Struct. Dev.*, *33*, 361–379.

Roth, L., & Willis, E. (1952). Tarsal structure and climbing ability of cockroaches. *Jour. Exp. Zool.*, *119*, 483–517.

Saranli, U., Buehler, M., & Koditschek, D. (2001). Rhex: A simple and highly mobile hexapod robot. *International Jour. or Robotics Research*, *20*(7), 616–631.

Savazzi, E. (1985). Functional morphology of the cuticular terraces in burrowing brachyuran decapods. *Lethaia*.

Seguin, A., Bertho, Y., Gondret, P., & Crassous, J. (2011). Dense granular flow around a penetrating object: Experiments and hydrodynamic model. *Phys. Rev. Let.*, *107*(048001).

Seymour, R., Withers, P., & Weathers, W. (1998). Energetics of burrowing, running and free-living in the Namib Deser golden mole (Eremitalpa namibensis). *Jour. Zoology*, *2434*(1), 107–117.

Sharpe, S., Ding, Y., & Goldman, D. (2012). Interaction with granular media influences muscle activation strategy in sandfish lizard (Scincus scincus). *Jour. Exp. Biol*, *216*.

Shepard, E., Wilson, R., Rees, W., Grundy, E., Lambertucci, S., & Vosper, S. (2013). Energy Landscapes Shape Animal Movement Ecology. *American Naturalist*, *182*(3), 298–312.

Sponberg, S., & Full, R. (2008). Neuromechanical response of musculo-skeletal structures in cockroaches during rapid running on rough terrain. *Jour. Exp. Biol*, *211*(3), 433–446.

Srinivasa, S., Ferguson, D., Helfrich, C., Berenson, D., Collet, A., Diankov, R., & Weghe, M. (2010). HERB: a home exploring robotic butler. *Autonomous Robots*, *28*(1), 5–20.

Tresguerres, M., Katz, S., & Rouse, G. (2013). How to get into bones: proton pump and carbonic anhydrase in Osedax boneworms. *Proc. Biol. Sci.*, *280*.

Trevor, J. (1978). The dynamics and mechanical energy expenditure of the polychaetes Nephtys cirrosa, Nereis diversicolor and Arenicola marina during burrowing. *Estuarine and Coastal Marine Science*, *6*(6), 605–619.

Trueman, E. (1970). The mechanism of burrowing of the mole crab, Emerita. *Jour. Exp. Biol*, 701–710.

Umbanhower, P., & Goldman, D. (2010). Granular impact and the critical packing state. *Phys. Rev. Let. E.*, *82*(010301).

Vleck, D. (1979). The Energy Cost of Burrowing by the Pocket Gopher Thomomys bottae. *Physiological Zoology*, *52*(2).

Warner, G. (1977). *The Biology of Crabs*. New York, NY: Van Nostrad Reinhold Company.

Weinstein R, & Full, R. (1994). Thermal dependence of locomotor energetics of the ghost crab, Ocypode quadrata. *Physiological Zoology*, *67*, 855–872.

Weinstein, R., & Full, R. (1992). Intermittent locomotion alters endurance in an eight-legged ectotherm. *Amer. J. Physiol.*, *262*, 852–859.

Weinstein, R., & Full, R. (1998). Performance limits of low temperature continuous locomotion are exceeded when locomotion is intermittent in ghost crabs. *Physiological Zoology*, *71*, 274–284.

White, C. (2001). The energetics of burrow excavation by the inland robust scorpion, Urodacus yashenkoi (Birula, 1903). *Australian Journal of Zoology*, *49*, 663–674.

Winter, A., Deits, R., & Hosoi, A. (2012). Localized fluidization burrowing mechanics of Ensis directus. *Jour. Exp. Biol*, *215*, 2072–2080.